Supporting Information for

Highly Active and Chemoselective Homobimetallic Ruthenium Catalyst for One-pot Reductive Amination in Water

Gopal Deshmukh, Thakur Rochak Kumar Rana, Nikita Yadav, Gopalan Rajaraman and Ramaswamy Murugavel

---

Genral Infromations

All the experimental procedures were conducted in a well-ventilated fume hood in an ambient atmosphere. The amines and aldehydes substrates employed in catalysis were used as available commercially. Other chemicals and solvents were procured commercially and used without any purification. The ruthenium compounds reported herein are air and moisture stable and no special measures were taken in handling them.

The ^{1}H and ^{13}C NMR spectra were recorded either on a Bruker Avance III 500 or Bruker AV III 400 MHz NMR spectrometer using $CDCl_3$ or DMSO-d_6 as solvents. The melting points were measured in glass capillaries and are reported uncorrected. FT-IR spectra were recorded on a PerkinElmer Spectrum One Infrared Spectrometer (Model number- 73465) in KBr diluted discs within the 4000–400 cm^{-1} frequency range. Elemental analyses were performed on a Thermo Finnigan (FLASH EA 1112) microanalyzer. ESI-MS measurements were performed on a Bruker Maxis Impact electrospray mass spectrometer. An Agilent 7890A GC system with an FID detector and a J & amp; WDB-1 column (10 m, 0.1 mm ID) was used to conduct GC-MS analysis., The catalytic product yields of the optimized reactions were determined for one of the starting materials. The UV-NIR-3600 spectrophotometer, Shimadzu was used for the UV-visible studies. Powder X-ray diffractions were recorded on a Rigaku SmartLab powder X-ray diffractometer using Cu-Kα radiation (λ= 1.54190 Å). The molecular structure of complexes **Ru1** and **Ru2** were determined using Mo-Kα radiation (λ = 0.71073 Å) Bruker D8 QUEST diffractometer.[1-4]

Procedure for preparation of formic acid: sodium formate buffer (HCOOH/HCOONa) aqueous solutions of various pH values.

Formic acid (98%, wt), sodium formate, and water were mixed in a conical flask to prepare the solutions with various pH values required to perform the reactions in Scheme 2. At 25 °C, the pH values were measured using a pH meter.

pH 3.5: 6.8 g of sodium formate (10 mmol), 3.7 mL of formic acid (98-100% by wt, 10 mmol), and 96 mL of water were mixed to attain pH 3.5 HCOONa and HCOOH buffer.

Using this all-other pH solutions have been prepared.

Table S1. Experiments for TON and TOF

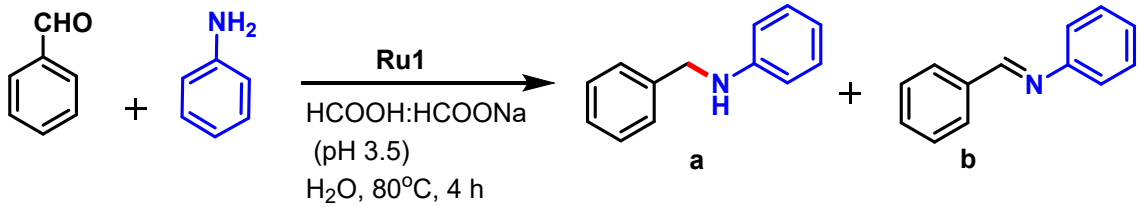

An oven-dried round bottom flask containing a stir bar was charged with benzaldehyde (5.0 mmol), aniline (5.0 mmol), and water (10 mL), and stirred under an ambient atmosphere for 5 minutes**. Ru1** (0.0001 mol% or 0.005 mol%) solution and buffer solution (HCOOH:HCOONa, pH 3.5, 15 mL) were added to the reaction mixture. The resulting reaction mixture was stirred at 80 °C for 4 h. After completion, the reaction mixture was extracted with ethyl acetate, dried over sodium sulfate, and analyzed by GC-MS (Figure S93-S95).

Entry	Catalyst (mol%)	Yield (%)		Conversion (%)	TON	TOF (h^{-1})
		a	b			
1	0.05	96	3	100	1920	480
2	0.005	79	14	100	15800	3950
3	0.001	73	26	>99	67000	16750
4	0.0001	43	56	>99	430000	107500

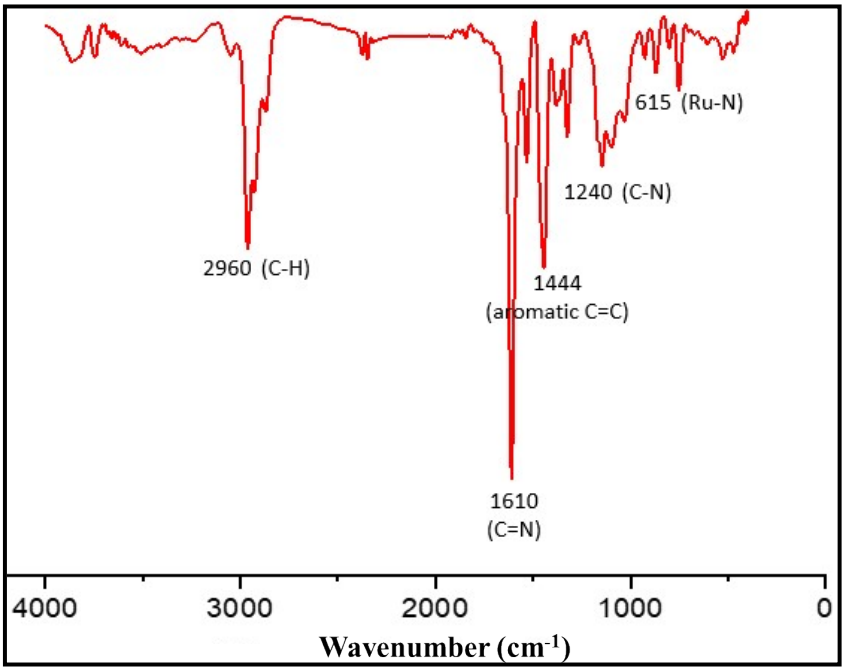

Figure S1. FT-IR spectrum of complex **Ru1**(as KBr diluted disk).

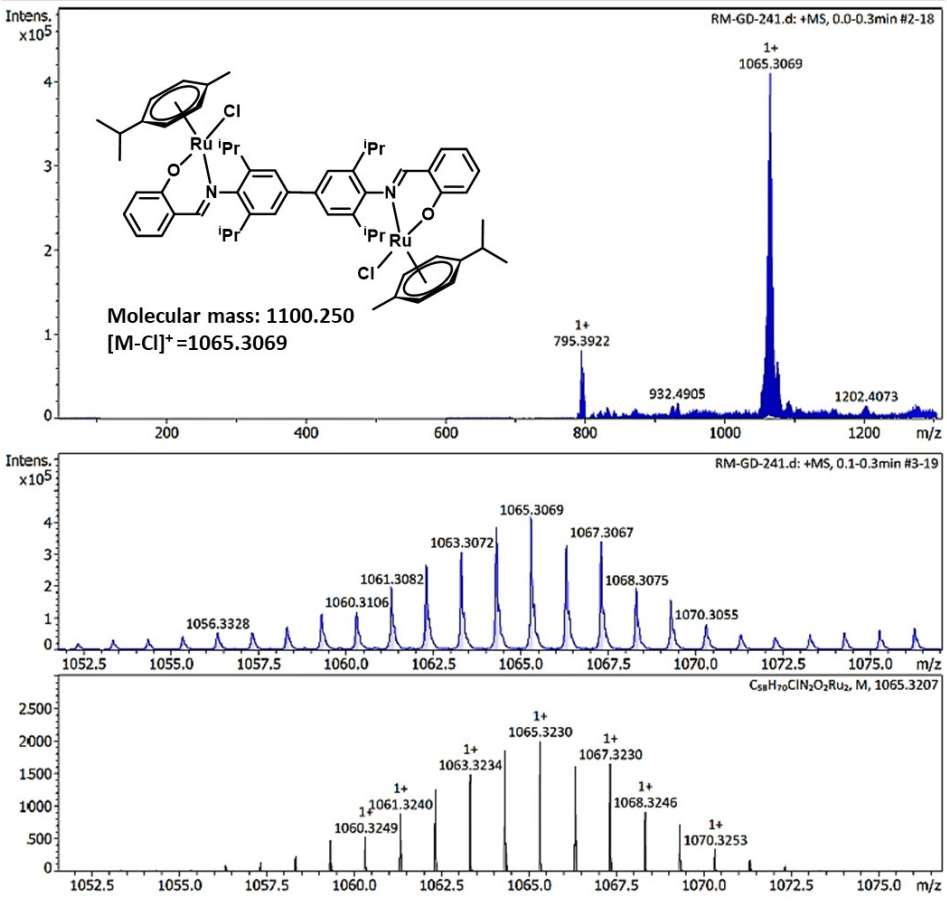

Figure S2. ESI-MS spectrum of complex **Ru1** in methanol showing experimental and simulated pattern for $[M-Cl]^+$ ion at *m/z* 1065.3069.

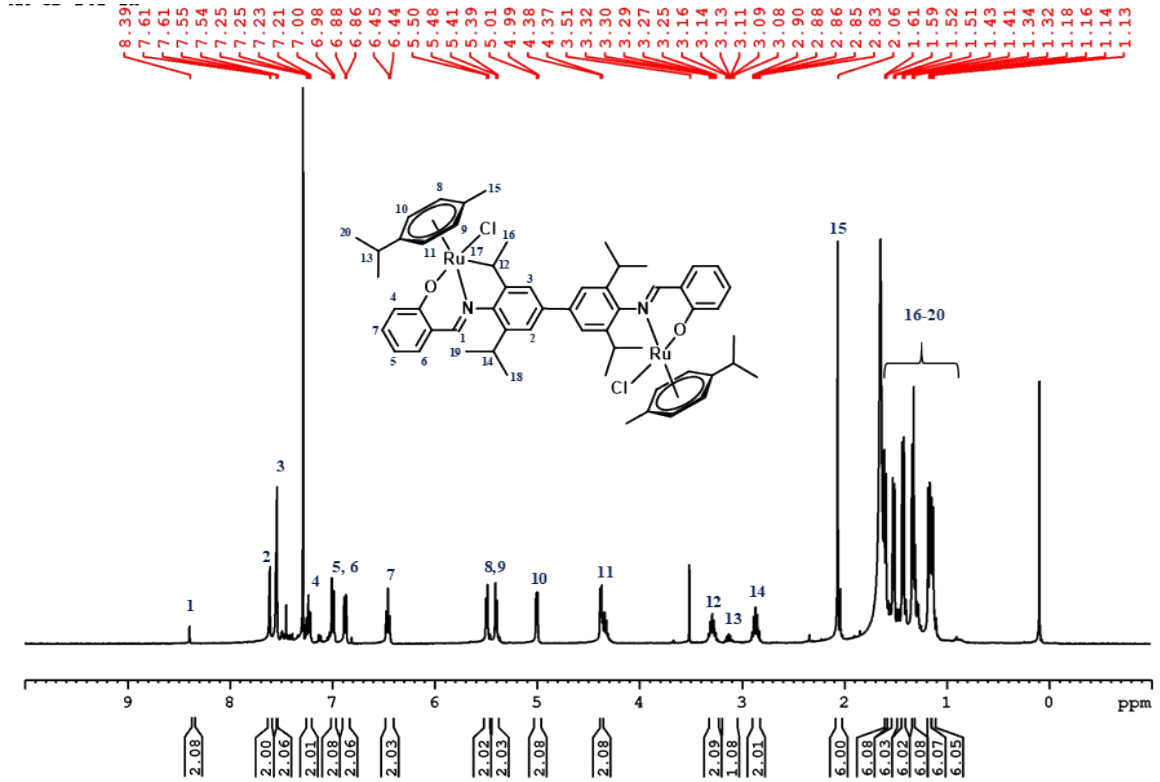

Figure S3. ^{1}H NMR spectrum of complex **Ru1** in $CDCl_3$ (400 MHz).

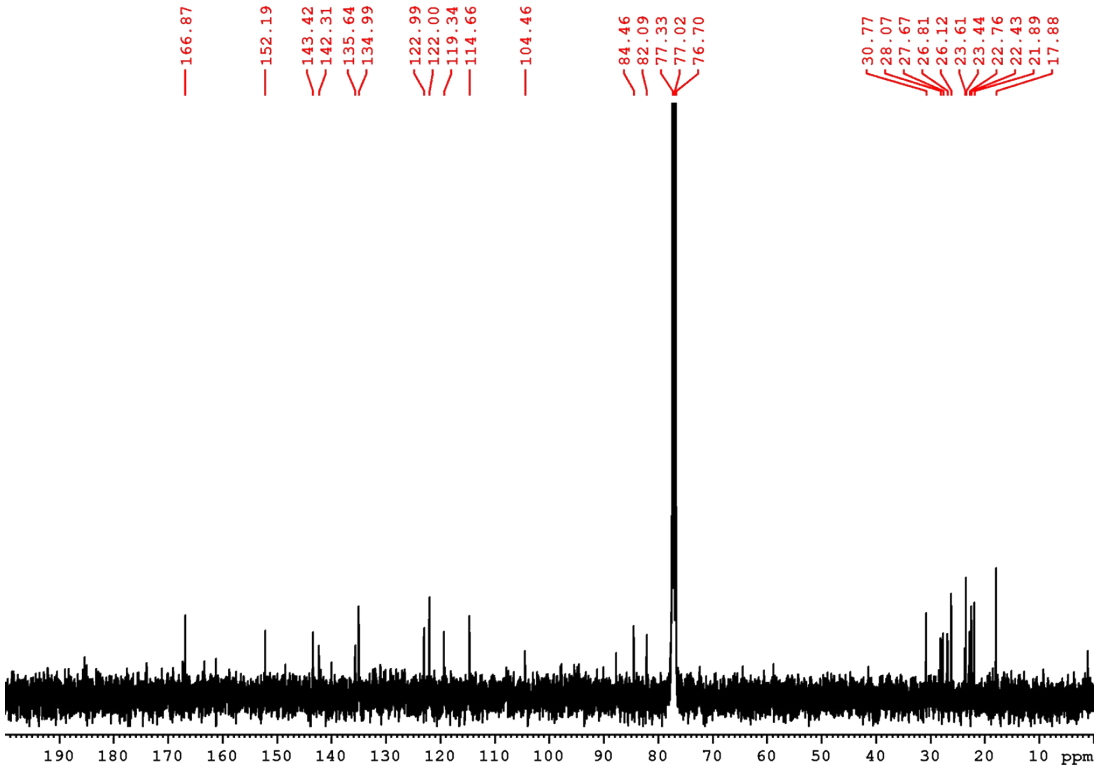

Figure S4. ^{13}C NMR spectrum of complex **Ru1** in $CDCl_3$ (100 MHz).

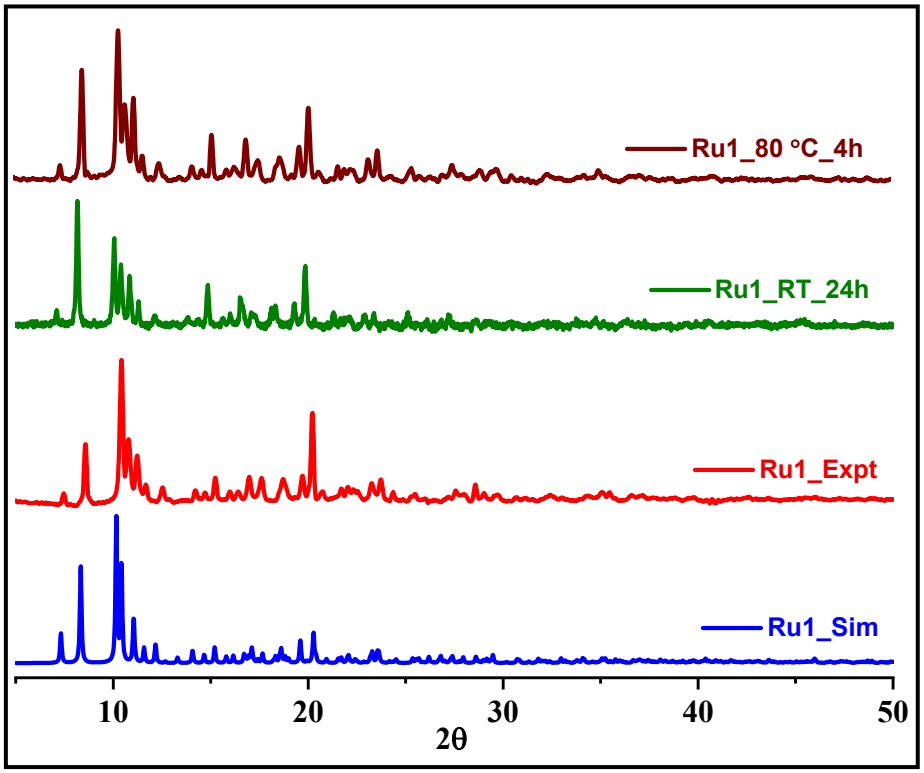

Figure S5. Powder X-ray diffraction pattern of complex **Ru1**. **Ru1_Expt** corresponding to assynthesed sample. **Ru1_RT_24h** corresponding to sample soaked in water for 24 hours. **Ru1_80 °C_4h** corresponding to sample soaked in water and heated at 80 °C for 4 hours.

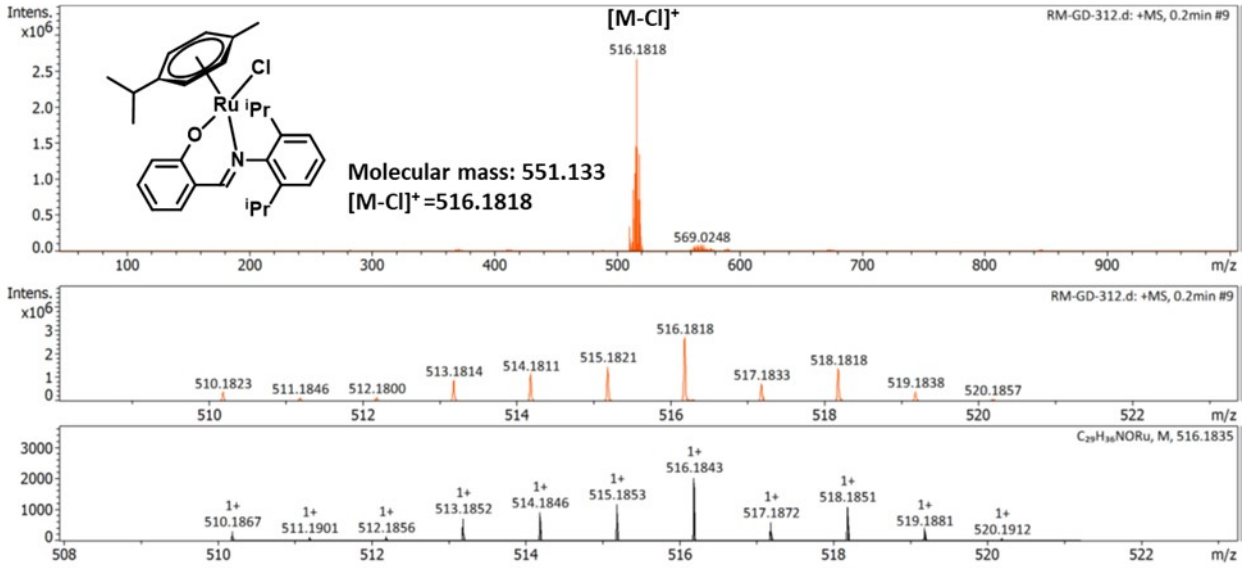

Figure S6. ESI-MS spectrum of complex **Ru2** in methanol showing experimental and simulated pattern for $[M\text{-}Cl]^+$ ion at *m/z* 516.1818.

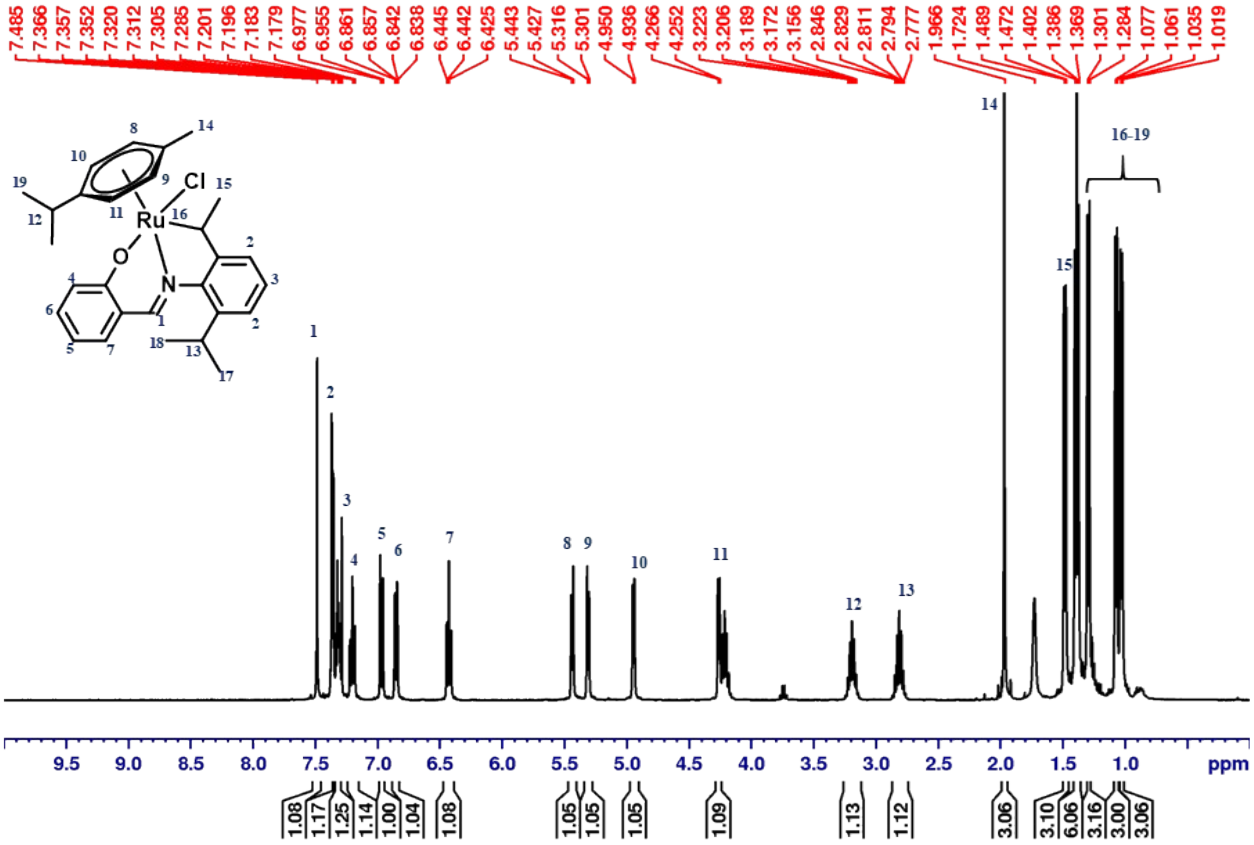

Figure S7. ^{1}H NMR spectrum of complex **Ru2** in $CDCl_3$ (400 MHz).

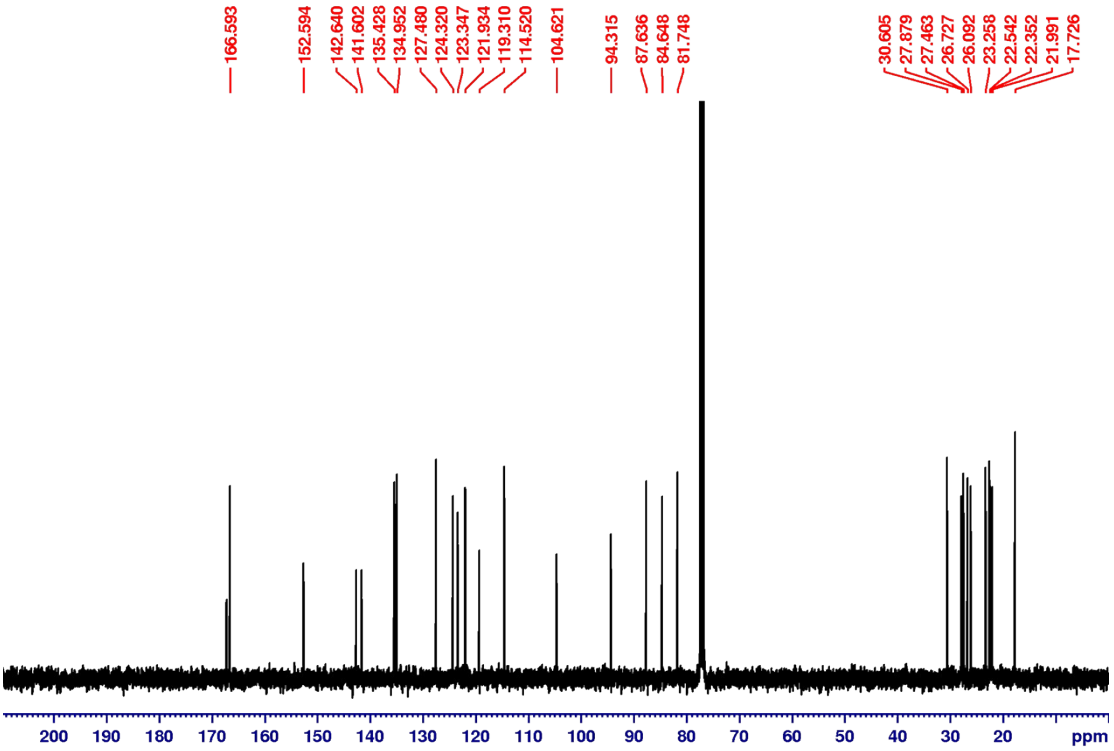

Figure S8. ^{13}C NMR spectrum of complex **Ru2** in $CDCl_3$ (100 MHz).

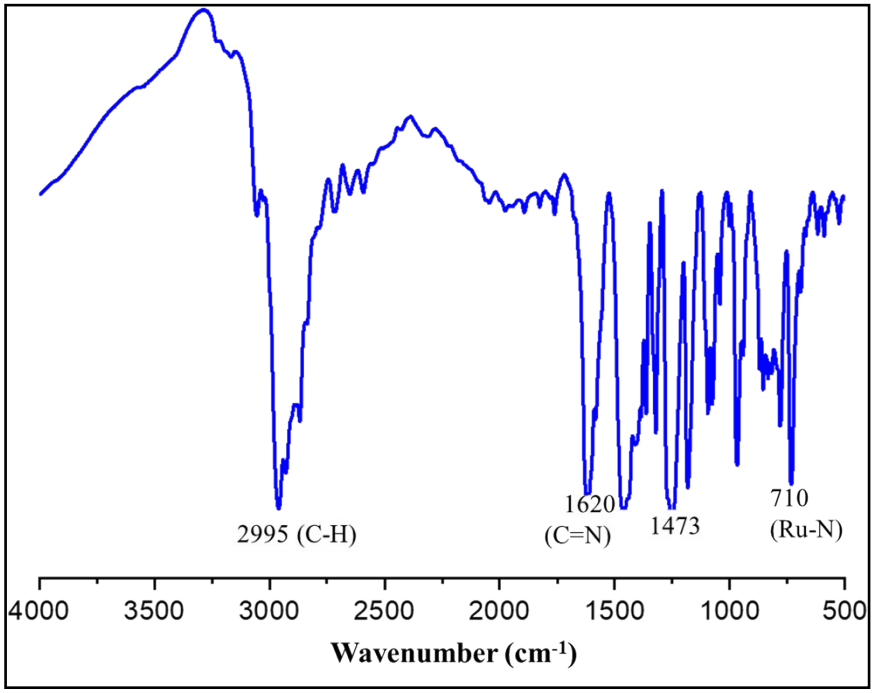

Figure S9. FT-IR spectrum of complex **Ru2** (as KBr diluted disk).

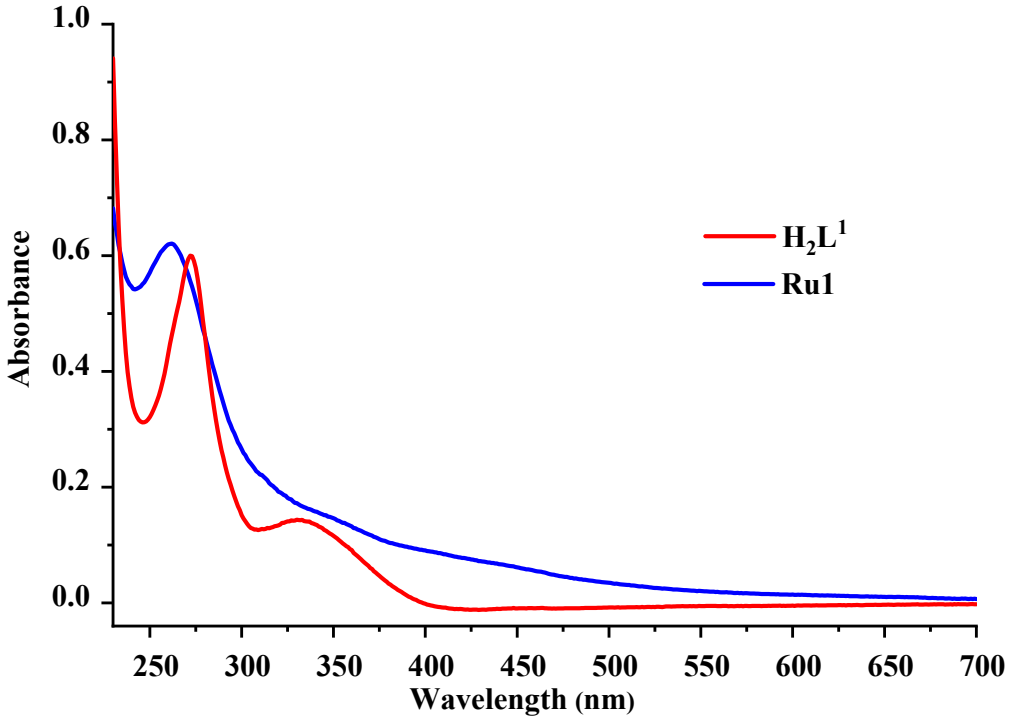

Figure S10. UV–vis spectra of the complex **Ru1** and $\mathbf{H_2L^1}$ ligand in DCM [λ_{max} (nm), ε(× 10^5 M^{-1} cm^{-1})) **Ru1**(4.52 mM); 226 (1.6), 266 (1.3), $\mathbf{H_2L^1}$(7.33 mM); 230 (1.2), 272 (0.8), 332(0.2)].

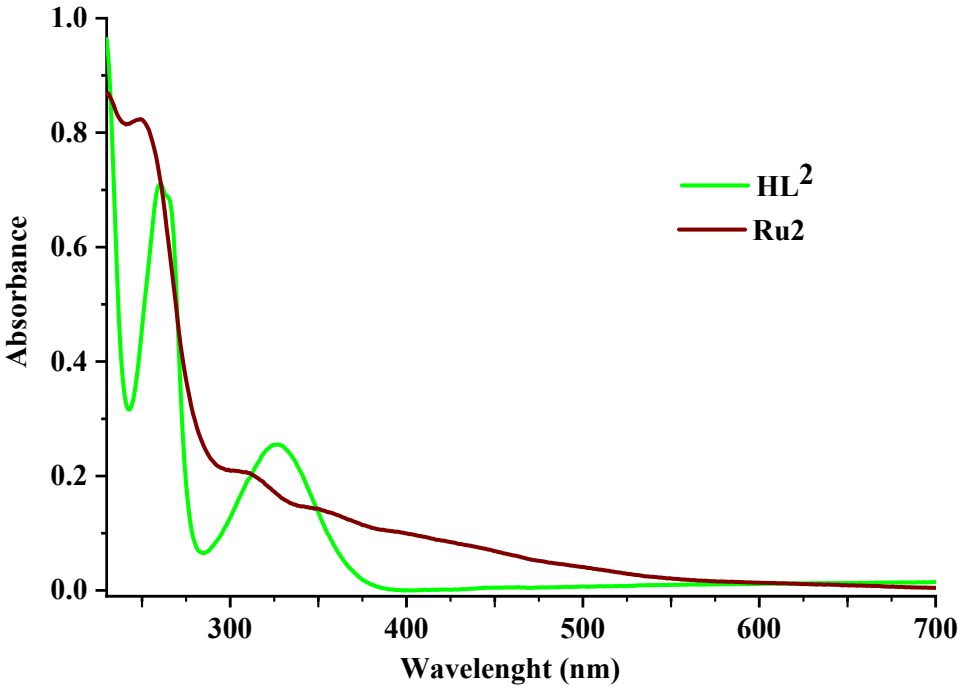

Figure S11. UV–vis spectra of the complex **Ru2** and **HL²** ligand in DCM [λ_{max} (nm), ε(× 10^5 M^{-1} cm^{-1})) **Ru2** (12.00 mM); 230 (0.7), 261 (0.6), **HL²** (18.40 mM); 230 (0.5), 260 (0.4), 327(0.2)].

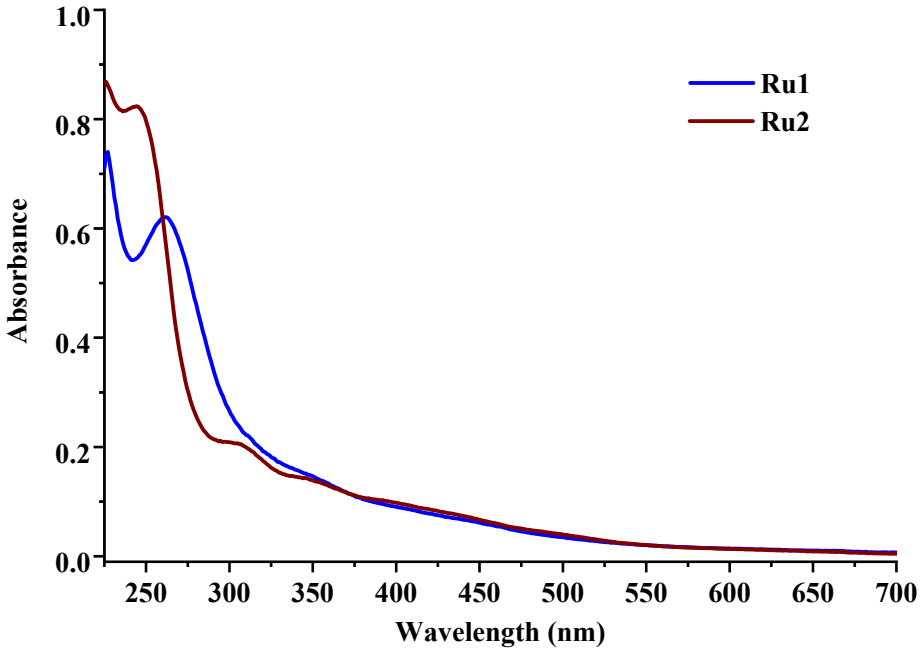

Figure S12. UV–vis spectra of the complex **Ru1** and **Ru2** in DCM [λ_{max} (nm), ε(× 10^5 M^{-1} cm^{-1})) **Ru1** (4.52 mM); 226 (1.6), 266 (1.3), **Ru2** (12.00 mM); 230 (0.7), 261 (0.6)].

Detection of intermediates II and III by ESI-MS

Ru1 (0.01 mmol) was mixed with 2.0 mL of water along with 3.0 mL of buffer (HCOOH:HCOONa, pH 3.5), and heated at 60 °C in the round bottom flask. Once the reaction started, an aliquot was taken at an interval of every five muinutes and analyzed by mass

spectrometry. The Ru-formato species **II** was identified at *m/z* 1121.29 after ten minutes 32 (Figure S15); this species immediately changed into Ru-hydride species **III**, which was also detected in mass spectrometry at *m/z* 1033.32 (Figure S14). A prominent change in color in the reaction mixture was observed that occurred once the species converted to Ru-hydride from Ru-formato intermediate.

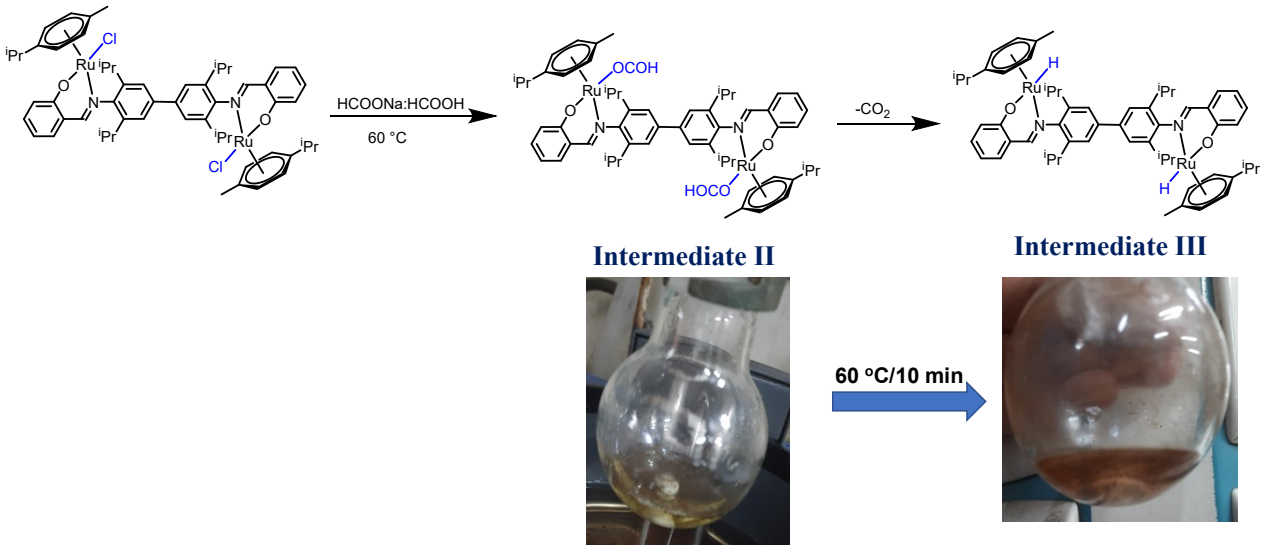

Figure S13. Catalytic intermediate for RA (picture showing the color change from pale yellow to brown during reaction).

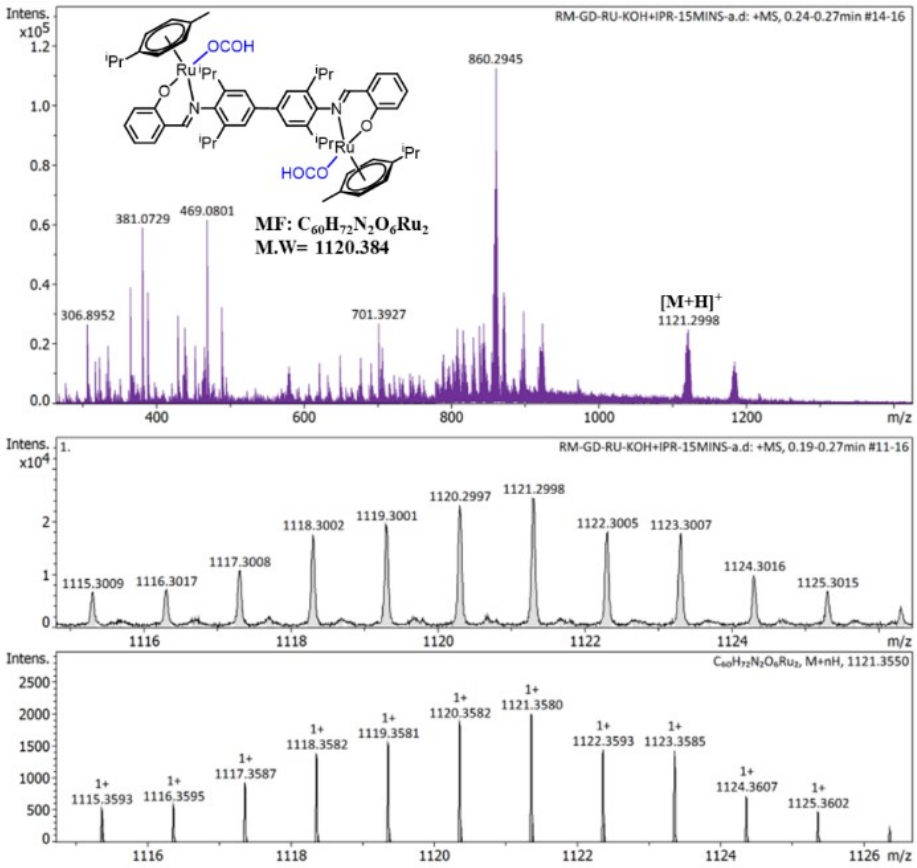

Figure S14. ESI-MS spectrum of intermediate **II** in methanol showing experimental and simulated pattern for $[M+H]^+$ ion at *m/z* 1121.2998.

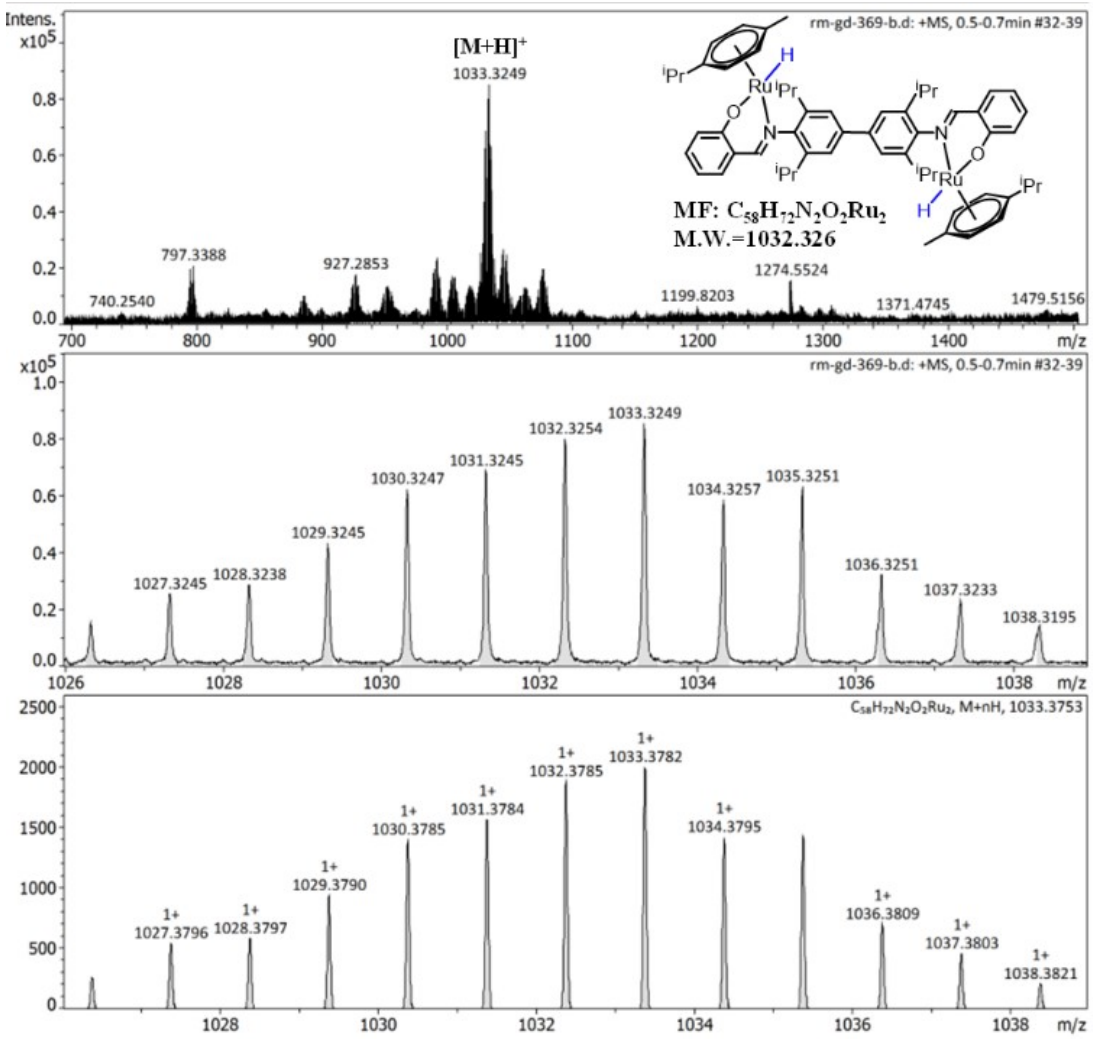

Figure S15. ESI-MS spectrum of intermediate **III** in methanol showing experimental and simulated pattern for $[M+H]^+$ ion at *m/z* 1033.3249.

Table S2. Comparison of reaction parameter with selected complexes for reductive amination reaction

Sr. No.	Catalyst	mol%	Additives	Solvent	Time (h)/ Temp. (°C)	Yield (%)	TON	TOF (h^{-1})	Refernce
1	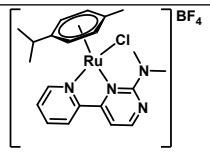	1.5	-	^{i}PrOH	6/90	60	40	7	S5
2	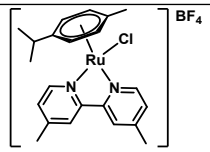	0.5	HCOOH:HCOONa (pH 4.4)	H_2O: Toluene	4 / 80	63	126	32	S6
3	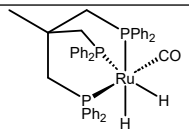	2	AcOH, H_2 30 bar	MeOH	4 / 80	87	44	22	S7
4	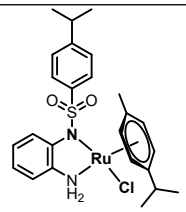	1	HCOOH:HCOONa (pH 4.8)	H_2O	1/80	53	53	27	S8
5	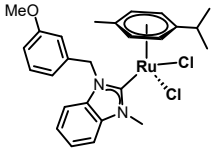	1	$PhSiH_3$, 4 Å molecular sieves	Ethanol	0.5/30	97	97	194	S9
6	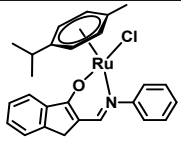	0.1	HCOOH:HCOONa (pH 4.8) or H_2 3 bar	H_2O or MeOH: H_2O	5/60	92	920	184	S10
7	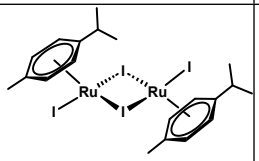	0.05	tris(*p*-chlorophenyl) phosphine , 50 bar CO/ KI	THF	20/160	77	1540	77	S11
8	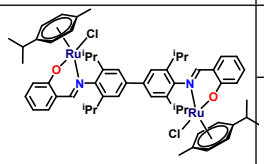	0.05	HCOOH:HCOONa (pH 3.5)	H_2O	4/80	96	1920	480	**Present Work**
		0.0001				43	430000	107500	

Table S3. Comparison of green metrics with selected complexes for reductive amination reaction.

Sr. No.	Catalyst	Atom economy (%)	Atom efficiency (%)	Reaction mass efficiency (%)	Reference
1	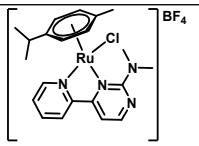	91.97	55.18	55.27	S5
2	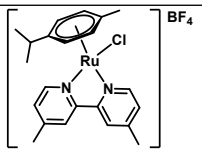		57.94	57.93	S6
3	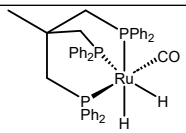		79.98	80.42	S7
4	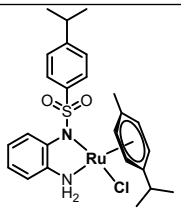		57.62	48.64	S8
5	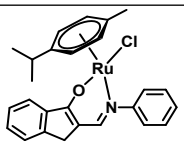		84.72	84.67	S10
6	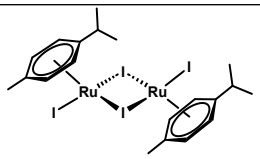		70.07	70.82	S11
7	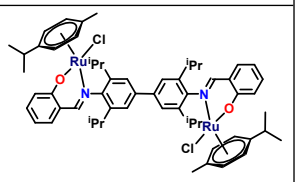		**89.21**	**89.69**	**Present Work**

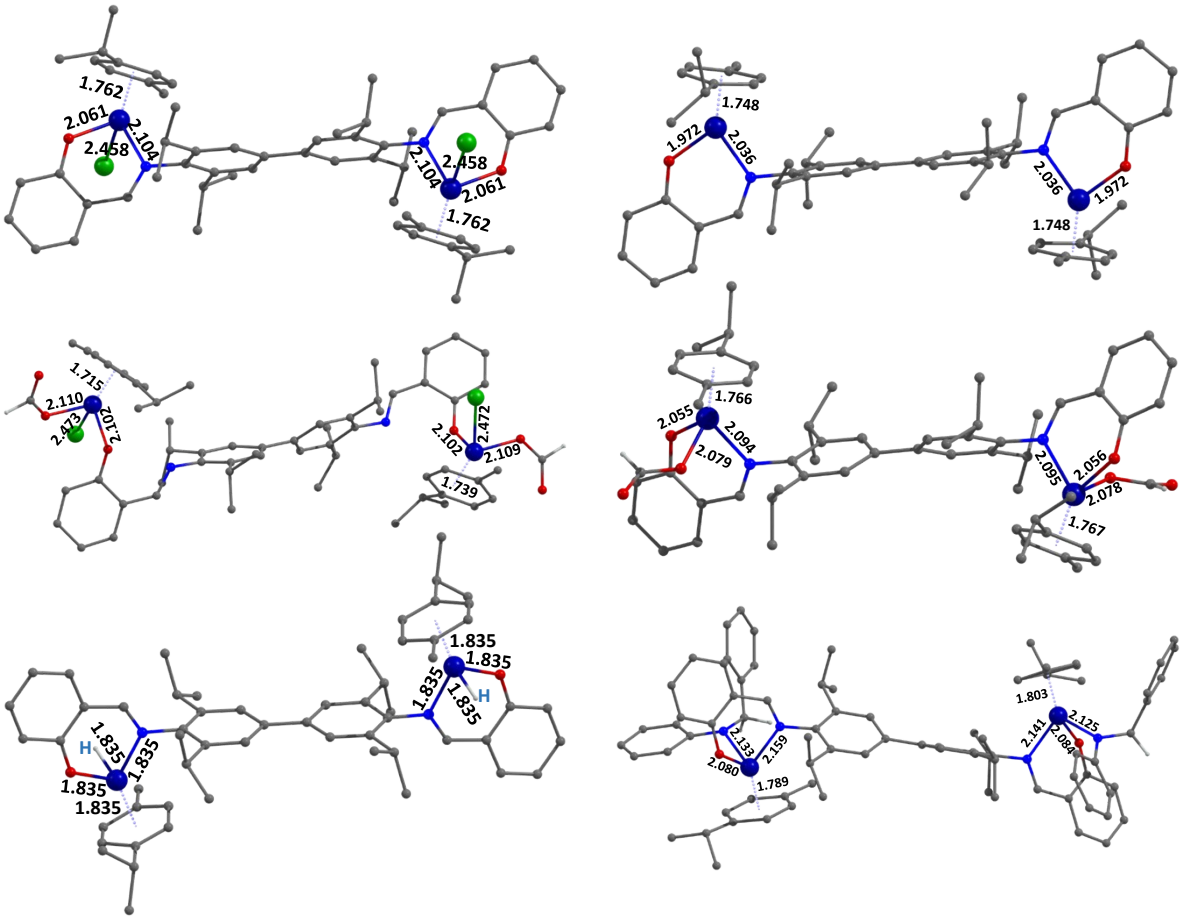

Figure S16. The DFT optimized geometry and structural parameters for bimetallic study for both active sides.

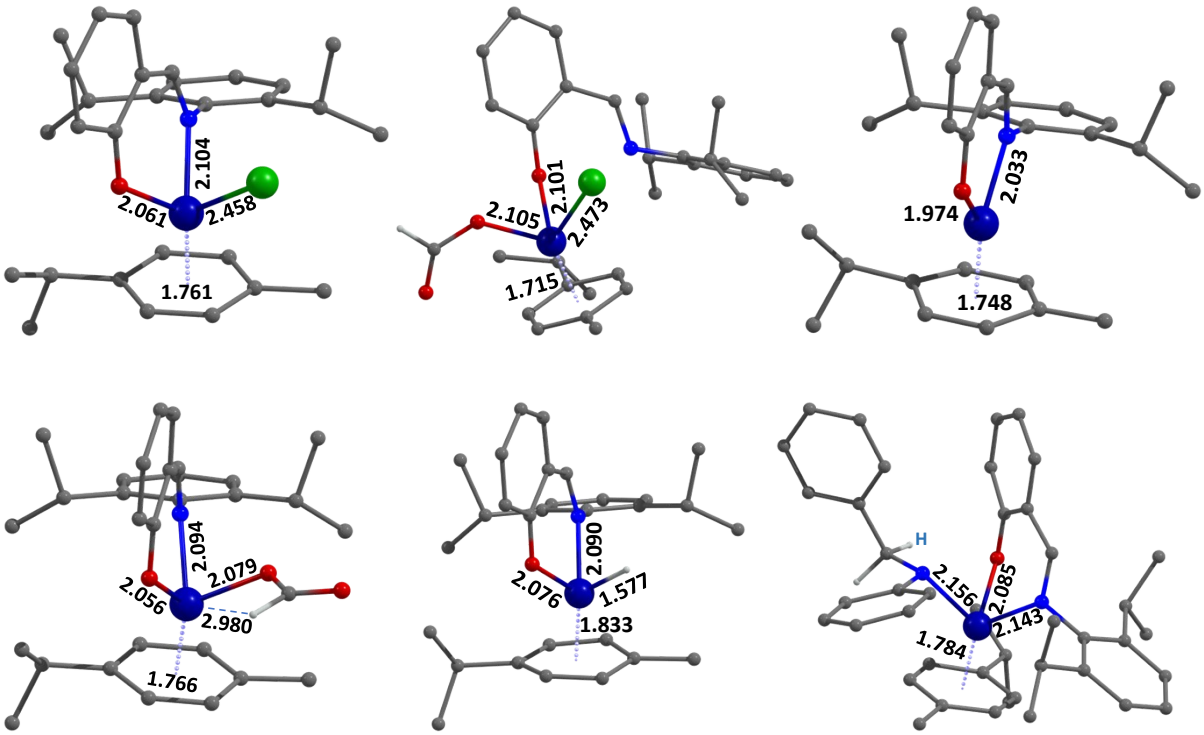

Figure S17. The DFT optimized geometry and structural parameters for monometallic study.

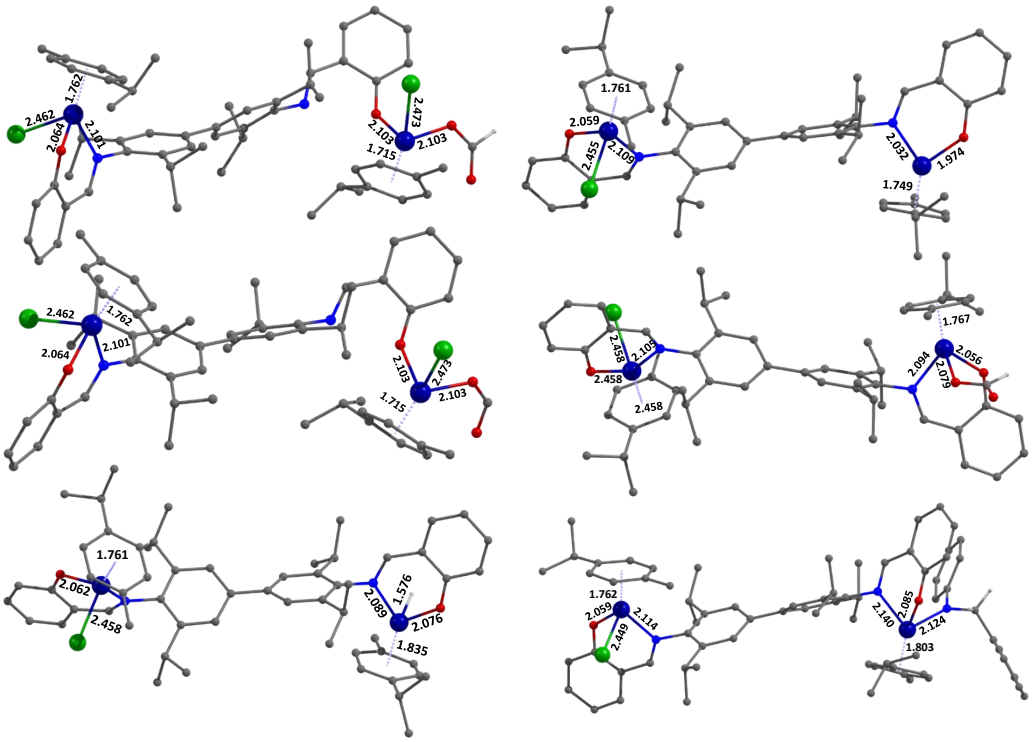

Figure S18. The DFT optimized geometry and structural parameters for bimetallic study for one active side.

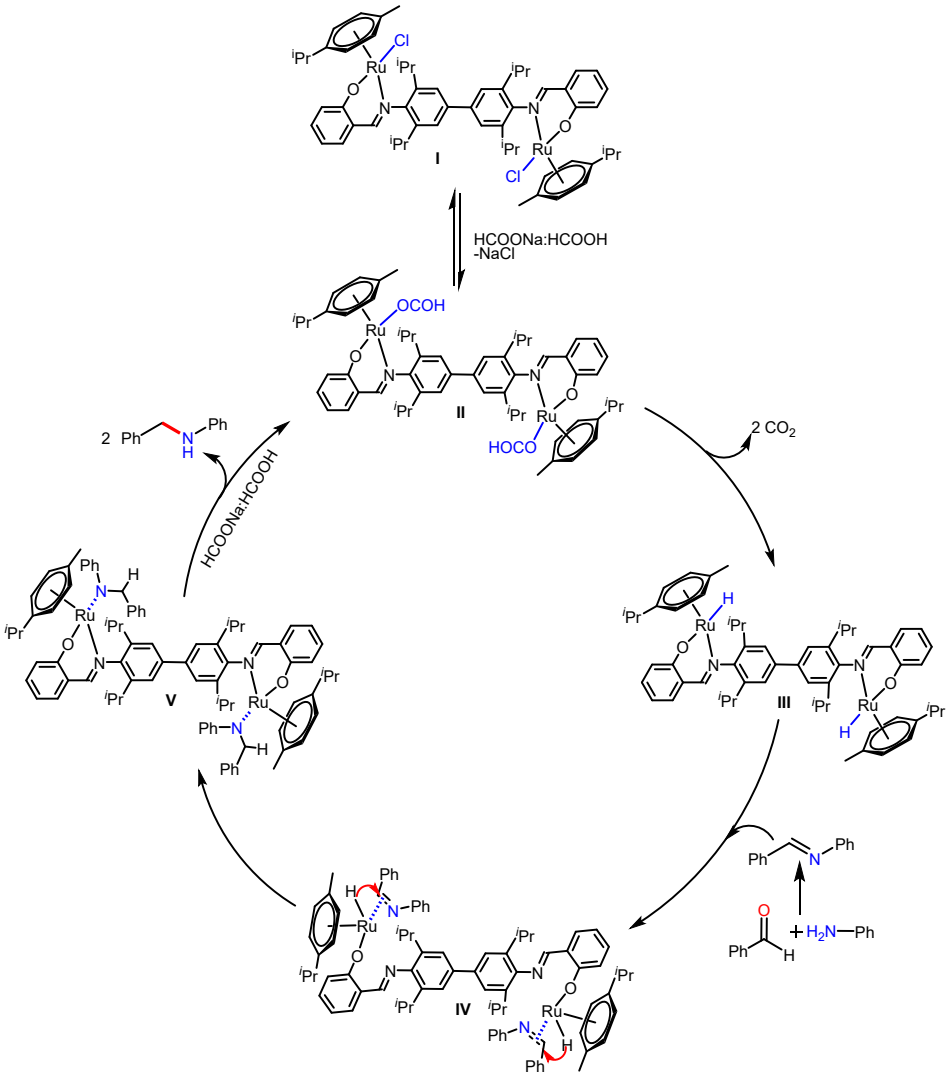

Scheme S1. Proposed a mechanism for reductive amination with **Ru1** catalyst.

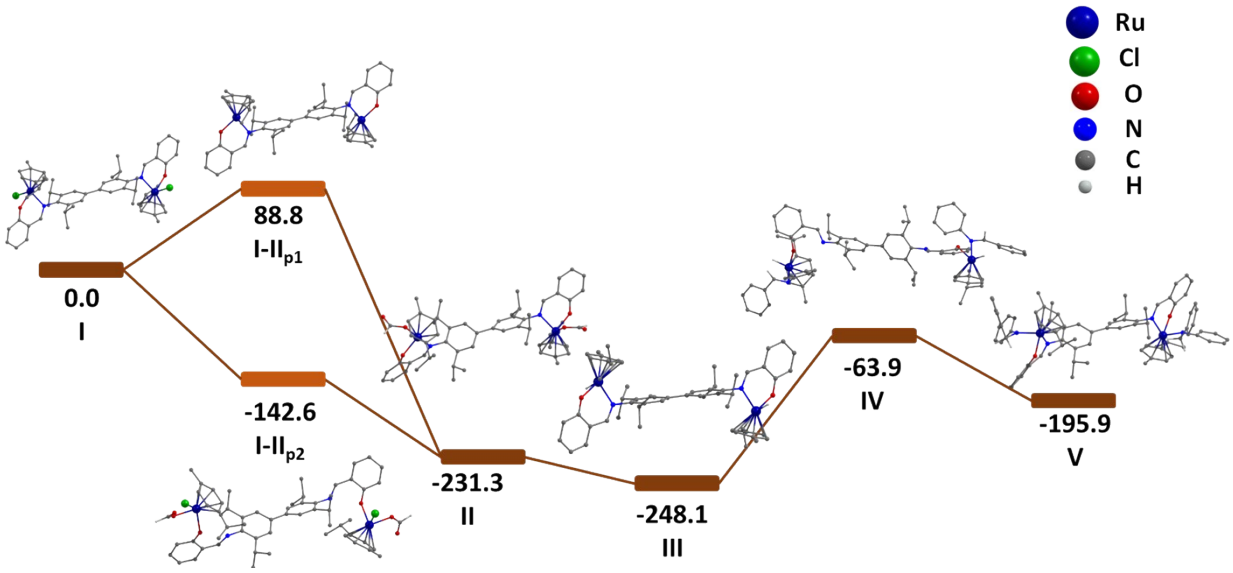

Figure S19: DFT-computed potential energy diagram (kJ/mol) of the reductive amination for the bimetallic study.

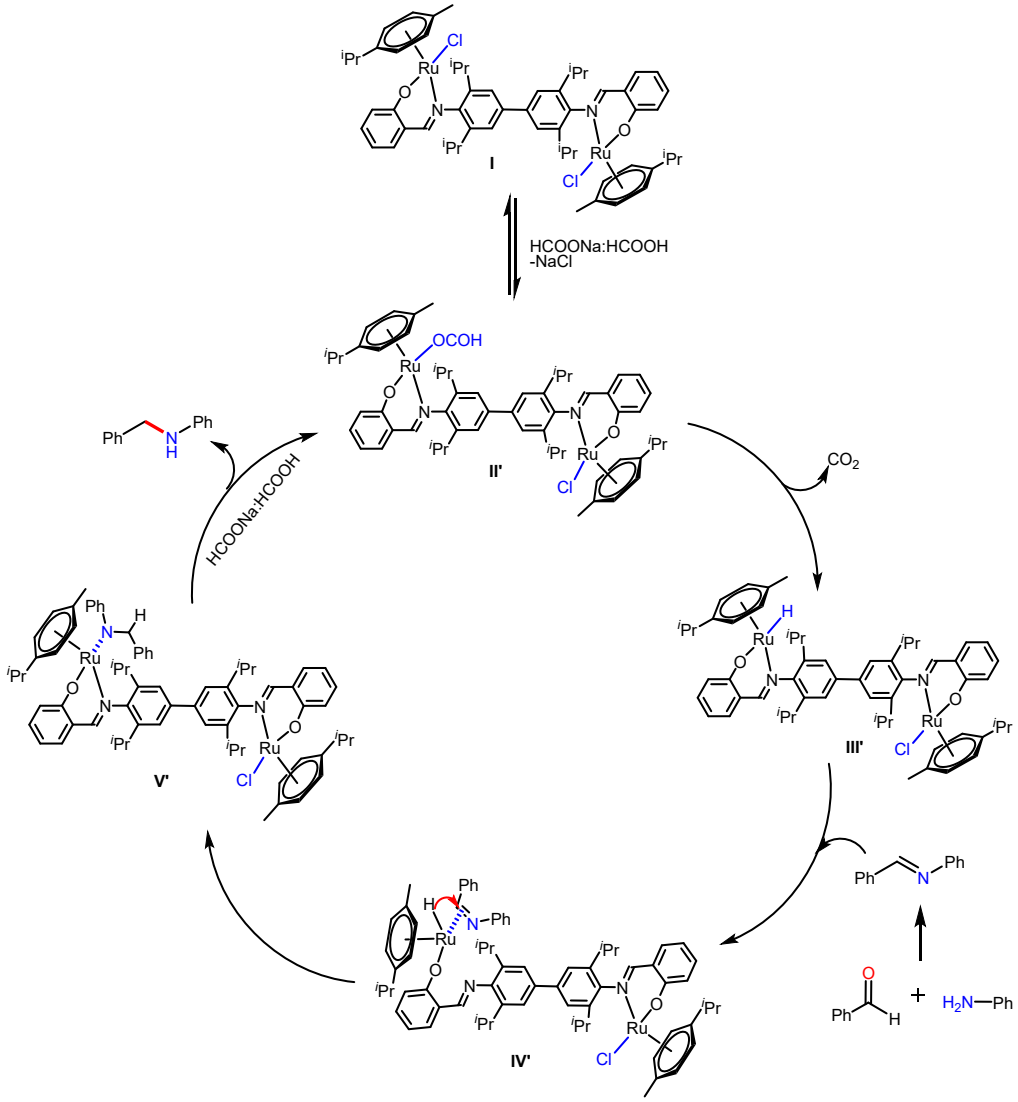

Scheme S2. Proposed a mechanism for reductive amination with **Ru1** catalyst at one side of Ru center

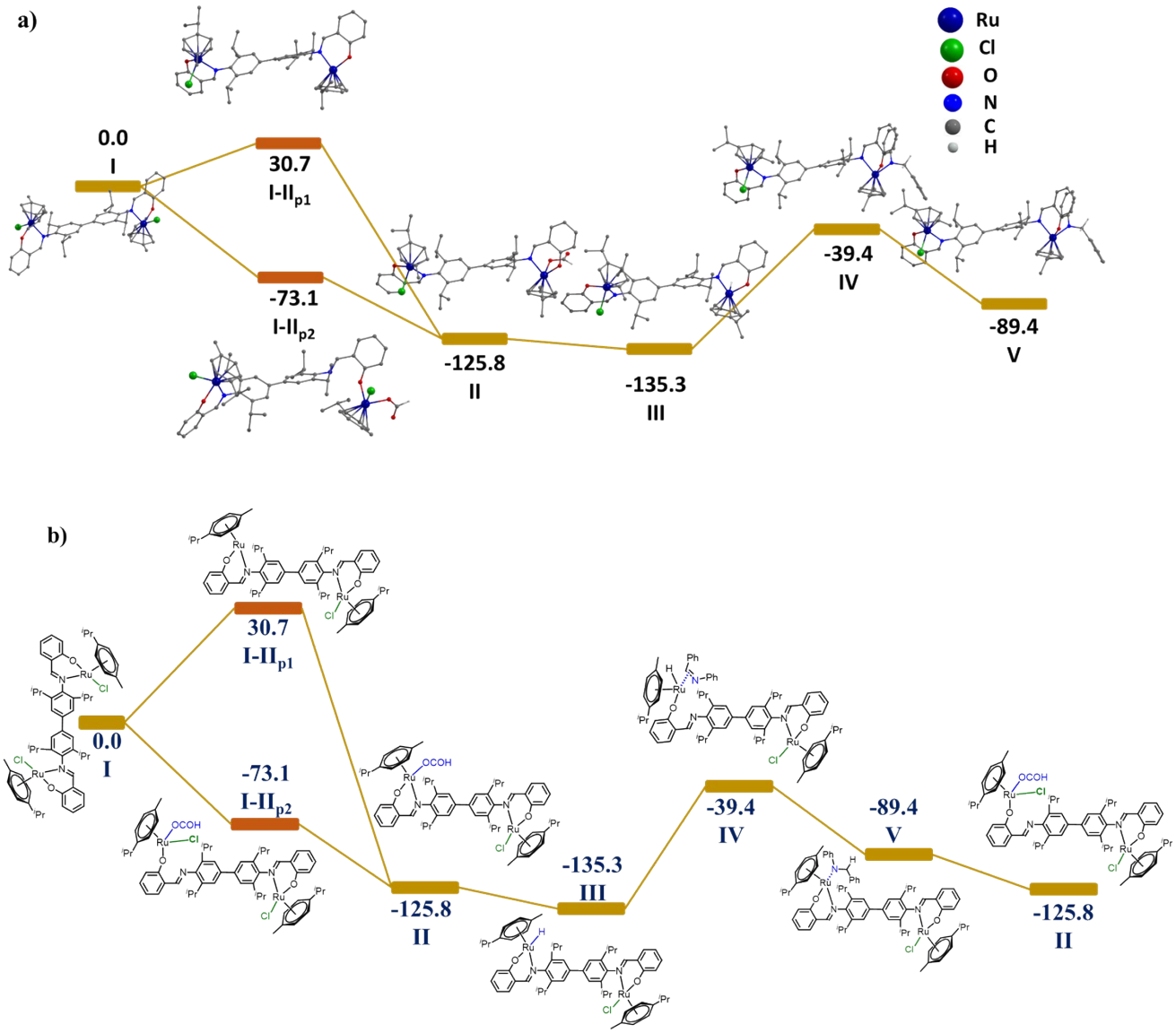

Figure S20: a) DFT-computed potential energy diagram (kJ/mol) of the reductive amination for the bimetallic study at one side of Ru center. (**b**) The corresponding Chemdraw energy profile.

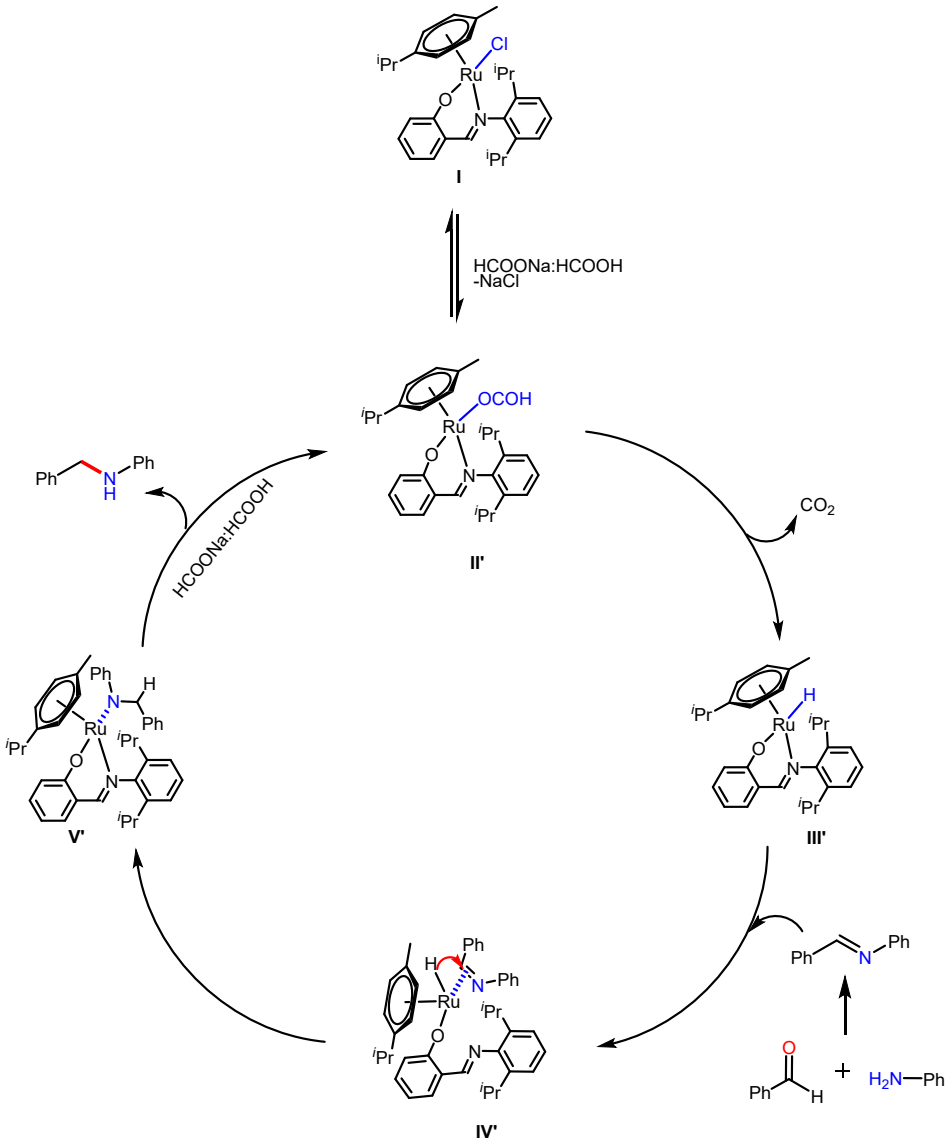

Scheme S3. Proposed a mechanism for reductive amination with **Ru2** catalyst.

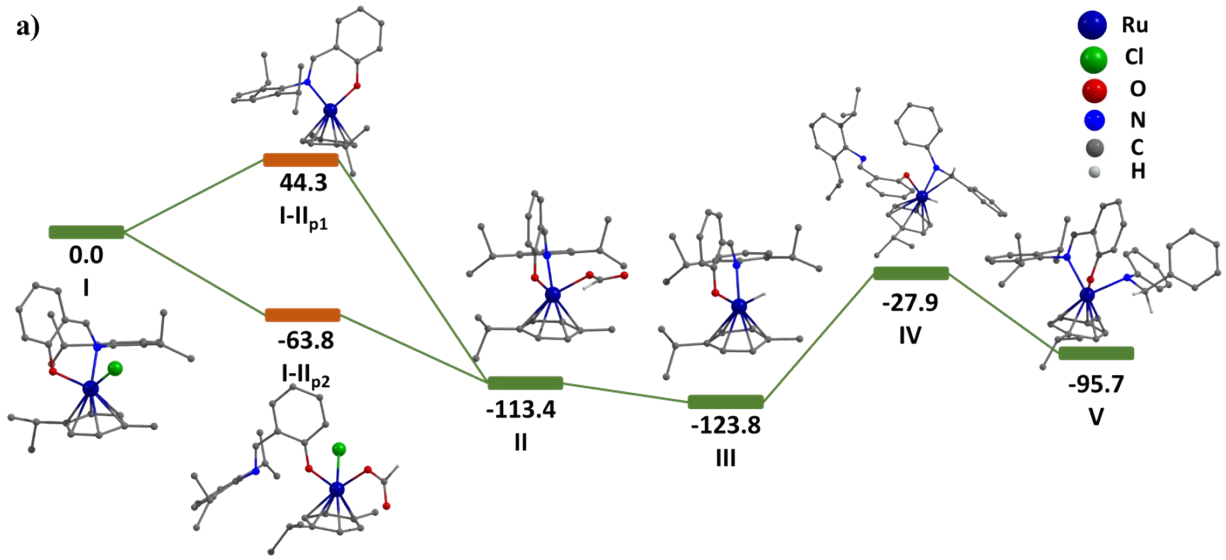

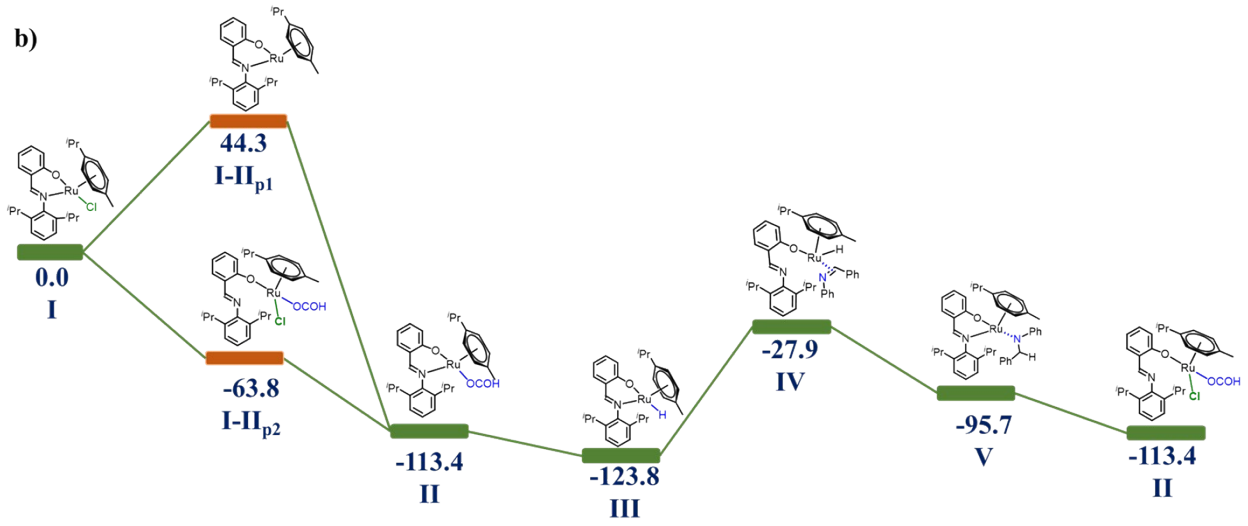

Figure S21: a) DFT-computed potential energy diagram (kJ/mol) of the reductive amination for the **Ru2** monometallic study. (**b**) The corresponding Chemdraw energy profile

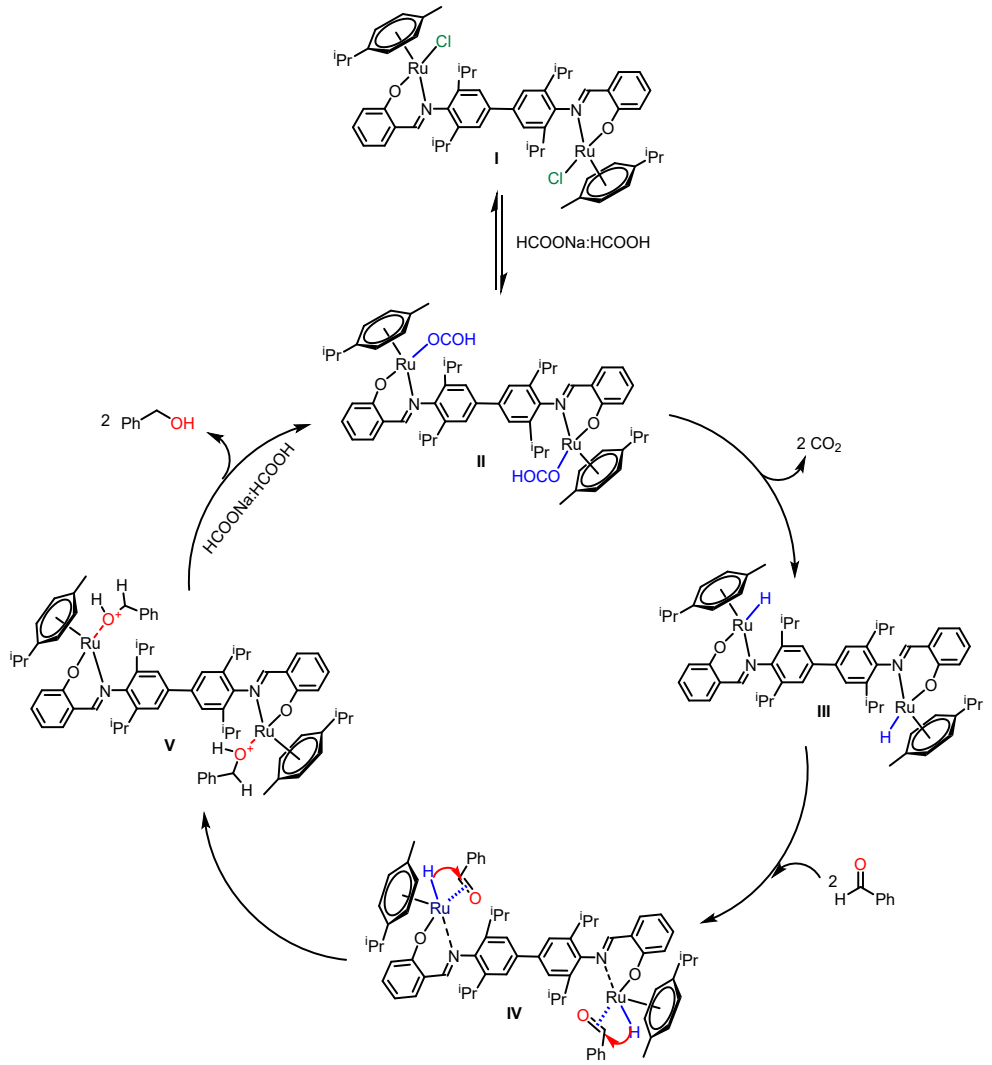

Scheme S4. Proposed a mechanism for alcohol formation with **Ru2** catalyst.

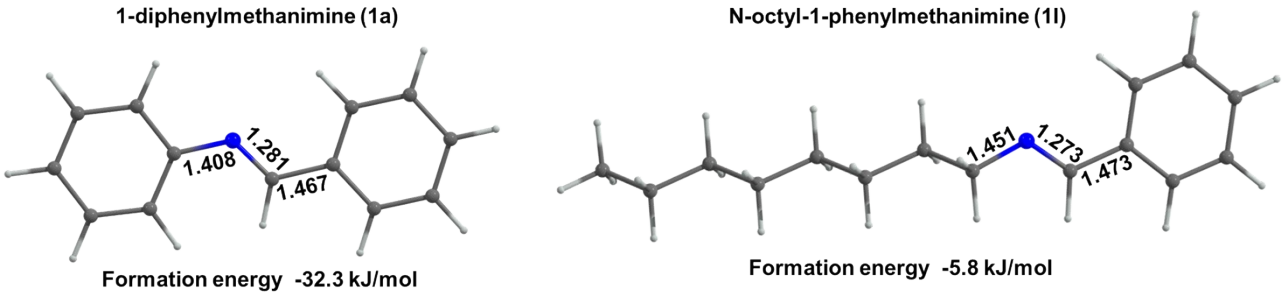

Figure S22 Optimized geometry of substrate **1a** and **1l** and their formation energies.

Table S4: Compression of the structural parameter optimized geometry with experiments

Ru1	**Experimental Data**	**Computational Data**
Ru(1)- Cl(1)	2.435	2.458
Ru(1)- O(1)	2.047	2.061
Ru(1)- N(1)	2.108	2.104
Ru(1) – *p*-cymene	1.680	1.762
∠O(1)-Ru(1)-Cl(1)	83.47	85.2
∠O(1)-Ru(1)-N(1)	86.81	86.7
∠N(1)-Ru(1)-Cl(1)	84.76	86.3
∠C(21)-C(21)-C(22)-C(23)	176.8	179.1
Ru2	**Experimental Data**	**Computational Data**
Ru(1)- Cl(1)	2.438	2.458
Ru(1)- O(1)	2.056	2.061
Ru(1)- N(1)	2.107	2.104
Ru(1) - *p*-cymene	1.680	1.761
∠O(1)-Ru(1)-Cl(1)	82.99	85.2
∠O(1)-Ru(1)-N(1)	87.60	86.6
∠N(1)-Ru(1)-Cl(1)	85.81	86.4

Table S5. Crystallographic details of complex **Ru1** and **Ru2.**

Compound	**Ru1**	**Ru2**
Identification code	RM_GD_241_0m	RM_GD_312
Empirical formula	$C_{63}H_{70}Cl_2N_2O_5Ru_2$	$C_{29}H_{36}ClNORu$
Formula weight	1208.35	551.11
Temperature/K	150.00	104.5(7)
Crystal system	triclinic	monoclinic
Space group	$P\bar{1}$	$P2_1/n$
a/Å	10.829(1)	11.3984(1)
b/Å	11.297(1)	12.3026(1)
c/Å	12.205(1)	18.3366(2)
α/°	82.474(4)	90
β/°	89.037(4)	99.3510(10)

γ/°	78.850(4)	90
Volume/Å^3	1452.3(3)	2537.17(4)
Z	1	4
ρ_{calc}g/cm^3	1.400	1.443
μ/mm^{-1}	0.662	0.745
F(000)	640.0	1144.0
Crystal size/mm^3	0.461 × 0.311 × 0.192	0.201 × 0.057 × 0.023
Radiation	MoKα (λ = 0.71073)	Mo Kα (λ = 0.71073)
2Θ range for data collection/°	5.08 to 50.28	4.502 to 50.038
Index ranges	-12 ≤ h ≤ 12, -13 ≤ k ≤ 13, -14 ≤ l ≤ 14	-13 ≤ h ≤ 13, -14 ≤ k ≤ 14, -21 ≤ l ≤ 21
Reflections collected	51543	44264
Independent reflections	5178 [R_{int} = 0.0486, R_{sigma} = 0.0238]	4454 [R_{int} = 0.0357, R_{sigma} = 0.0150]
Data/restraints/parameters	5178/6/322	4454/0/305
Goodness-of-fit on F^2	1.119	1.033
Final R indexes [I>=2σ (I)]	R_1 = 0.0555, wR_2 = 0.1455	R_1 = 0.0212, wR_2 = 0.0542
Final R indexes [all data]	R_1 = 0.0635, wR_2 = 0.1523	R_1 = 0.0221, wR_2 = 0.0549
Largest diff. peak/hole / e Å^{-3}	1.55/-0.7	0.45/-0.43

Table S6. Selected bond distances (Å) and angles (º) in compound **Ru1.**

Ru(1)-Cl(1)	2.439(1)	O(1)- Ru(1)- Cl(1)	83.5(1)
Ru(1)-O(1)	2.051(3)	O(1)- Ru(1)- N(1)	86.8 (1)
Ru(1)-N(1)	2.114(4)	N(1)- Ru(1)- Cl(1)	84.8(1)
Ru(1)- C(20)	2.204(5	C(1)- O(1)- Ru(1)	127.7(3)
Ru(1)- C(21)	2.176(5)	C(7)-N(1)- Ru(1)	124.3(3)
Ru(1)- C(22)	2.189(5)	C(7)-N(1)-(C8)	116.5(4)
Ru(1)- C(23)	2.201(5)	C(8)-N(1)- Ru(1)	119.0(3)
Ru(1)- C(24)	2.203(5)		
Ru(1)- C(25)	2.189 (5)		
N(1)- C(7)	1.291(6)		
N(1)- C(8)	1.453(6)		

Table S7. Selected bond distances (Å) and angles (º) in compound **Ru2.**

Ru(1)-Cl(1)	2.4385(4)	O(1)- Ru(1)- Cl(1)	82.99(4)
Ru(1)-O(1)	2.057(1)	O(1)- Ru(1)- N(1)	87.60(5)
Ru(1)-N(1)	2.107(2)	N(1)- Ru(1)- Cl(1)	85.81(4)
Ru(1)- C(20)	2.21(2)	C(1)- O(1)- Ru(1)	126.94(1)
Ru(1)- C(21)	2.202(2)	C(7)-N(1)- Ru(1)	123.63(1)
Ru(1)- C(22)	2.214(2)	C(7)-N(1)-(C8)	116.83(2)
Ru(1)- C(23)	2.194(2)	C(8)-N(1)- Ru(1)	119.42(1)
Ru(1)- C(24)	2.185(2)		
Ru(1)- C(25)	2.175(2)		
N(1)- C(7)	1.296(2)		
N(1)- C(8)	1.296(2)		

Calculation of green metrics for reductive amination optimized substrate

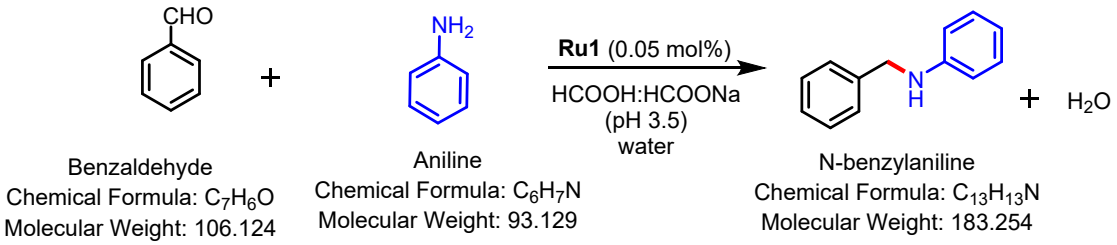

Benzaldehyde
Chemical Formula: C_7H_6O
Molecular Weight: 106.124

Aniline
Chemical Formula: C_6H_7N
Molecular Weight: 93.129

N-benzylaniline
Chemical Formula: $C_{13}H_{13}N$
Molecular Weight: 183.254

Total = 106.124 + 93.129 = 199.253

Product yield = 97% (178.5 mg)

Reactant 1	Benzaldehyde	106 mg	Formula wt. 106.124
Reactant 1	Aniline	93 mg	F.W. 93.129
Additives	HCOONa:HCOOH	3 mL	F.W. 105.01
Solvent	Water	2 mL	F.W. 18.01
Products	N-benzylaniline	178.5	F.W. 183.254
By products	Water	-	F.W. 18.01

Atom economy = Reactant total molecular weight / Product molecular weight

= 183.254 / 199.253 = 91.97 %

Atom efficiency = Product yield × (atom economy/ 100)

= 97 × (91.97/100) = 89.21%

Carbon efficiency = No. C in product / no. total **C** in reactant = 100%

Reaction mass efficiency = Product experimental weight / total weight of reactant used

= 178.5 mg / (106 + 93) × 100 = 89.69%

Calculation of green metrics for gram scale reaction

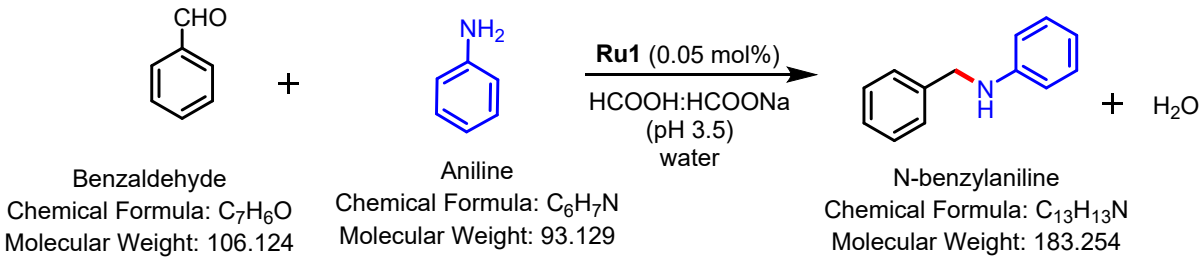

Benzaldehyde
Chemical Formula: C_7H_6O
Molecular Weight: 106.124

Aniline
Chemical Formula: C_6H_7N
Molecular Weight: 93.129

N-benzylaniline
Chemical Formula: $C_{13}H_{13}N$
Molecular Weight: 183.254

Total = 106.124 + 93.129 = 199.253

Product yield = 89% (3.2 g)

Reactant 1	Benzaldehyde	2.1 g	Formula wt. 106.124
Reactant 1	Aniline	1.8 mg	F.W. 93.129
Additives	HCOONa:HCOOH	25 mL	F.W. 105.01
Solvent	Water	15 mL	F.W. 18.01
Products	N-benzylaniline	3.2 g	F.W. 183.254
By products	Water	-	F.W. 18.01

Atom economy = Reactant total molecular weight / Product molecular weight

= 183.254 / 199.253 = 91.97 %

Atom efficiency = Product yield × (atom economy/ 100)

= 89 × (91.97/100) = 81.85%

Carbon efficiency = No. C in product / no. total **C** in reactant = 100%

Reaction mass efficiency = Product experimental weight / total weight of reactant used

= 3.2 g / (2.1g + 1.8g) × 100 = 82.05%

NMR data for secondary amines product:

1.

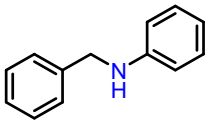

167 mg; 91% yield; ^{1}H NMR (400 MHz, $CDCl_3$): δ 7.37-7.25 (m, 4H), 7.24-7.20 (m, 1H), 7.18-7.14 (m, 2H), 6.72-6.65 (m, 1H), 6.68-6.61 (m, 2H), 4.31 (s, 2H), 4.01 (br, 1H) ppm. ^{13}C NMR (100 MHz, $CDCl_3$) δ 148.18, 139.46, 129.30, 128.67, 127.54, 127.26, 117.59, 112.87, 48.35 ppm.

2.

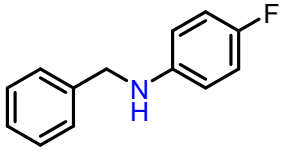

178 mg; 90% yield; ^{1}H NMR (400 MHz, $CDCl_3$) δ 7.37 – 7.29 (m, 5H), 6.91-6.87 (m, 2H), 6.58-6.54 (m, 2H), 4.30 (s, 3H), 3.96 (s, 1H) ppm. ^{13}C NMR (100 MHz, $CDCl_3$) δ 144.50, 139.26, 128.69, 127.51, 127.33, 115.80, 115.57, 113.70, 113.63, 48.95 ppm.

3.

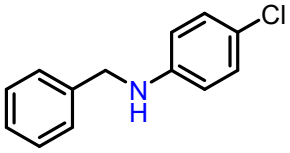

199 mg; 92% yield; ^{1}H NMR (400 MHz, $CDCl_3$) δ 7.37 – 7.26 (m, 5H), 7.11 (d, *J* = 8.8 Hz, 2H), 6.55 (d, *J* = 8.8 Hz, 2H), 4.31 (s, 2H), 4.08 (s, 1H) ppm. ^{13}C NMR (100 MHz, $CDCl_3$) δ 146.67, 138.96, 129.25, 129.09, 128.73, 127.43, 122.11, 114.03, 113.86, 48.36 ppm.

4.

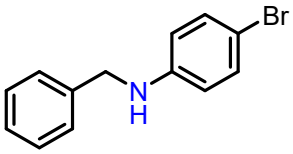

244 mg; 93% yield; ^{1}H NMR (400 MHz, $CDCl_3$) δ 7.38 (d, *J* = 4.5 Hz, 2H), 7.36 – 7.24 (m, 5H), 6.53 (d, *J* = 8.9 Hz, 2H), 4.33 (s, 2H), 4.11 (s, 1H) ppm. ^{13}C NMR (100 MHz, $CDCl_3$) δ 147.07, 138.87, 131.95, 128.72, 127.41, 114.43, 109.13, 48.24 ppm.

5.

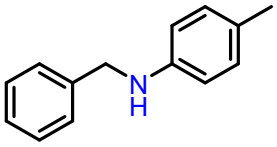

180 mg; 92% yield; ^{1}H NMR (400 MHz, $CDCl_3$): δ 7.44-7.33 (m, 5H), 6.64 (d, J = 7.3 Hz, 2H), 6.61 (d, J = 7.6Hz, 2H), 4.36 (s, 2H) 3.95 (s, 1H), 2.31 (s, 3H) ppm. ^{13}C NMR (100 MHz, $CDCl_3$) δ 146.01, 139.75, 129.83, 128.67, 127.57, 127.22, 126.79, 113.07, 48.69, 29.81, 20.49 ppm.

6.

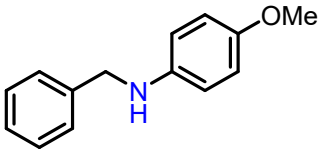

205 mg; 96% yield; ^{1}H NMR (400 MHz, $CDCl_3$) δ 7.42 – 7.01 (m, 5H), 6.85 (d, *J* = 8.9 Hz, 5H), 6.67 (d, *J* = 8.9 Hz, 2H), 4.33 (s, 2H), 3.79 (s, 3H) ppm. ^{13}C NMR (100 MHz, $CDCl_3$) δ 153.55, 128.58, 128.19, 127.51, 116.20, 114.80, 55.71, 50.41, 29.71, 22.60, 14.04 ppm.

7.

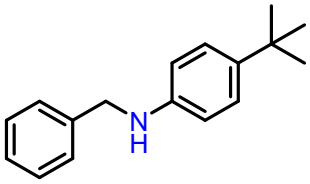

240 mg; 99% yield; ^{1}H NMR (400 MHz, $CDCl_3$) δ 7.44 – 7.31 (m, 5H), 7.27 (d, *J* = 8.3 Hz, 2H), 6.66 (d, *J* = 8.4 Hz, 2H), 4.36 (s, 2H), 3.98 (s, 1H), 1.34 (s, 9H) ppm. ^{13}C NMR (100 MHz, $CDCl_3$) δ 145.91, 140.35, 139.73, 128.65, 127.61, 127.22, 126.08, 112.59, 48.66, 31.91, 31.60 ppm.

8.

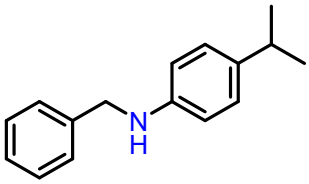

223 mg; 98% yield; ^{1}H NMR (400 MHz, $CDCl_3$) δ 7.42 – 7.25 (m,5), 7.09 (d, *J* = 8.5 Hz, 2H), 6.64 (d, *J* = 8.4 Hz, 2H), 4.34 (s, 3H), 3.04 – 2.64 (sept, J=6.8 Hz 1H), 1.25 (d, *J* = 6.9 Hz, 6H) ppm. ^{13}C NMR (100 MHz, $CDCl_3$) δ 146.26, 139.70, 138.12, 128.61, 127.57, 127.19, 127.13, 112.89, 48.69, 33.18, 24.26 ppm.

9.

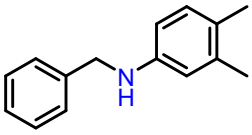

204 mg; 97% yield; ^{1}H NMR (400 MHz, $CDCl_3$) δ 7.41 – 7.29 (m, 5H), 6.97 (s,1H), 6.52 (s, 1H), 6.46 – 6.43 (m,1H), 4.33(s, 2H), 2.21 (s, 6H) ppm. ^{13}C NMR (100 MHz, $CDCl_3$) δ 146.42, 139.81, 137.38, 130.33, 128.63, 127.55, 127.16, 125.61, 114.75, 110.26, 48.67, 20.12, 18.76 ppm.

10.

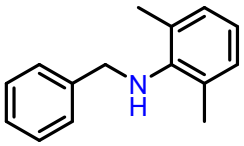

188 mg; 88% yield; ^{1}H NMR (400 MHz, $CDCl_3$) δ 7.39 – 7.30 (m, 5H), 7.03 (d, *J* = 7.5 Hz, 2H), 6.88 (t, *J* = 7.4 Hz, 1H), 4.12 (s, 2H), 2.29 (s, 3H) ppm. ^{13}C NMR (100 MHz, $CDCl_3$) δ 145.91, 140.46, 129.85, 128.85, 128.59, 127.99, 127.30, 122.21, 52.90, 18.48 ppm.

11.

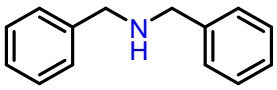

162 mg; 82% yield; ^{1}H NMR (400 MHz, $CDCl_3$) δ 7.38 – 6.87 (m, 10H), 3.82 (s, 4H) ppm.^{13}C NMR (100 MHz, $CDCl_3$) δ138.91, 133.18, 132.69, 121.72, 53.47 ppm.

12.

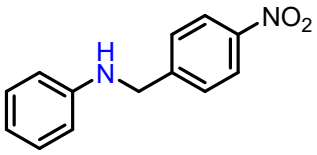

223 mg; 98% yield; ^{1}H NMR (400 MHz, $CDCl_3$) δ 8.21 (d, *J* = 4.8 Hz, 2H), 7.55 (d, *J* = 8.9 Hz, 2H), 7.17 (t, *J* = 7.6 Hz, 2H), 6.75 – 6.69 (m, 1H), 6.59 (d, *J* = 7.8 Hz, 2H), 4.48 (s, 2H), 4.25 (s, 1H) ppm. ^{13}C NMR (100 MHz, $CDCl_3$) δ 147.47, 147.31, 129.41, 127.71, 123.91, 118.26, 112.93, 47.65 ppm.

13.

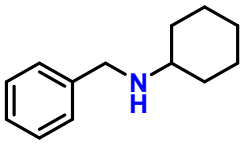

180 mg; 95% yield; ^{1}H NMR (400 MHz, CDCl3) δ 7.20 (t, J = 7.1 Hz, 2H), 6.10 (t, J = 6.9 Hz, 1H), 6.14 (d, J = 7.4 Hz, 2H), 3.79 (s, 1H), 3.10 (d, J = 5.9 Hz, 2H), 1.50 – 1.56 (m, 5H), 1.50-1.34 (m, 1H), 1.30 – 1.19 (m, 3H), 1.00-0.89 (m, 2H) ppm. 13C NMR (100 MHz, CDCl3) δ 150.34, 130.52, 128.26, 113.59, 51.78, 36.39, 30.45, 27.00, 25.31 ppm.

14.

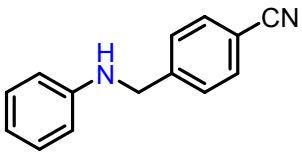

202 mg; 98% yield; ^{1}H NMR (400 MHz, $CDCl_3$) δ 7.66 (d, *J* = 8.3 Hz, 2H), 7.50 (d, *J* = 8.5 Hz, 2H), 7.26 – 7.12 (m, 2H), 6.84 – 6.52 (m, 3H), 4.46 (s, 2H), 4.22 (s, 1H) ppm. ^{13}C NMR (100 MHz, $CDCl_3$) δ 147.40, 145.38, 132.48, 129.41, 127.74, 127.65, 118.89, 113.00, 112.78, 110.97, 47.82 ppm.

15.

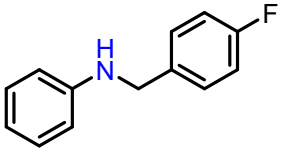

180 mg; 88% yield; ^{1}H NMR (400 MHz, $CDCl_3$) δ 7.38 – 7.31 (m, 2H), 7.22 – 7.14 (m, 2H), 7.05 (t, *J* = 8.7 Hz, 2H), 6.75 (t, *J* = 7.3 Hz, 1H), 6.66 (d, *J* = 7.6 Hz, 2H), 4.33 (s, 2H), 4.05 (s, 1H) ppm. ^{13}C NMR (100 MHz, $CDCl_3$) δ 147.95, 135.13, 129.30, 128.97, 117.76, 115.56, 115.35, 112.89, 47.63 ppm.

16.

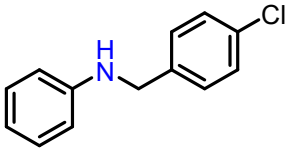

198 mg; 90% yield; ^{1}H NMR (400 MHz, $CDCl_3$) δ 7.38 – 7.17 (m, 5H), 6.75 (d, *J* = 7.3 Hz, 2H), 6.63 (d, *J* = 7.6 Hz, 2H), 4.33 (s ,2H), 4.05 (s, 1H) ppm. ^{13}C NMR (100 MHz, $CDCl_3$) δ 147.85, 138.02, 132.88, 129.32, 128.77, 128.71, 128.29, 117.83, 112.91, 47.63 ppm.

17.

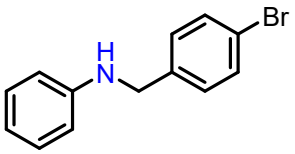

242 mg; 92% yield; ^{1}H NMR (400 MHz, $CDCl_3$) δ 7.47 (d, *J* = 8.4 Hz, 2H), 7.32 – 7.09 (m, 5H), 6.62 (d, *J* = 7.6 Hz, 2H), 4.30 (s, 2H), 3.20 (s, 2H) ppm. ^{13}C NMR (100 MHz, $CDCl_3$) δ147.84, 138.60, 131.73, 129.35, 129.09, 120.94, 117.86, 112.94, 47.667 ppm.

18.

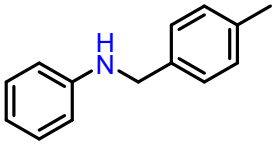

173 mg; 88% yield; ^{1}H NMR (400 MHz, $CDCl_3$) δ 7.22 – 7.15 (m, 5H), 6.73 (d, *J* = 8.4 Hz, 2H), 6.66 (d, *J* = 7.6 Hz, 2H), 4.31 (s, 2H), 2.37 (s, 3H) ppm.^{13}C NMR (100 MHz, $CDCl_3$) δ 148.25, 136.90, 136.38, 129.34, 129.28, 127.56, 117.52, 112.87, 48.11, 21.14 ppm.

19.

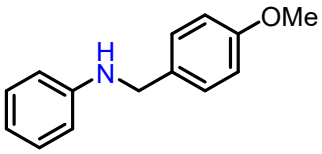

200 mg; 93% yield; ^{1}H NMR (400 MHz, $CDCl_3$) δ 7.35 (d, *J* = 8.7 Hz, 2H), 7.23 (t, *J* = 15.6 Hz, 2H), 6.94 (d, *J* = 8.67 Hz, 2H), 6.72 (dd, *J* = 1.8, 2.7 Hz, 3H), 4.30 (s, 2H), 3.85 (s, 3H) ppm. ^{13}C NMR (100 MHz, $CDCl_3$) δ 158.88, 148.25, 131.45, 129.29, 128.85, 117.54, 115.16, 112.88, 55.34, 47.82 ppm.

20.

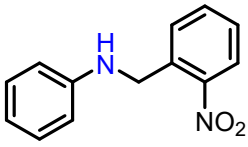

206 mg; 90% yield; ^{1}H NMR (400 MHz, $CDCl_3$) δ 8.09 (d, *J* = 8.1 Hz, 1H), 7.71 (d, *J* = 8.3 Hz, 1H), 7.59 (t, *J* = 7.0 Hz, 1H), 7.45 (t, *J* = 7.7 Hz, 1H), 7.26 – 7.12 (m, 2H), 6.75 (t, *J* = 7.3 Hz, 1H), 6.60 (d, *J* = 8.6 Hz, 1H), 4.76 (s, 2H), 4.38 (s, 1H) ppm.^{13}C NMR (100 MHz, $CDCl_3$) δ 147.37, 135.70, 133.71, 129.79, 129.36, 128.00, 125.22, 118.04, 112.89, 45.78 ppm.

21.

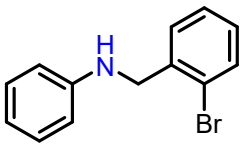

225 mg; 86% yield; ^{1}H NMR (400 MHz, $CDCl_3$) δ 7.62 (d, *J* = 9.1 Hz, 1H), 7.45 (d, *J* = 7.4 Hz, 1H), 7.31-720 (m, 5H), 6.79 (d, *J* = 9.5 Hz, 2H), 4.44 (s, 2H) ppm. ^{13}C NMR (100 MHz, $CDCl_3$) δ 147.73, 138.21, 132.84, 129.33, 129.19, 128.72, 127.60, 123.29, 117.89, 112.98, 48.43 ppm.

22.

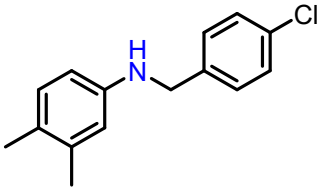

231 mg; 92% yield; ^{1}H NMR (400 MHz, $CDCl_3$) δ 7.33 (s, 1H), 6.93 (d, *J* = 8.1 Hz, 2H), 6.46 (d, *J* = 2.4 Hz, 2H), 6.36 (d, *J* = 8.0 Hz, 2H), 4.28 (s, 2H), 3.85 (s, 1H) ppm.^{13}C NMR (100 MHz, $CDCl_3$) δ 146.04, 138.37, 137.40, 130.32, 128.70, 128.28 125.85, 114.77, 110.27, 47.93, 20.05, 18.69 ppm.

23.

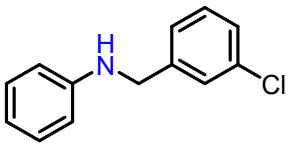

203 mg; 94% yield; ^{1}H NMR (400 MHz, $CDCl_3$) δ 7.42 (s, 1H), 7.31-7.21 (m, 5H), 6.80 (t, *J* = 13.5 Hz, 1H), 6.66 (d, *J* = 8.5 Hz, 2H), 4.36 (s, 2H) ppm.^{13}C NMR (100 MHz, $CDCl_3$) δ 147.81, 141.78, 134.54, 129.95, 129.36, 127.44, 127.40, 125.45, 117.88, 112.93, 47.78 ppm.

24.

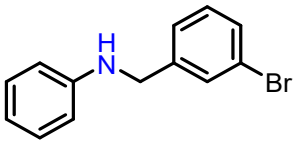

245 mg; 93% yield;^{1}H NMR (400 MHz, $CDCl_3$) δ 7.56 (s, 1H), 7.34-7.20 (m, 5H), 6.78 (t, *J* = 15.5 Hz, 1H), 6.66 (d, *J* = 8.5 Hz, 2H), 4.34 (s, 2H) ppm. ^{13}C NMR (100 MHz, $CDCl_3$) δ 147.79, 142.05, 130.33, 130.25, 129.36, 125.92, 122.79, 120.93, 117.89, 112.93, 47.74 ppm.

25.

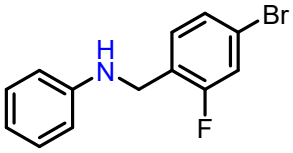

255 mg; 89% yield; ^{1}H NMR (400 MHz, $CDCl_3$) δ 7.29-7.19 (m, 5H), 6.79 (t, *J* = 7.3 Hz, 1H), 6.66 (d, *J* = 8.6 Hz, 2H), 4.39 (s, 2H), 4.10 (s, 1H) ppm. ^{13}C NMR (100 MHz, $CDCl_3$) δ 147.47, 130.45, 129.35, 127.54, 125.79, 120.91, 119.13, 118.89, 118.04, 112.95, 41.48 ppm.

26.

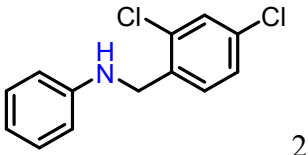

231 mg; 92% yield; ^{1}H NMR (400 MHz, $CDCl_3$) δ 7.50 – 7.26 (m, 2H), 7.18 (d, *J* = 10.9 Hz, 3H), 6.79 – 6.68 (m, 1H), 6.61 (d, *J* = 8.6 Hz, 2H), 4.78 (s,2H), 4.43 (s, 1H)

ppm.^{13}C NMR (100 MHz, $CDCl_3$) δ 147.44, 135.37, 133.74, 129.74, 129.35, 129.31, 127.22, 118.00, 112.92, 45.45 ppm.

27.

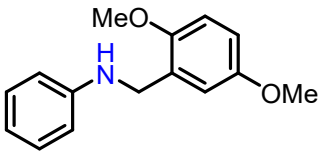

236 mg; 97% yield; ^{1}H NMR (400 MHz, $CDCl_3$) δ 7.23 (dd, *J* = 8.8 Hz, 2H), 6.99 (s, 1H), 6.86 – 6.70 (m, 5H), 4.37 (s,2H), 3.88 (s, 3H), 3.79 (s, 3H) ppm. ^{13}C NMR (100 MHz, $CDCl_3$) δ 153.68, 151.62, 148.41, 129.34, 128.69, 118.57, 117.48, 115.34, 113.17, 112.23, 111.25, 55.92, 55.74, 43.55 ppm.

28.

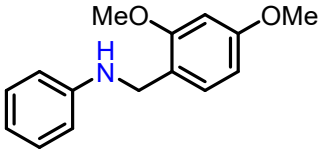

206 mg; 84% yield; ^{1}H NMR (400 MHz, $CDCl_3$) δ 7.24 (s, 1H), 7.23 – 7.15 (m, 2H), 6.83 – 6.62 (m,2H), 6.51 (d, *J* = 2.3 Hz, 1H), 6.46 (dd, *J* = 8.2, 2.4 Hz, 2H), 4.28 (s, 2H), 3.86 (s, 3H), 3.83 (s, 3H) ppm.^{13}C NMR (100 MHz, $CDCl_3$) δ 160.20, 158.44, 148.51, 129.71, 129.17, 117.30, 115.13, 103.86, 98.62, 55.40, 55.37, 43.17 ppm.

29.

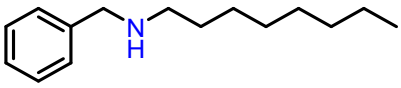

157 mg; 71% yield; ^{1}H NMR (500 MHz, $CDCl_3$) δ 7.49 – 7.20 (m, 5H), 3.82 (s, 2H), 2.67 (t, *J* = 7.3 Hz, 2H), 1.76 (s, 2H), 1.64 – 1.49 (m, 2H), 1.34 (m, 10H), 0.95 (t, *J* = 6.8 Hz, 3H) ppm. ^{13}C NMR (125 MHz, $CDCl_3$) δ 140.53, 128.37, 128.14, 126.87, 54.12, 49.55, 31.98, 30.15, 29.70, 29.41, 27.44, 22.75, 14.17 ppm.

30.

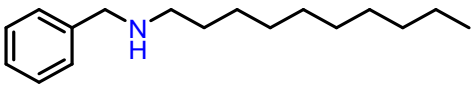

191 mg; 76% yield; ^{1}H NMR (500 MHz, $CDCl_3$) δ 7.36 – 7.27 (m, 5H), 3.82 (s, 2H), 2.66 (t, *J* = 7.4 Hz, 2H), 1.75 (s, 2H), 1.57 – 1.45 (m, 2H), 1.32 (m, 14H), 0.94 (q, *J* = 6.8 Hz, 3H) ppm. ^{13}C NMR (125 MHz, $CDCl_3$) δ 140.52, 128.36, 128.13, 126.86, 54.12, 49.55, 31.98, 30.15, 29.70, 29.66, 29.41, 29.41, 27.44, 22.75, 14.17 ppm.

31.

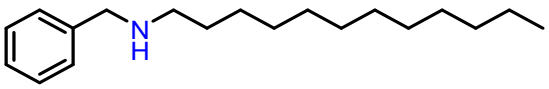

223 mg; 80% yield; ^{1}H NMR (500 MHz, $CDCl_3$) δ 7.35 – 7.27 (m, 5H), 3.81 (s, 2H), 2.63 (t, *J* = 7.9 Hz, 2H), 1.54 (s, 2H), 1.55 – 1.50 (m, 2H), 1.29 (m, , 18H), 0.91 (q, *J* = 6.2 Hz, 3H) ppm. ^{13}C NMR (125 MHz, $CDCl_3$) δ 140.50, 128.39, 128.15, 126.89, 54.11, 49.54, 31.95, 30.28,30.11, 29.70, 29.67, 29.64, 29.60, 29.38, 27.72, 22.72, 14.17 ppm.

32.

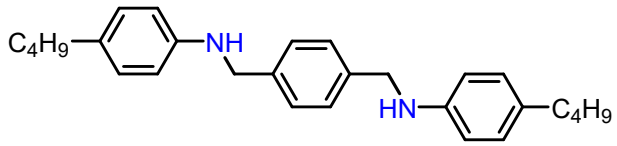

393 mg; 98% yield; ^{1}H NMR (400 MHz, $CDCl_3$) δ 7.39(s, 4H), 7.00 (d, J = 8.55 Hz, 4H), 6.59 (d, J = 8.65 Hz, 2H), 4.31 (s, 4H), 3.92 (s, 2H), 2.52 (t, J = 7.75 Hz, 4H), 1.60-1.52 (m, 4H), 1.39-1.33(m, 4H), 0.93 (t, J = 7.47, 6H) ppm. ^{13}C NMR (100 MHz, $CDCl_3$) δ 146.08, 138.64, 132.09, 129.15, 127.83, 112.89, 84.39, 34.73, 34.03 ppm.

33.

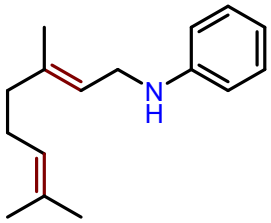

194 mg; 85% yield; ^{1}H NMR (400 MHz, $CDCl_3$) δ 7.22(t, J = 7.39 Hz, 2H), 6.76 (d, J = 7.36 Hz, 2H), 6.73 (t, J = 7.41 Hz, 2H), 5.25 (t, J = 6.13 Hz, 1H), 5.21 (t, J = 6.41 Hz, 1H), 3.81(d, J = 17.79 Hz, 1H), 3.59(d, J = 17.05 Hz, 1H), 2.18 (q, J = 7.82 Hz, 2H), 2.07-1.80 (m, 2H), 1.78 (s, 3H), 1.73 (s, 3H), 1.62 (s, 3H) ppm.

34.

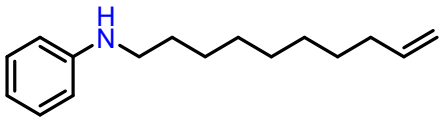

202 mg; 87 % yield; ^{1}H NMR (400 MHz, $CDCl_3$) δ 7.20 (t, J = 7.31 Hz, 2H), 6.71 (d, J = 7.33 Hz, 1H), 6.62 (t, J = 7.48 Hz, 2H), 5.85-581 (m, 1H), 5.00 (d, J = 17.12 Hz, 2H), 4.95 (d, J = 9.91 Hz, 2H), 3.13 (t, J = 7.09 Hz, 1H), 2.18 (q, J = 7.82 Hz, 2H), 2.07-1.80 (m, 2H), 1.78 (s, 3H), 1.73 (s, 3H), 1.62 (s, 3H) ppm. ^{13}C NMR (100 MHz, $CDCl_3$) δ 148.54, 139.19, 129.22, 117.08, 114.17, 112.69, 44.00, 33.79, 29.59, 29.43, 29.40, 29.07, 28.91, 27.17 ppm.

35.

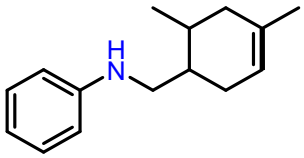

179 mg; 82% yield; ^{1}H NMR (400 MHz, $CDCl_3$) δ 7.24-7.20 (m, 2H), 6.64-6.62 (m, 1H), 6.51-6.48 (m, 2H), 5.25 (t, J= 6.23 Hz, 1H), 5.02 (s, 1H), 3.42 (dd, J=10.02 Hz, J=10.13 Hz, 1H), 3.15 (dd, J=10.18 Hz, J=10.12 Hz, 1H), 1.87-1.85(m, 2H), 1.70-1.57(m, 4H), 1.27 (s, 3H), 0.86 (q, J= 7.20 Hz, 3H) ppm. ^{13}C NMR (100 MHz, $CDCl_3$) δ 132.60, 128.97, 128.74, 127.79, 114.59, 110.88, 53.86, 47.74, 33.48, 29.71, 28.24, 22.94, 18.19 ppm.

Refernces

1. *CrysAlisPRO*, Oxford Diffraction/Agilent Technol. UKLtd, Yarnton, Oxford, UK .
2. L. J. Farrugia, *J. Appl. Crystallogr.*, 2012, **45**, 849–854.
3. O. V. Dolomanov, L. J. Bourhis, R. J. Gildea, J. A. K. Howard and H. Puschmann, *J. Appl. Crystallogr.*, 2009, **42**, 339–341.
4. G. M. Sheldrick, *Acta Crystallogr., Sect. C: Struct. Chem.*, 2015, **71**, 3–8.
5. C. Kerner, S. D. Straub, Y. Sun and W. R. Thiel, *Eur. J. Org. Chem.*, 2016, **18**, 3060–3064.
6. M. Ruiz-Castañeda, M. C. Carrión, L. Santos, B. R. Manzano, G. Espino and F. A. Jalón, *ChemCatChem*, 2018, **10**, 5541–5550.
7. F. Christie, A. Zanotti-Gerosa and D. Grainger, *ChemCatChem*, 2018, **10**, 1012–1018.
8. N. Kayacı, S. Dayan, N. Özdemir, O. Dayan and N. Kalaycıoğlu Özpozan, *Appl. Organomet. Chem.*, 2018, **32**, e4558.
9. L. Kathuria and A. G. Samuelson, *Eur. J. Inorg. Chem.*, 2020, **24**, 2372–2379
10. X. J. Yun, C. Ling, W. Deng, Z. J. Liu and Z. J. Yao, *Organometallics*, 2020, **39**, 3830–3838.
11. A. R. Fatkulin, O. I. Afanasyev, A. A. Tsygankov and D. Chusov, *J. Catal.*, 2022, **405**, 404–409.

NMR Spectra for secondary amines product

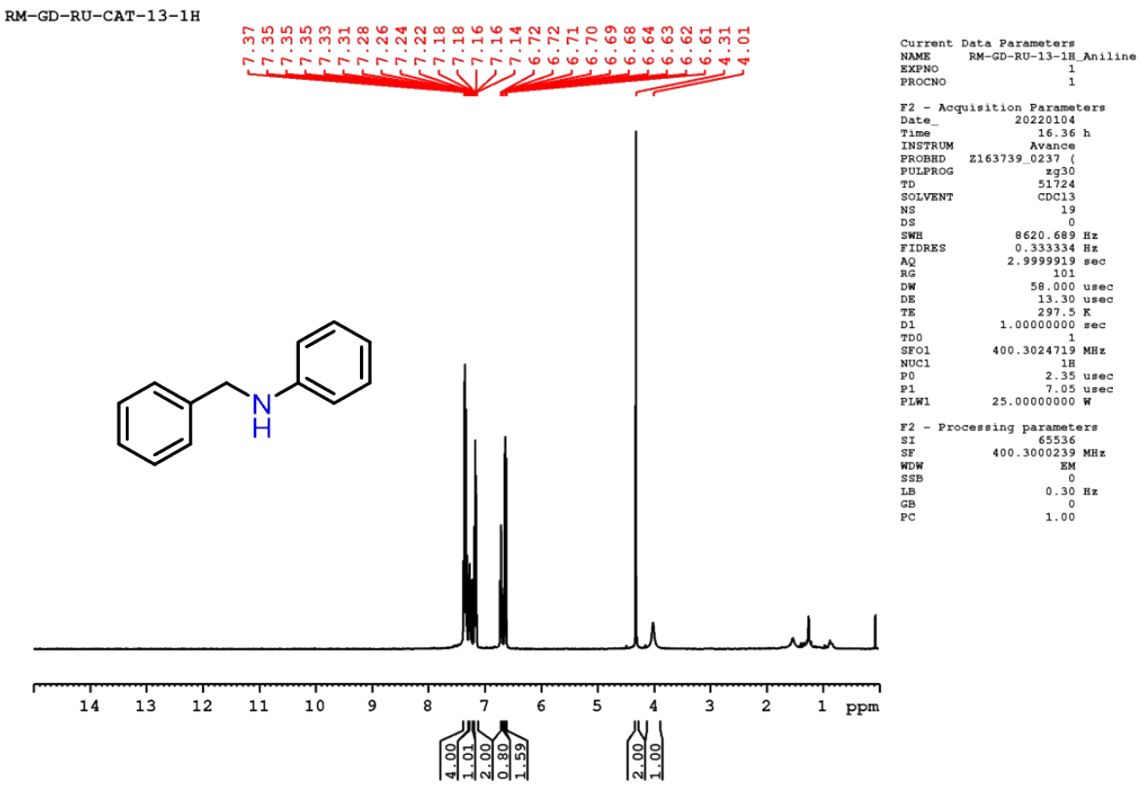

Figure S23. ^{1}H NMR spectrum of complex **1a** in $CDCl_3$ (400 MHz).

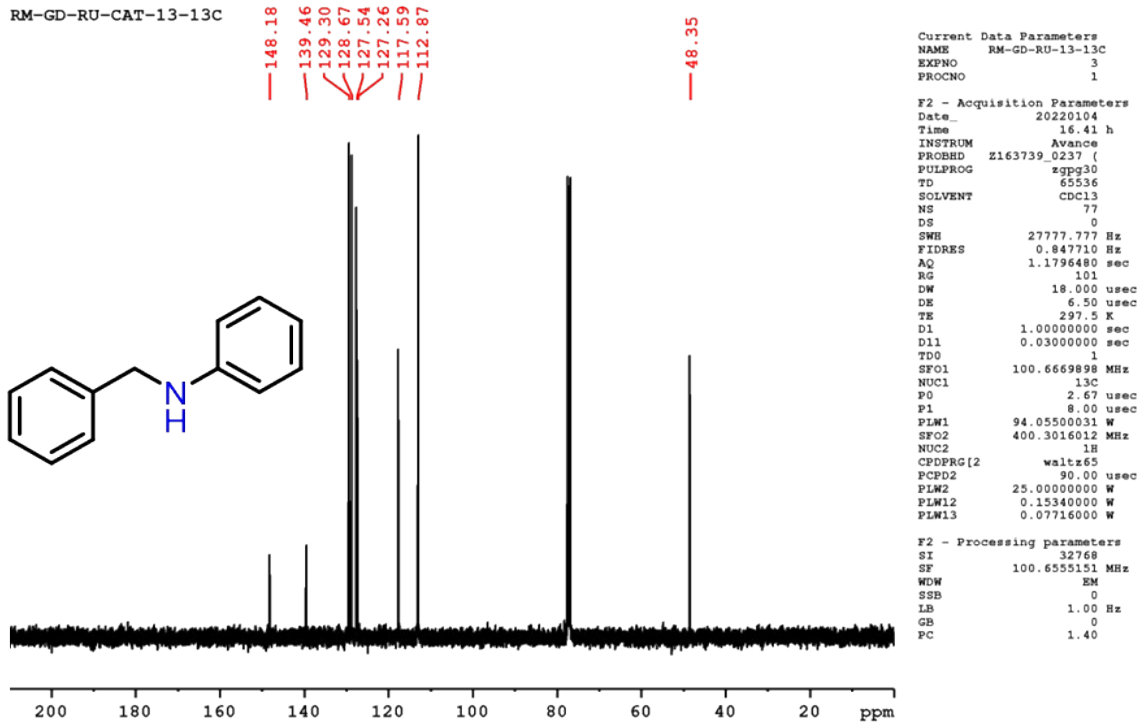

Figure S24. ^{13}C NMR spectrum of complex **1a** in $CDCl_3$ (100 MHz).

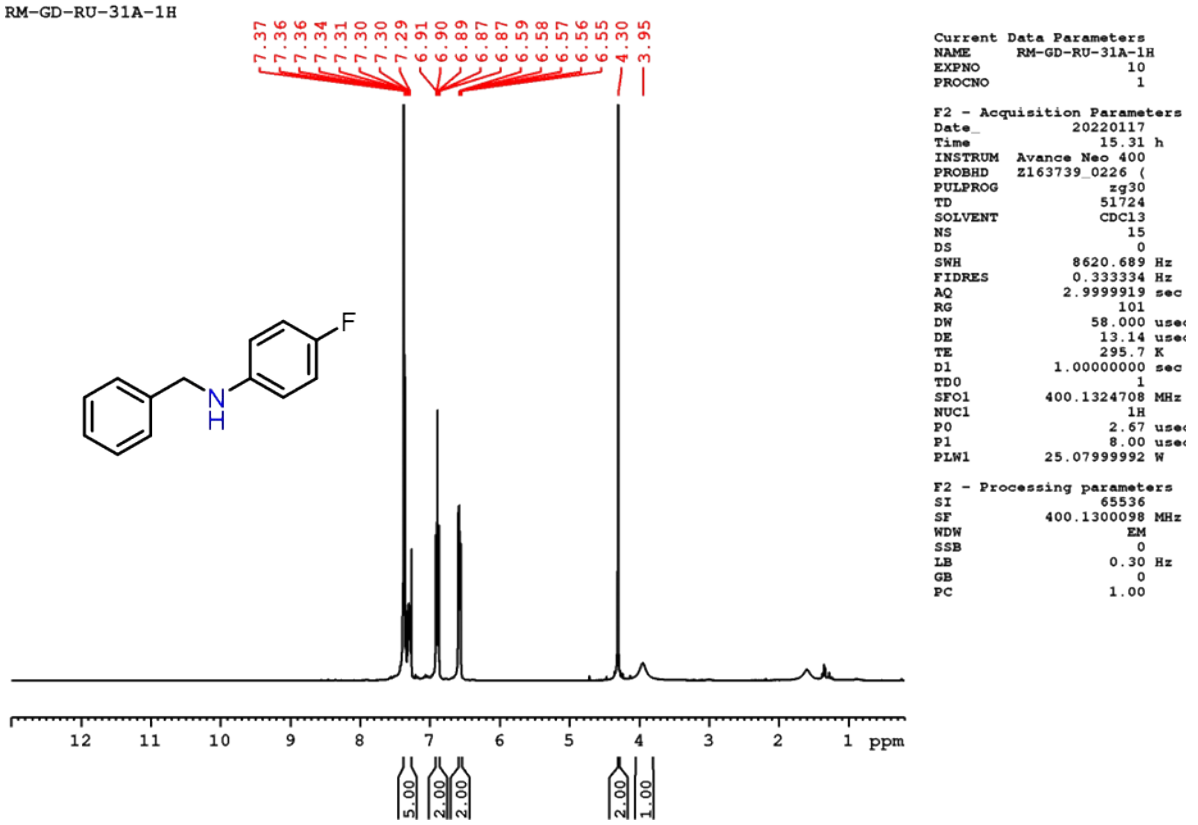

Figure S25. ^{1}H NMR spectrum of complex **1f** in $CDCl_3$ (400 MHz).

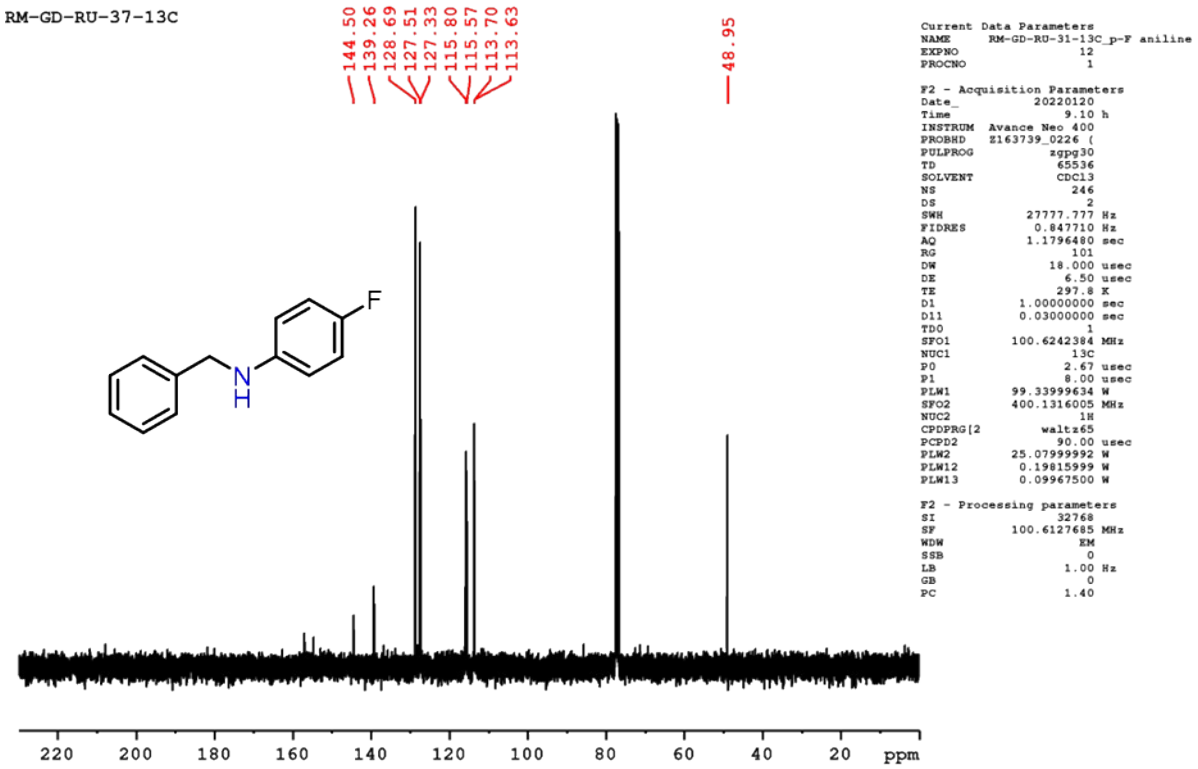

Figure S26. ^{13}C NMR spectrum of complex **1f** in $CDCl_3$ (100 MHz).

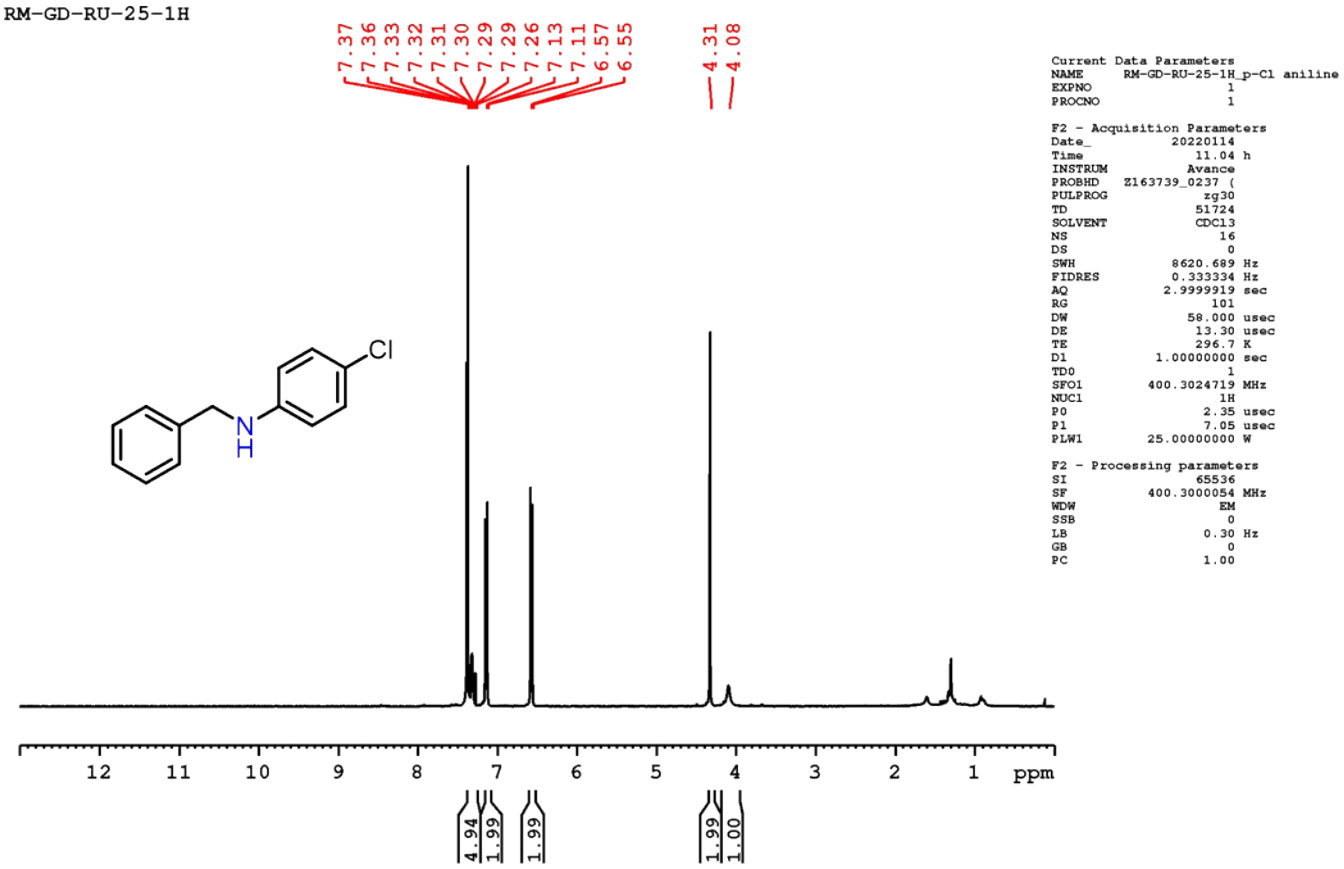

Figure S27. ^{1}H NMR spectrum of complex **1g** in $CDCl_3$ (400 MHz).

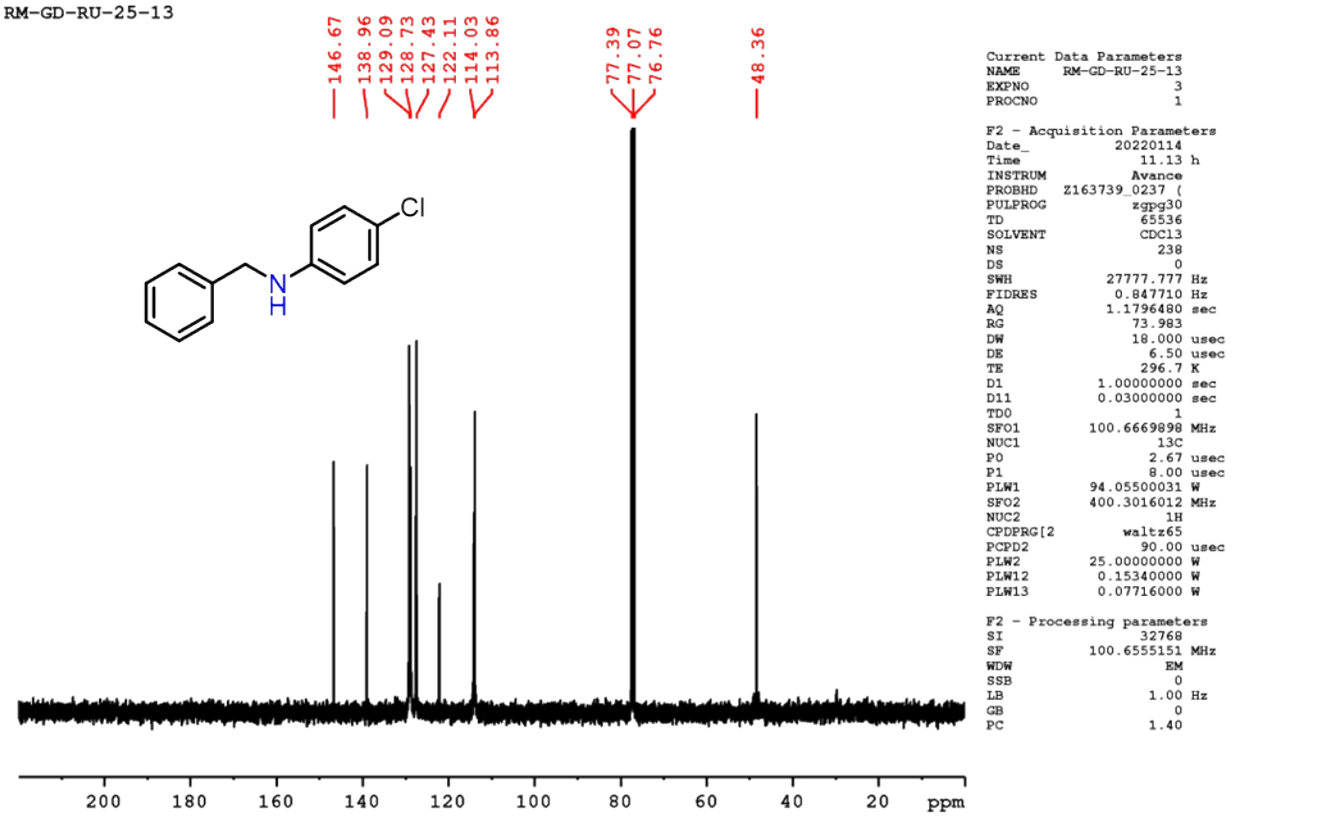

Figure S28. ^{13}C NMR spectrum of complex **1g** in $CDCl_3$ (100 MHz).

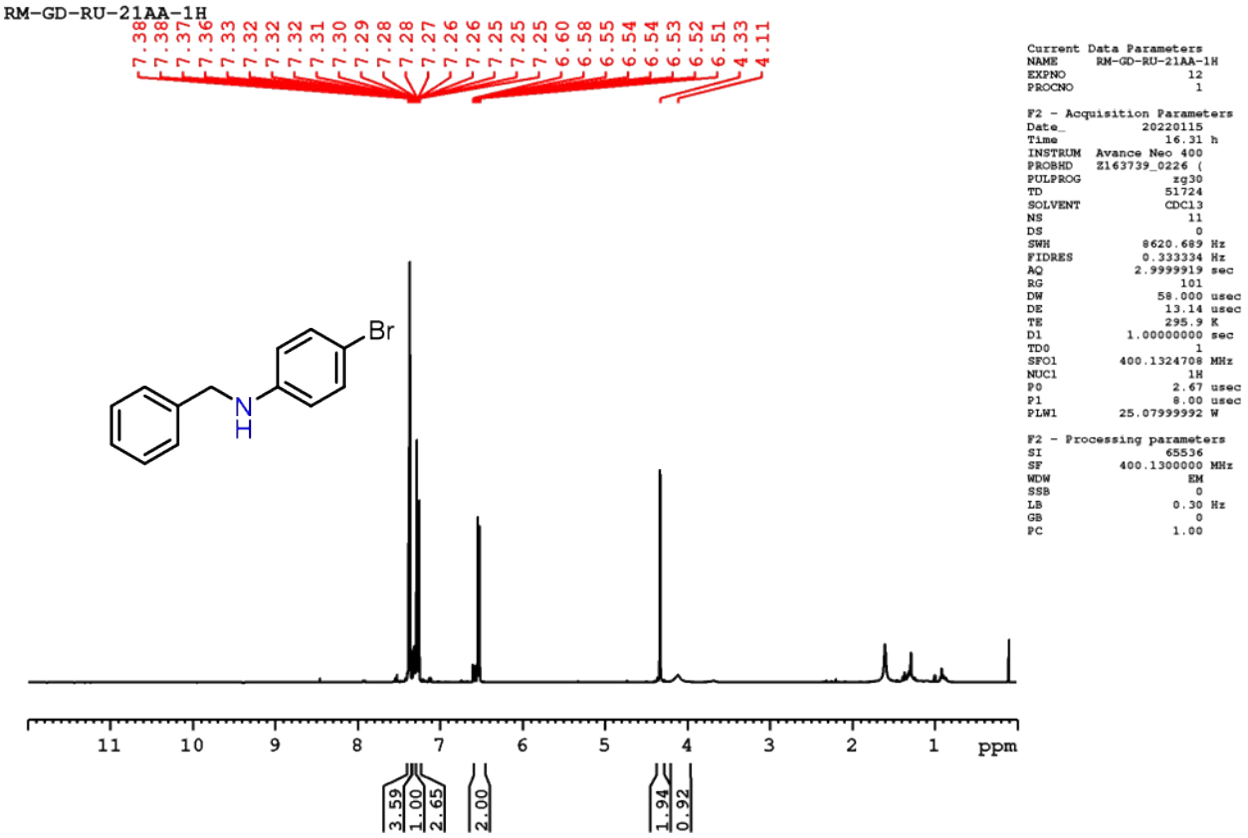

Figure S29. ^{1}H NMR spectrum of complex **1h** in $CDCl_3$ (400 MHz).

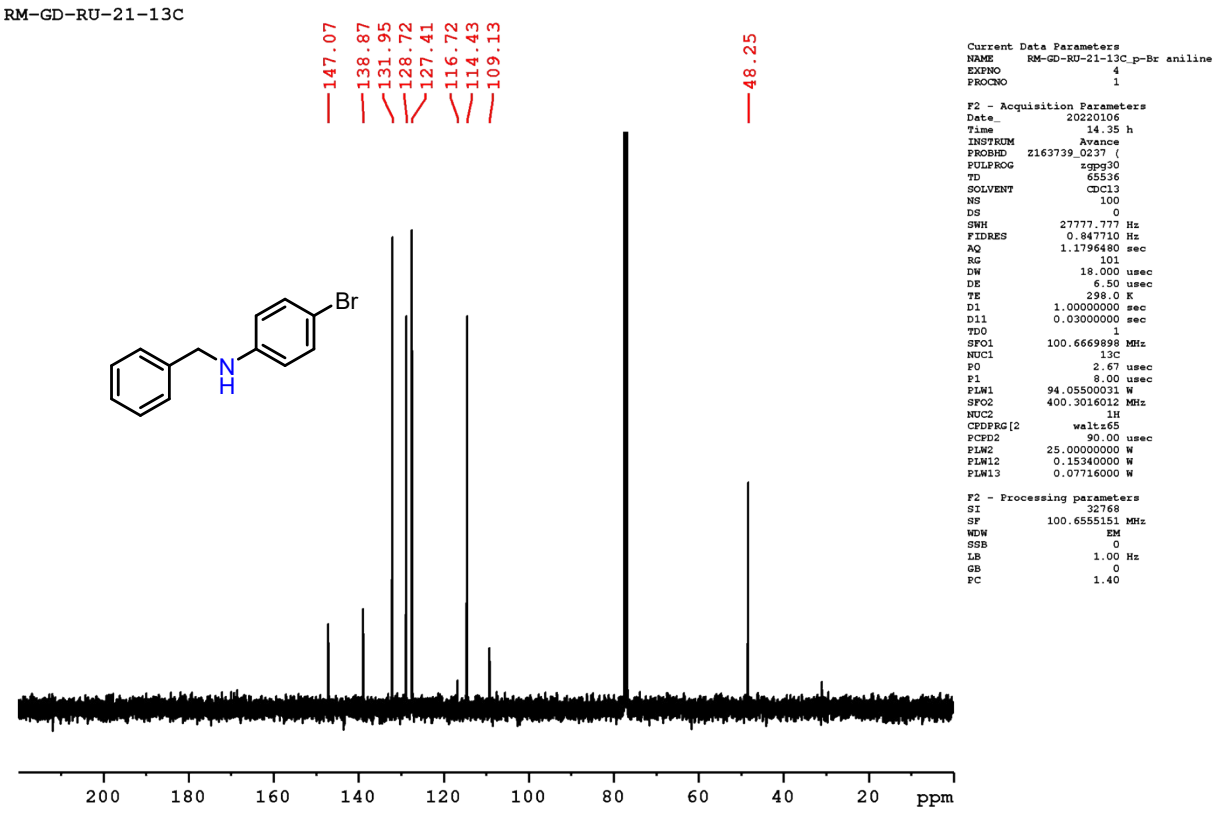

Figure S30. ^{13}C NMR spectrum of complex **1h** in $CDCl_3$ (100 MHz).

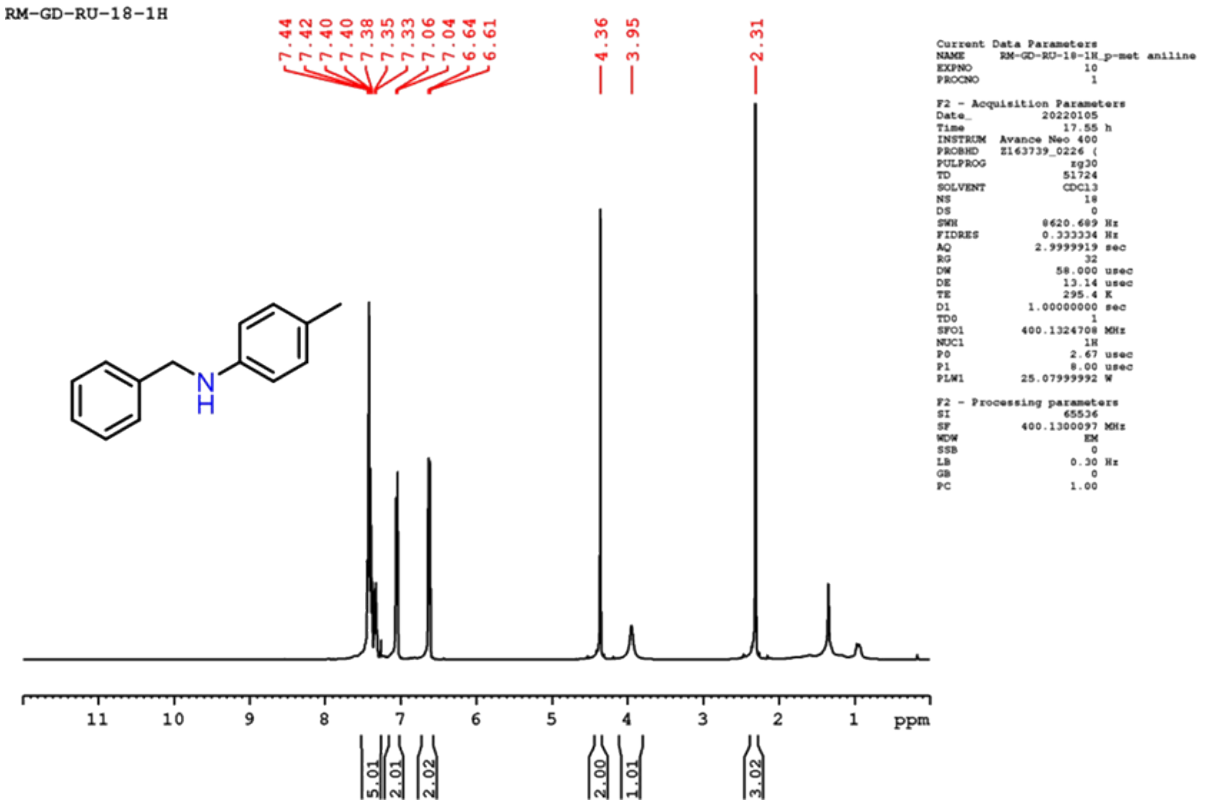

Figure S31. ^{1}H NMR spectrum of complex **1b** in $CDCl_3$ (400 MHz).

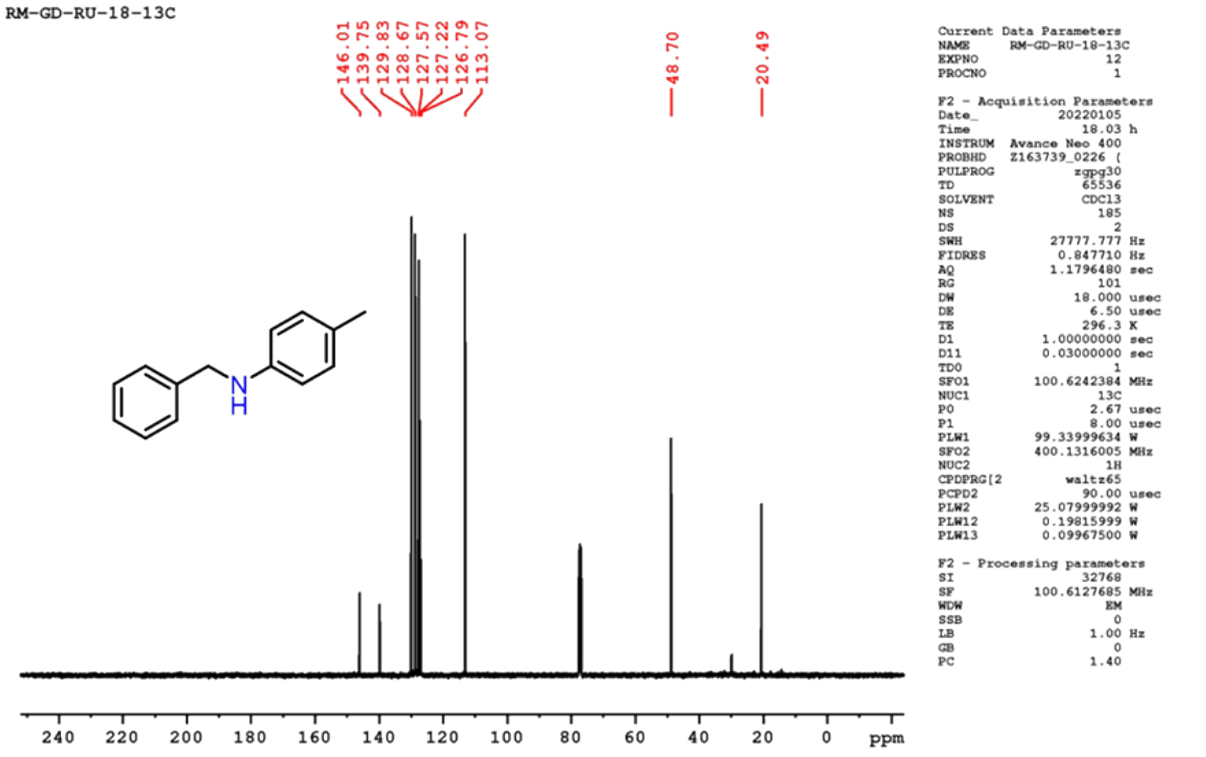

Figure S32. ^{13}C NMR spectrum of complex **1b** in $CDCl_3$ (100 MHz).

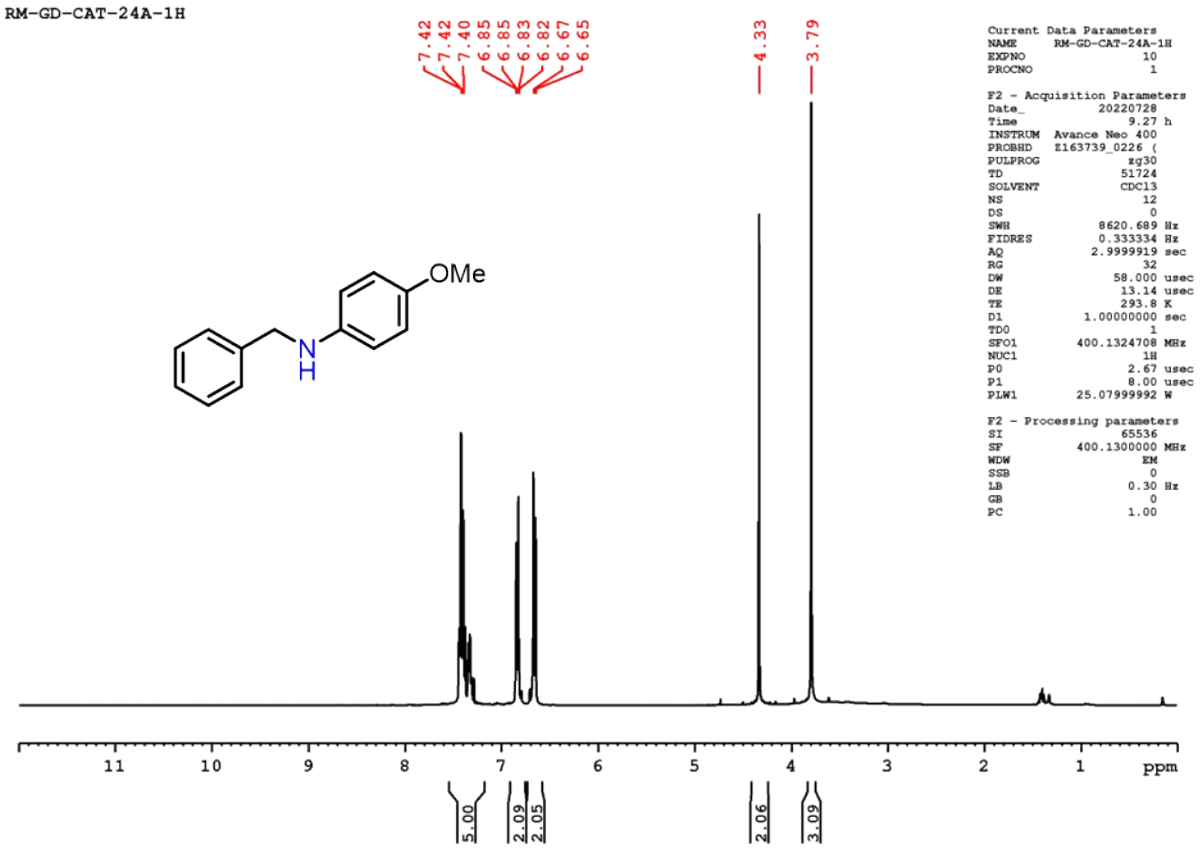

Figure S33. ^{1}H NMR spectrum of complex **1c** in $CDCl_3$ (400 MHz).

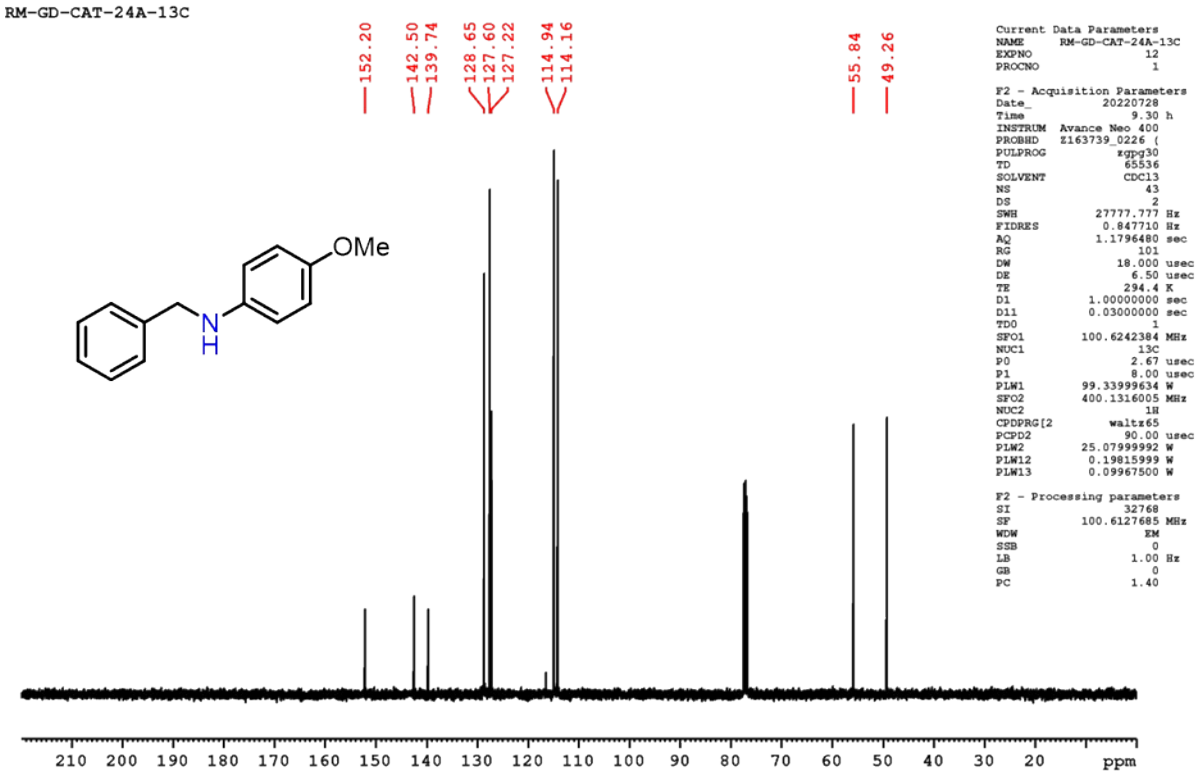

Figure S34. ^{13}C NMR spectrum of complex **1c** in $CDCl_3$ (100 MHz).

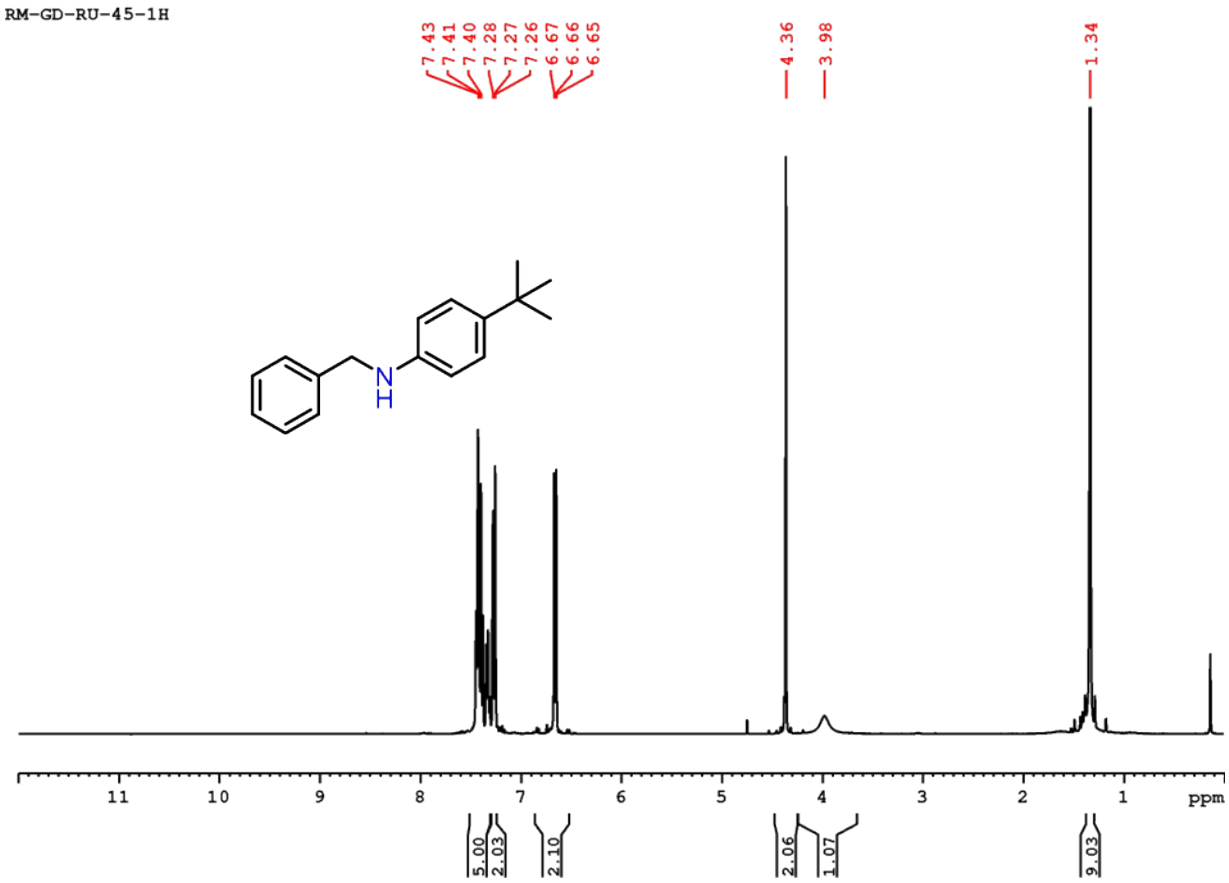

Figure S35. ^{1}H NMR spectrum of complex **1e** in $CDCl_3$ (400 MHz).

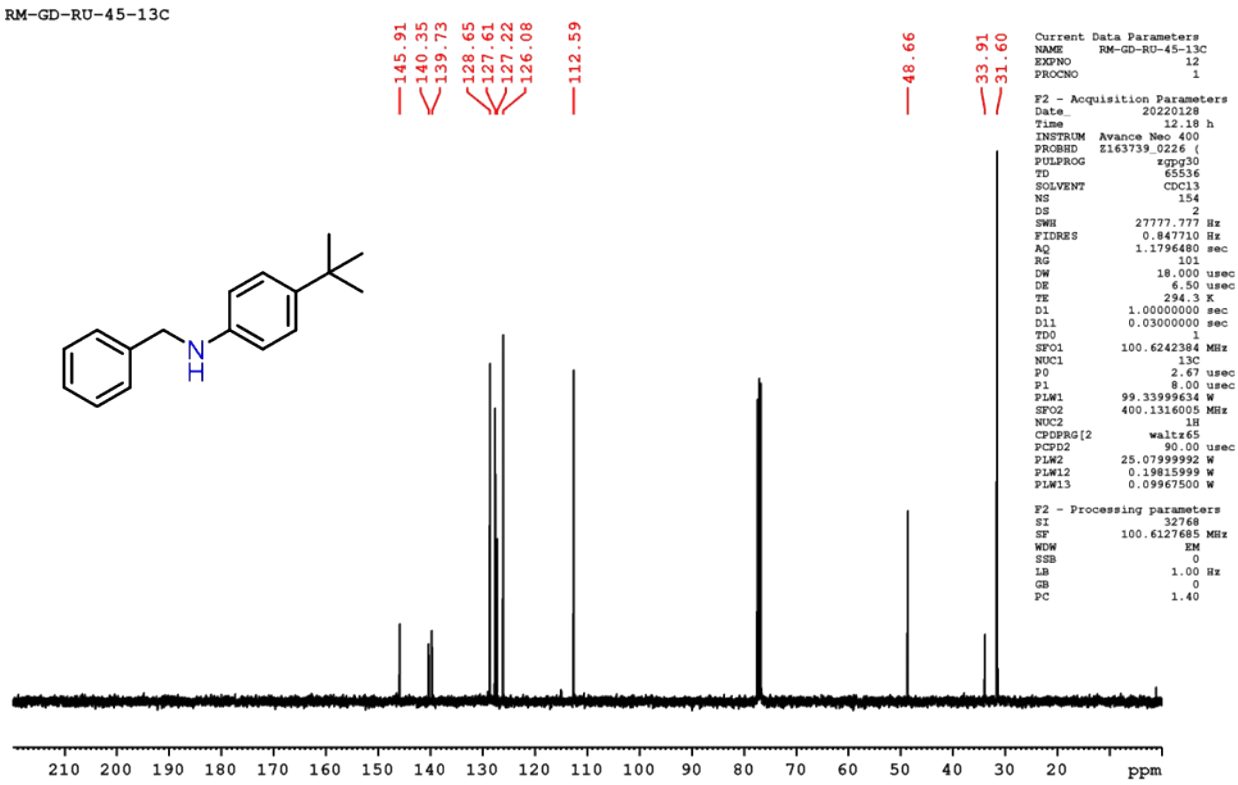

Figure S36. ^{13}C NMR spectrum of complex **1e** in $CDCl_3$ (100 MHz).

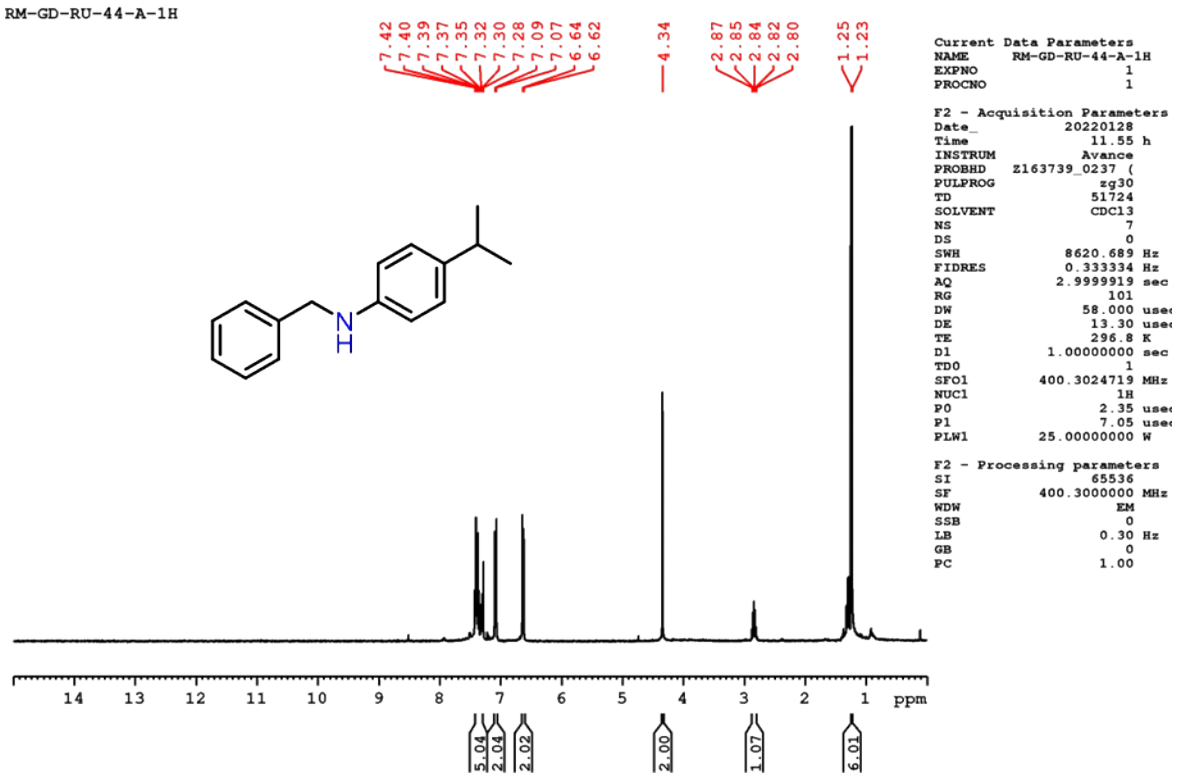

Figure S37. ^{1}H NMR spectrum of complex **1d** in $CDCl_3$ (400 MHz).

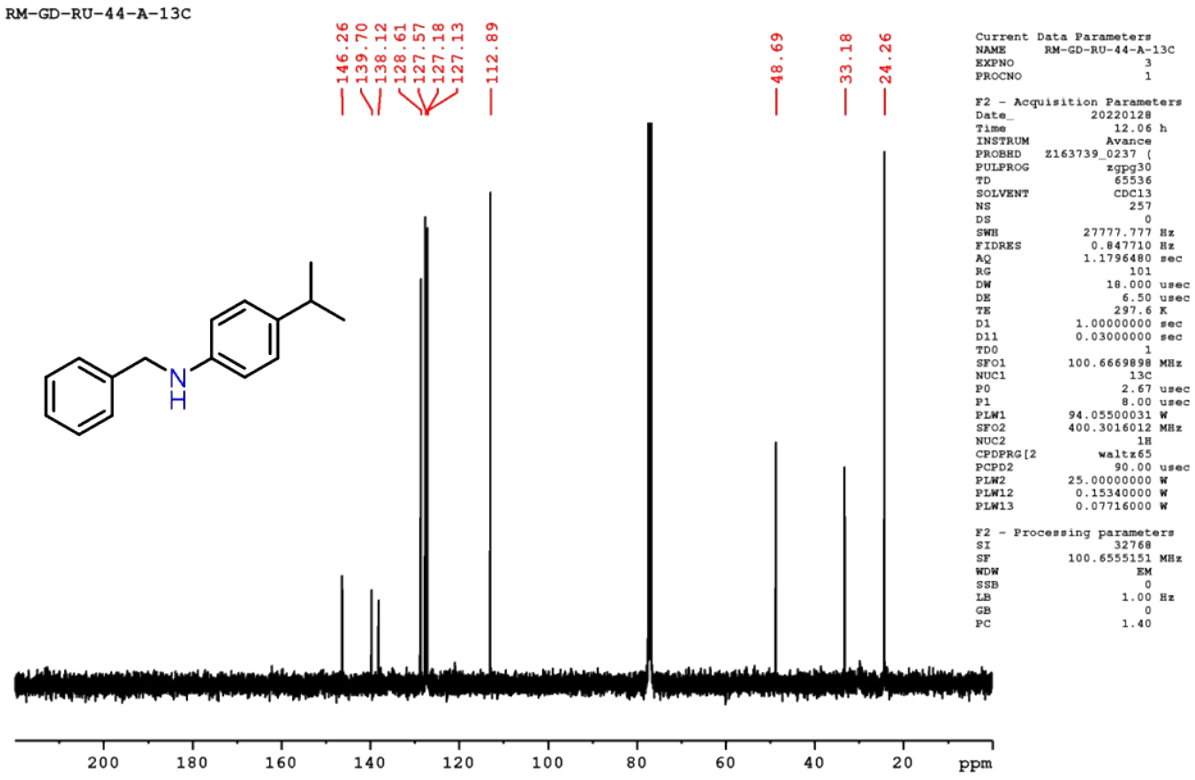

Figure S38. ^{13}C NMR spectrum of complex **1d** in $CDCl_3$ (100 MHz).

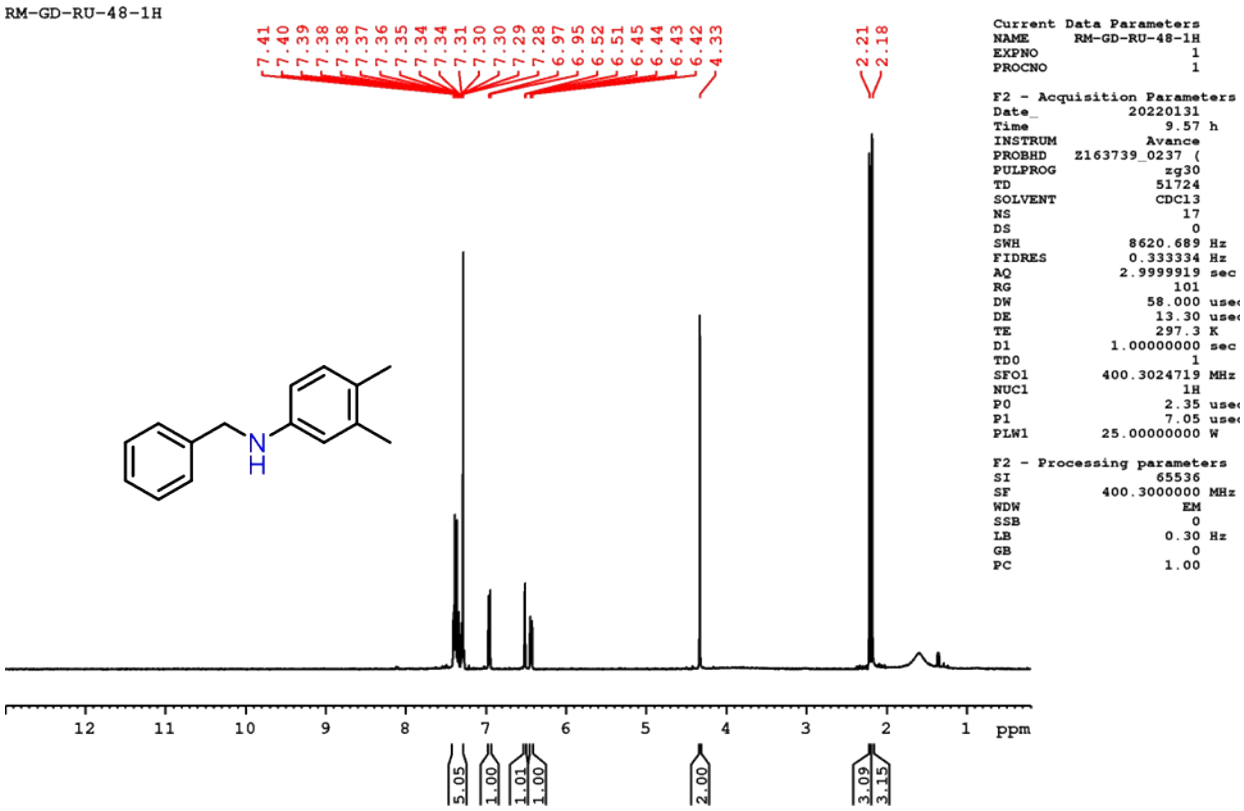

Figure S39. ^{1}H NMR spectrum of complex **1j** in $CDCl_3$ (400 MHz).

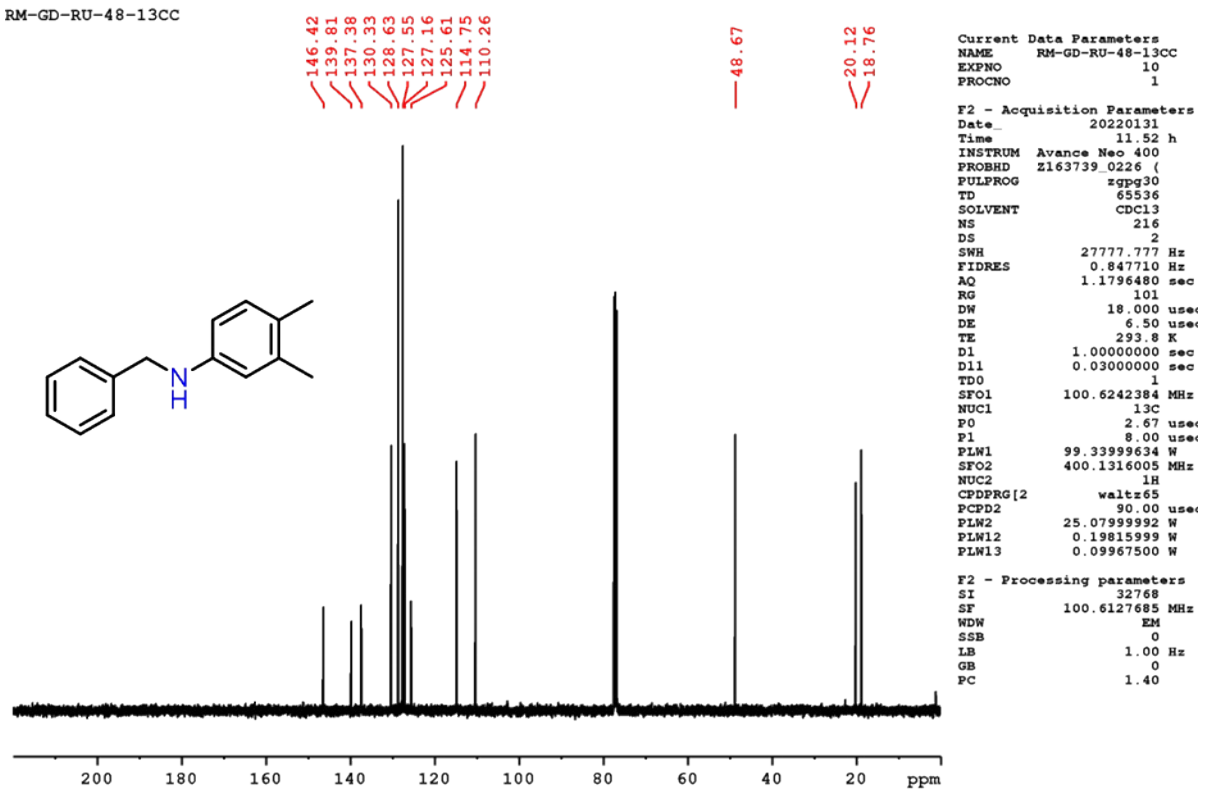

Figure S40. ^{13}C NMR spectrum of complex **1j** in $CDCl_3$ (100 MHz).

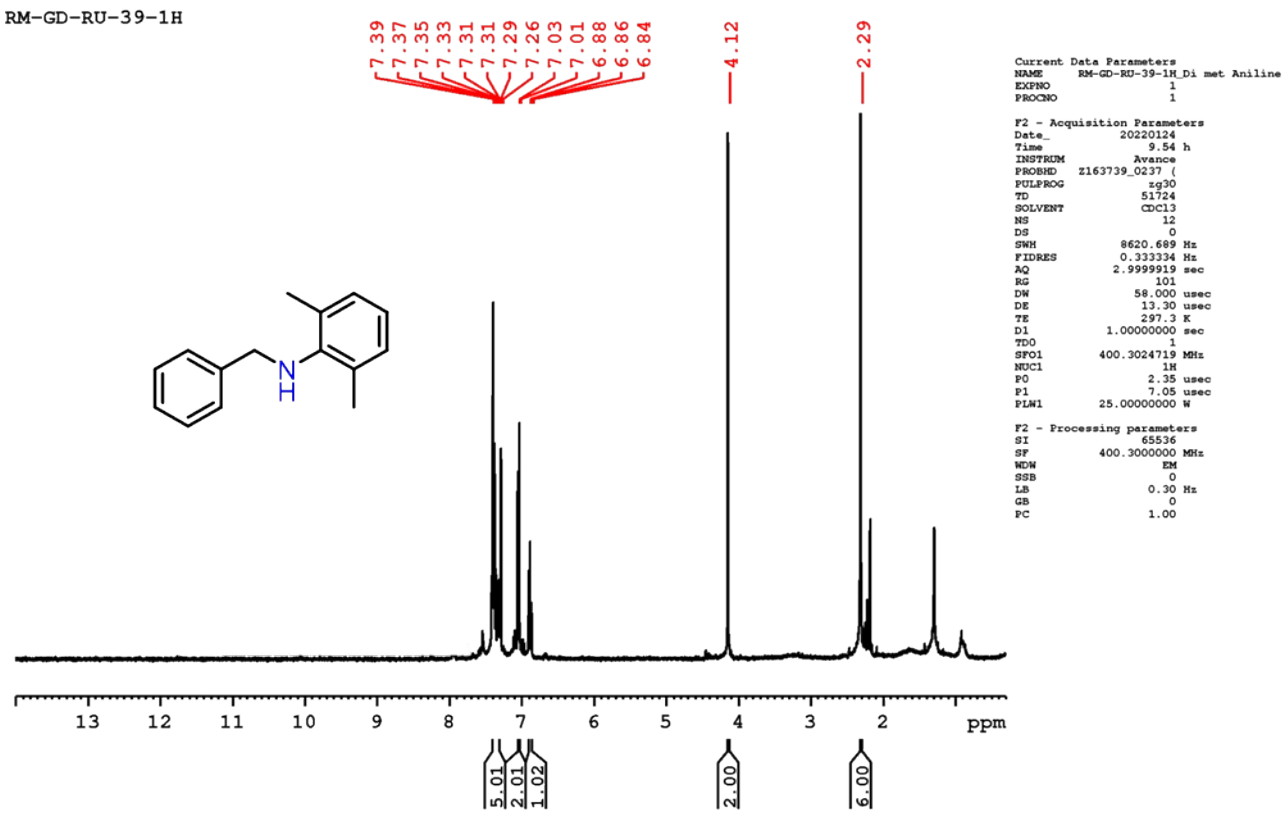

Figure S41. ^{1}H NMR spectrum of complex **1o** in $CDCl_3$ (400 MHz).

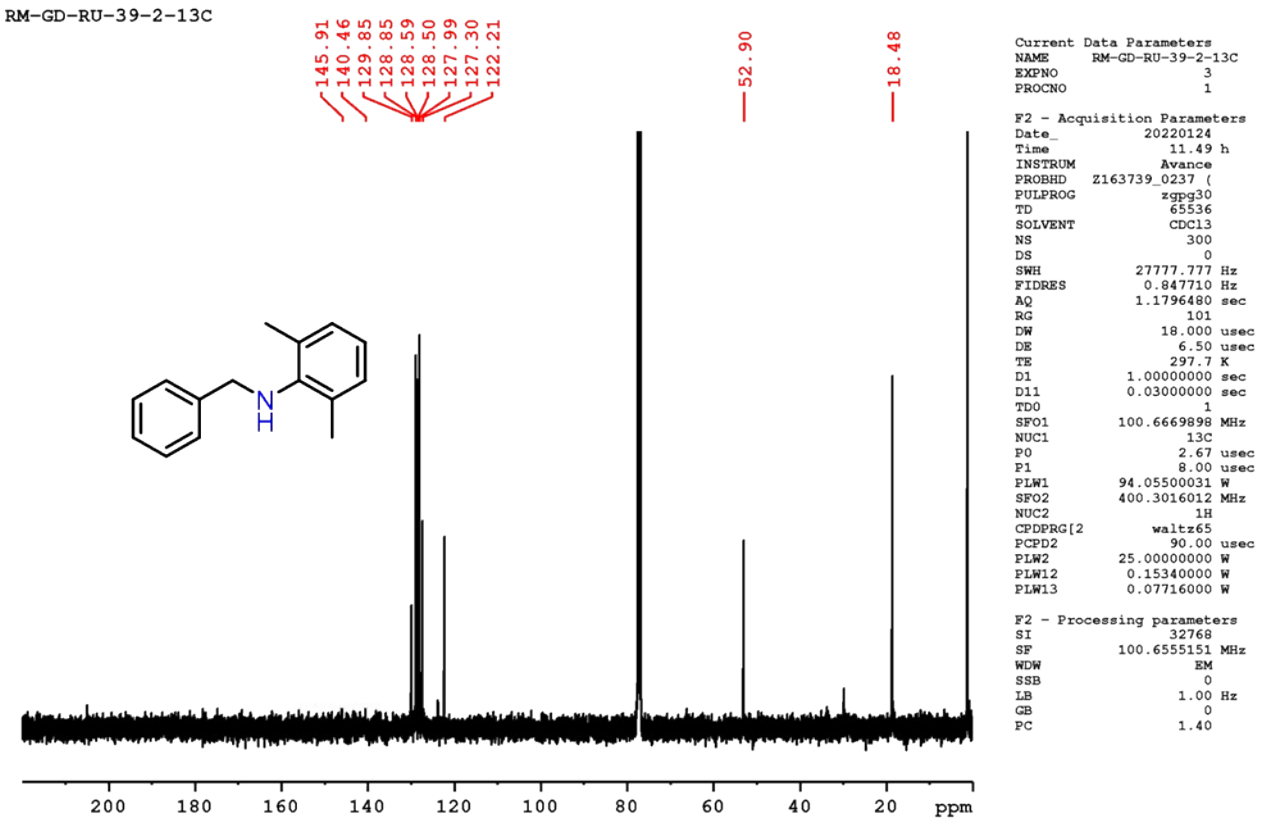

Figure S42. ^{13}C NMR spectrum of complex **1o** in $CDCl_3$ (100 MHz).

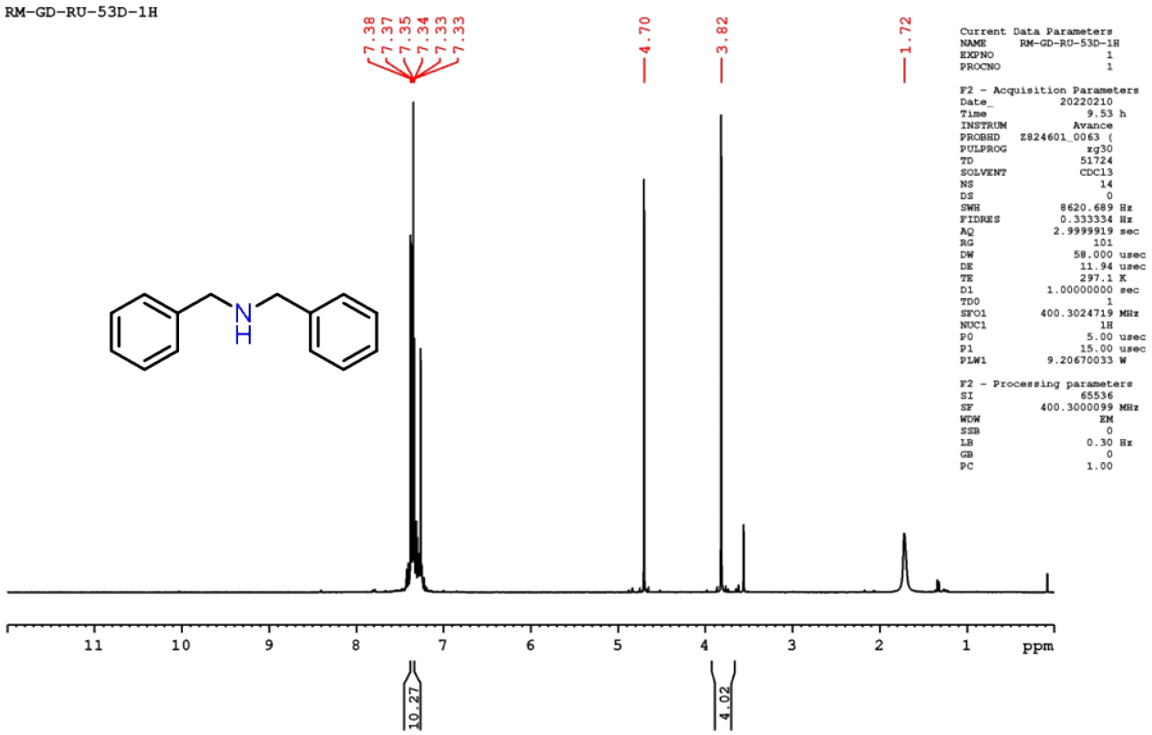

Figure S43. ^{1}H NMR spectrum of complex **1k** in $CDCl_3$ (400 MHz).

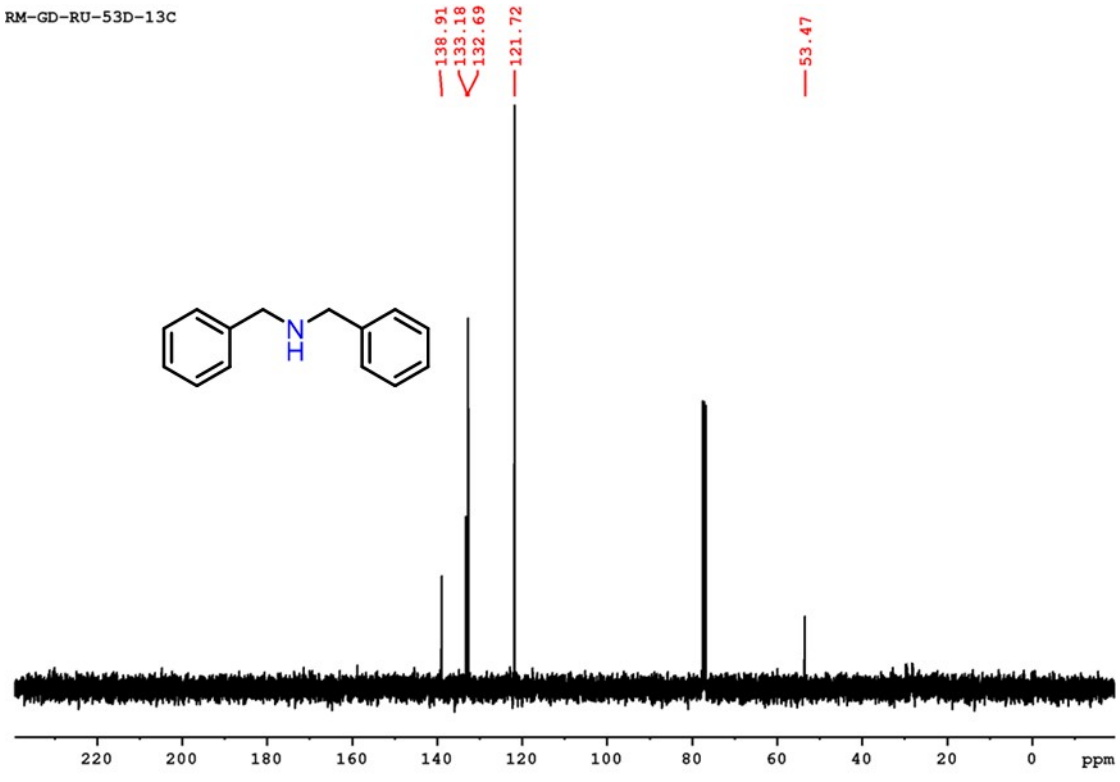

Figure S44. ^{13}C NMR spectrum of complex **1k** in $CDCl_3$ (100 MHz).

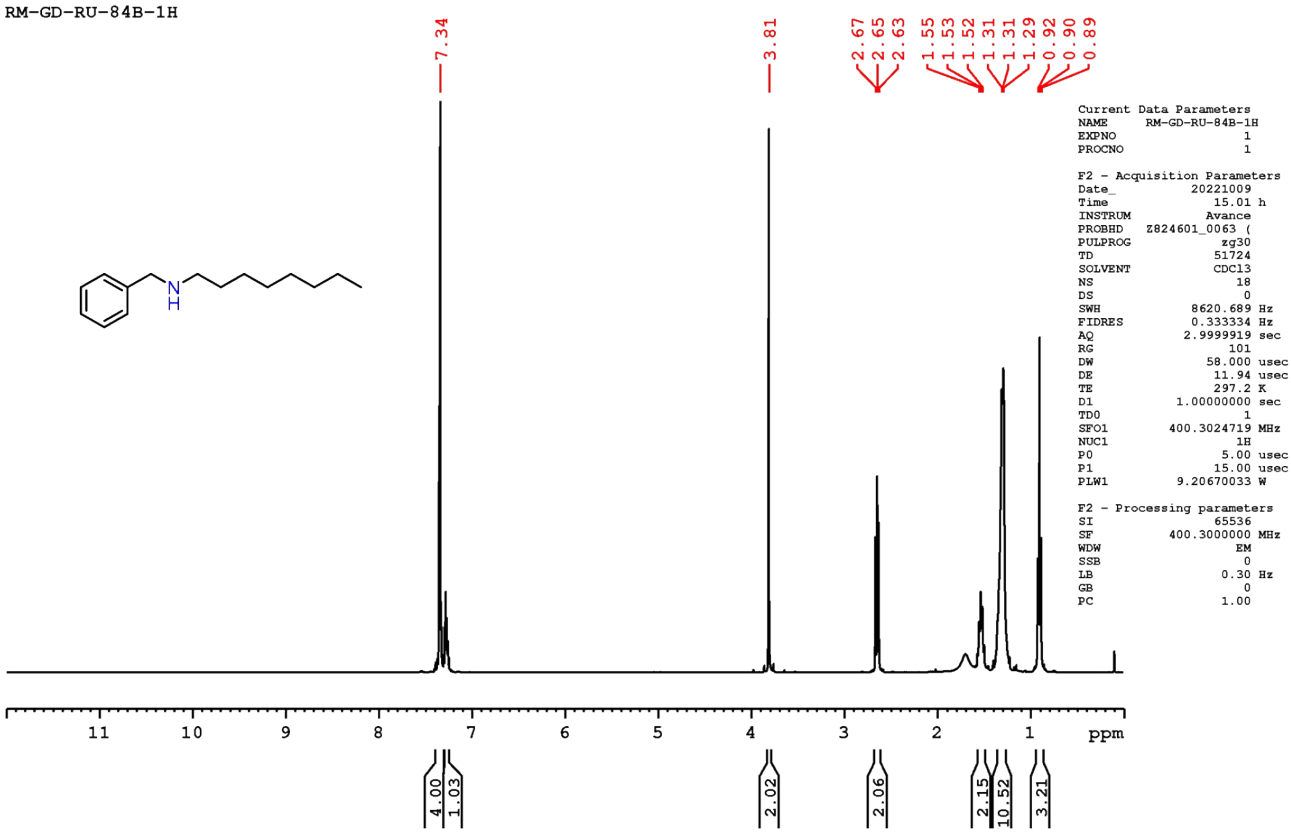

Figure S45. ^{1}H NMR spectrum of complex **1l** in $CDCl_3$ (400 MHz).

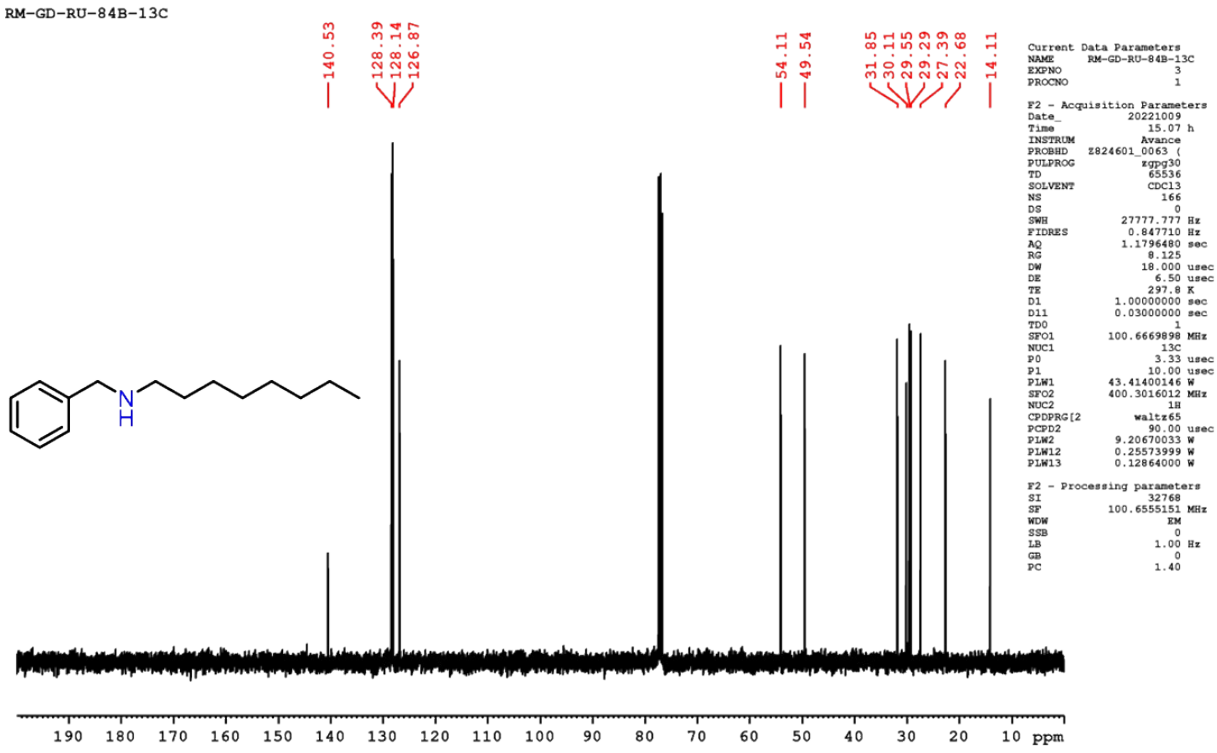

Figure S46. ^{13}C NMR spectrum of complex **1l** in $CDCl_3$ (100 MHz).

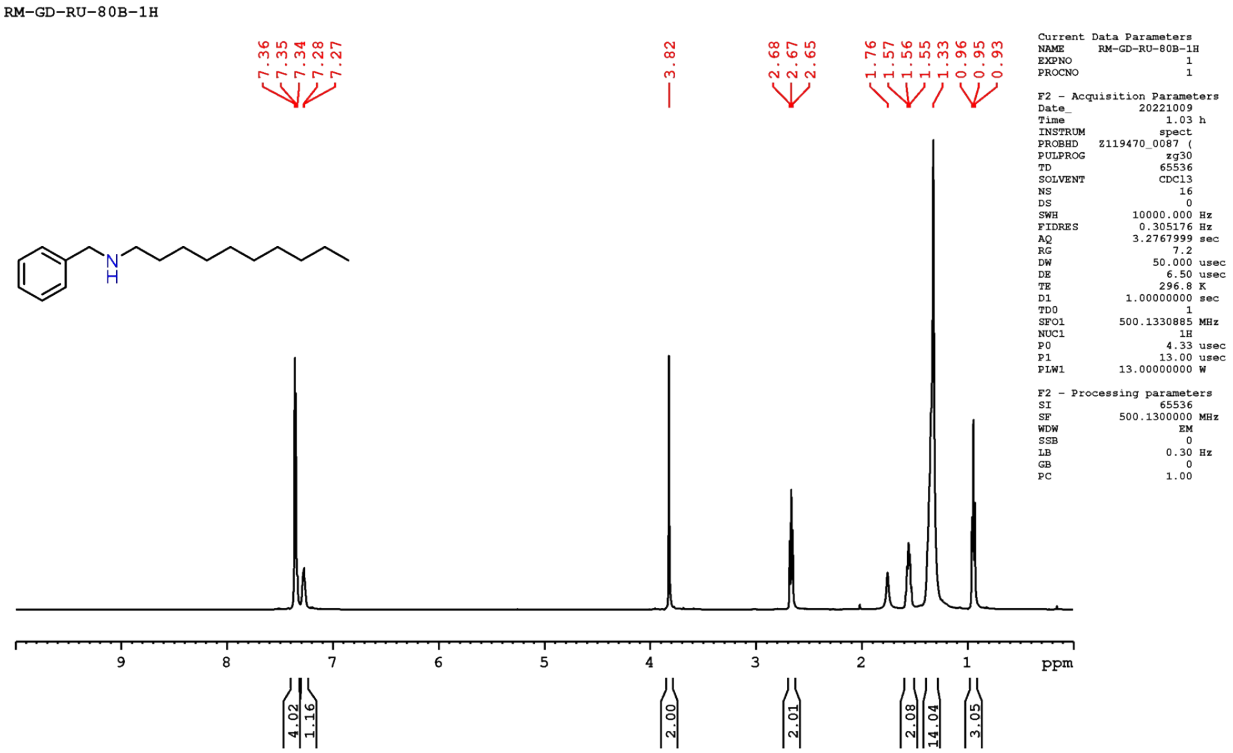

Figure S47. ^{1}H NMR spectrum of complex **1m** in $CDCl_3$ (400 MHz).

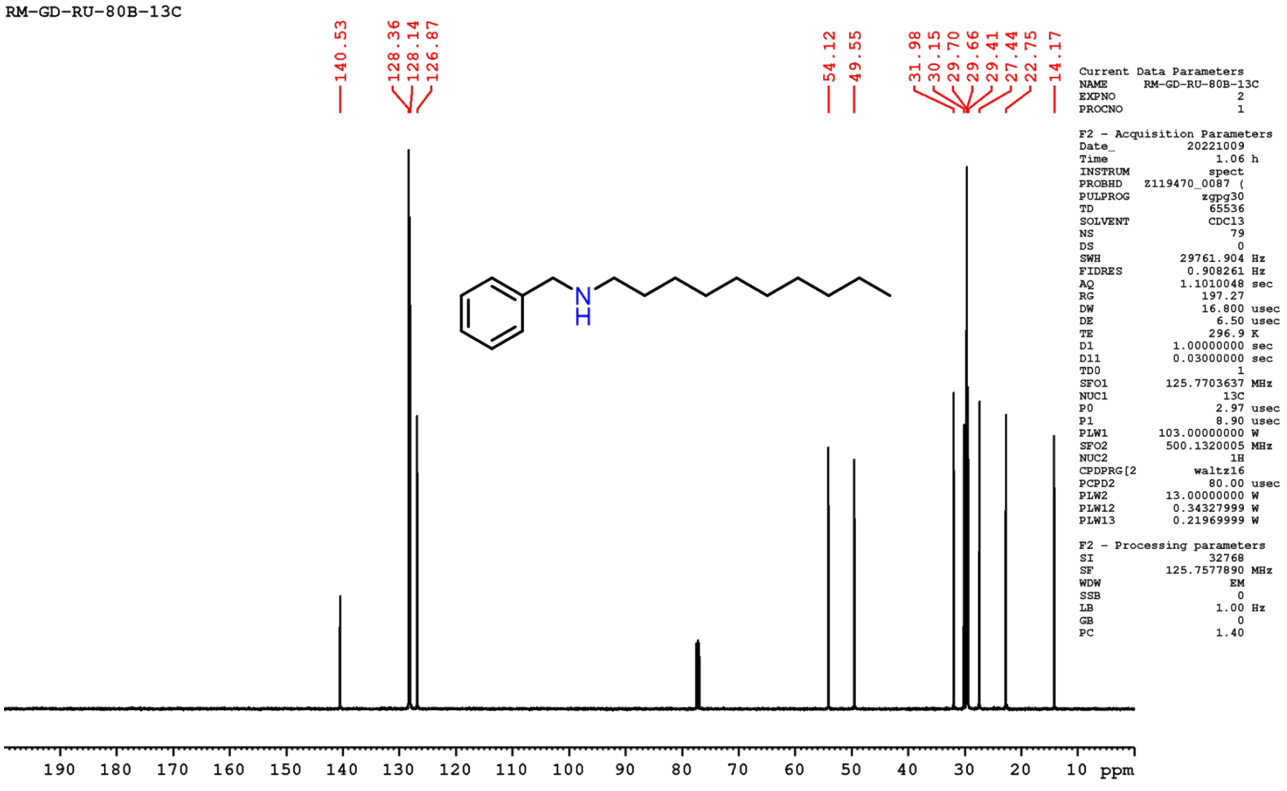

Figure S48. ^{13}C NMR spectrum of complex **1m** in $CDCl_3$ (100 MHz).

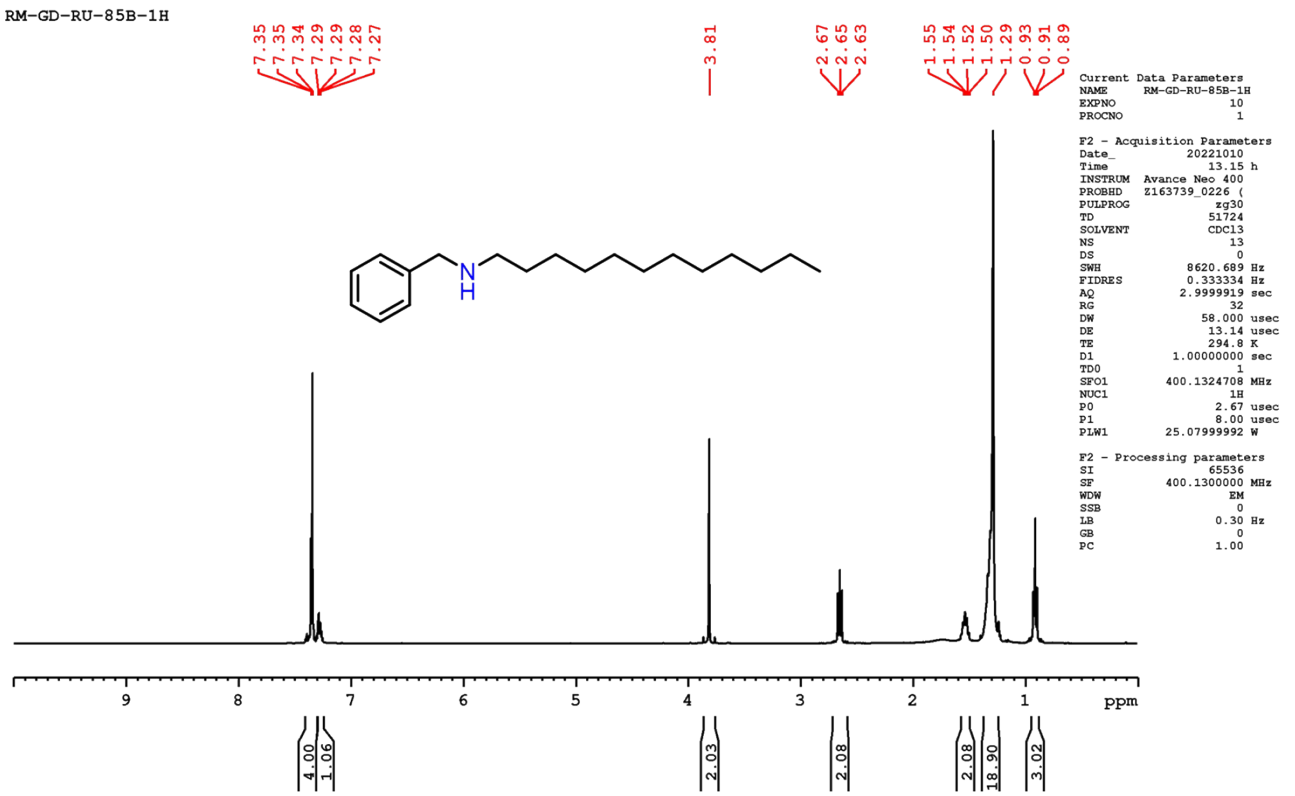

Figure S49. ^{1}H NMR spectrum of complex **1n** in $CDCl_3$ (400 MHz).

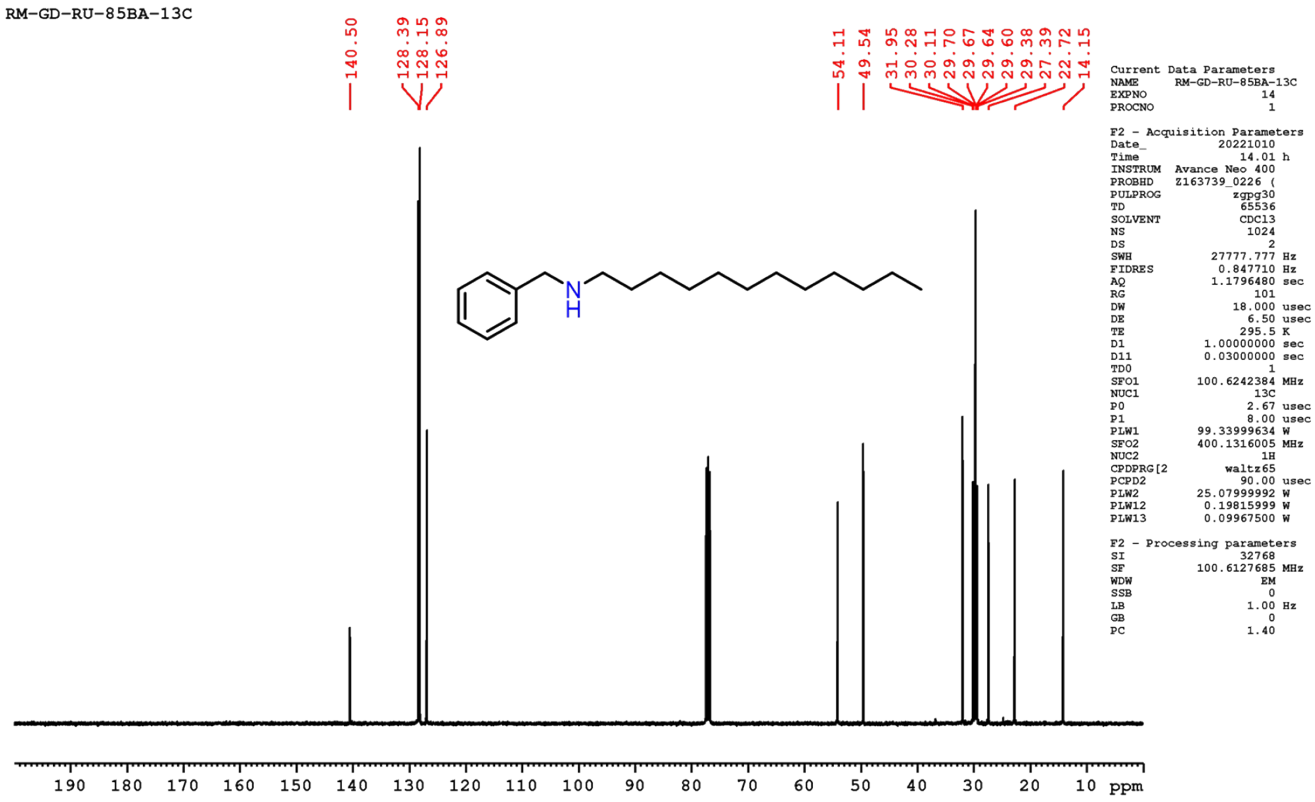

Figure S50. ^{13}C NMR spectrum of complex **1n** in $CDCl_3$ (100 MHz).

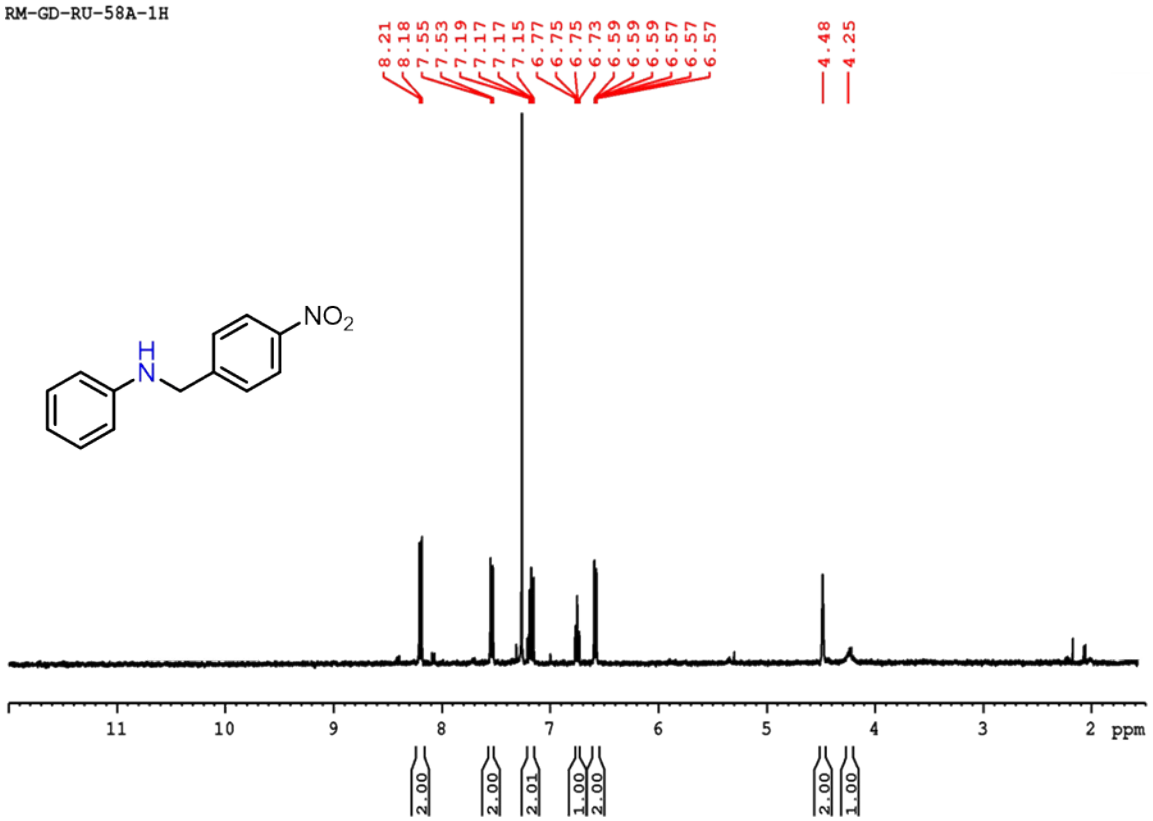

Figure S51. ^{1}H NMR spectrum of complex **2b** in $CDCl_3$ (400 MHz).

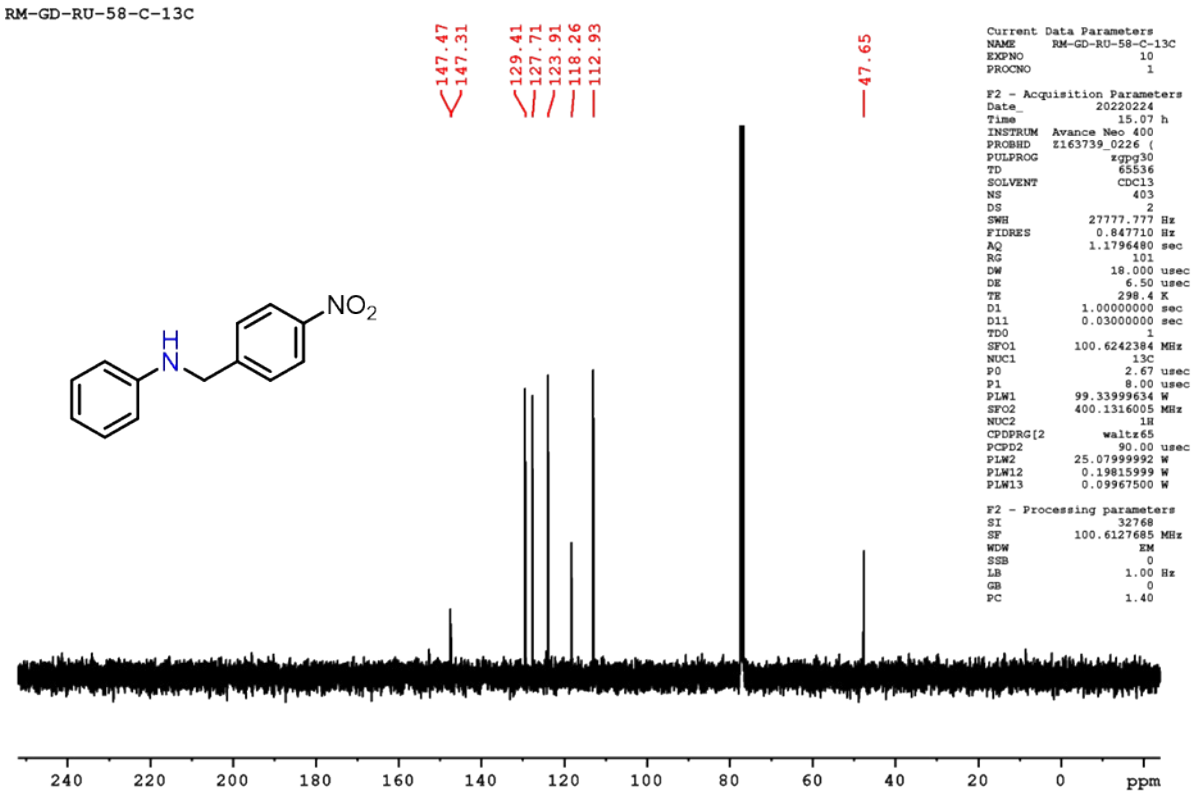

Figure S52. ^{13}C NMR spectrum of complex **2b** in $CDCl_3$ (100 MHz).

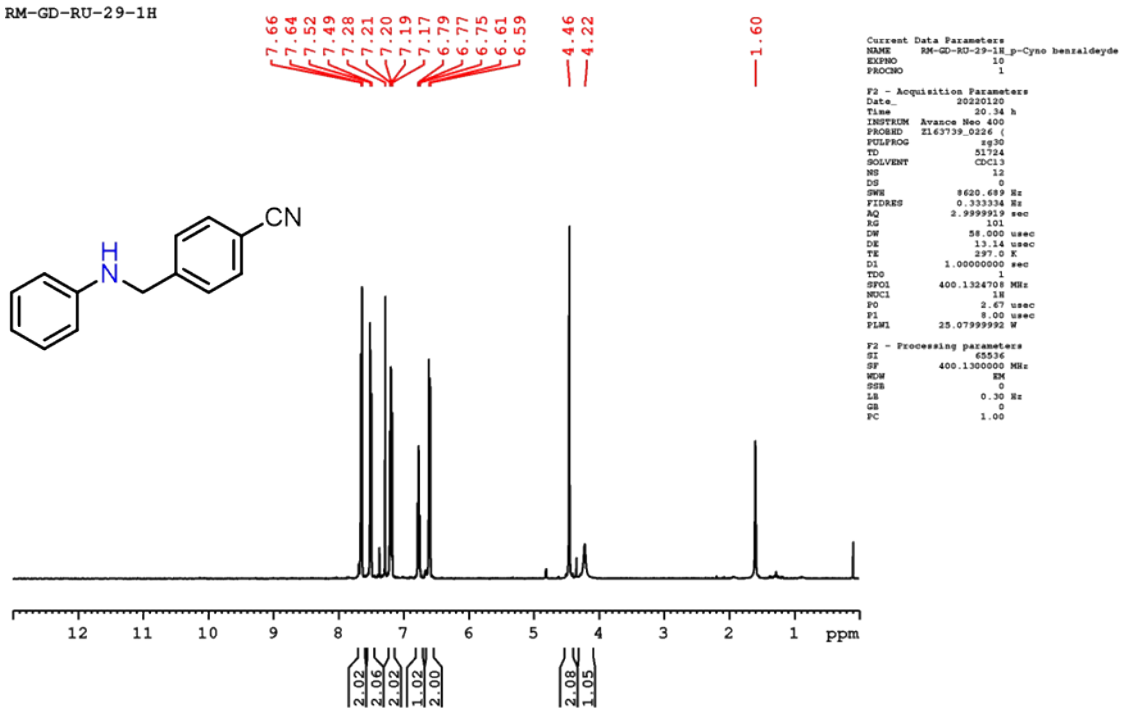

Figure S53. ^{1}H NMR spectrum of complex **2c** in $CDCl_3$ (400 MHz).

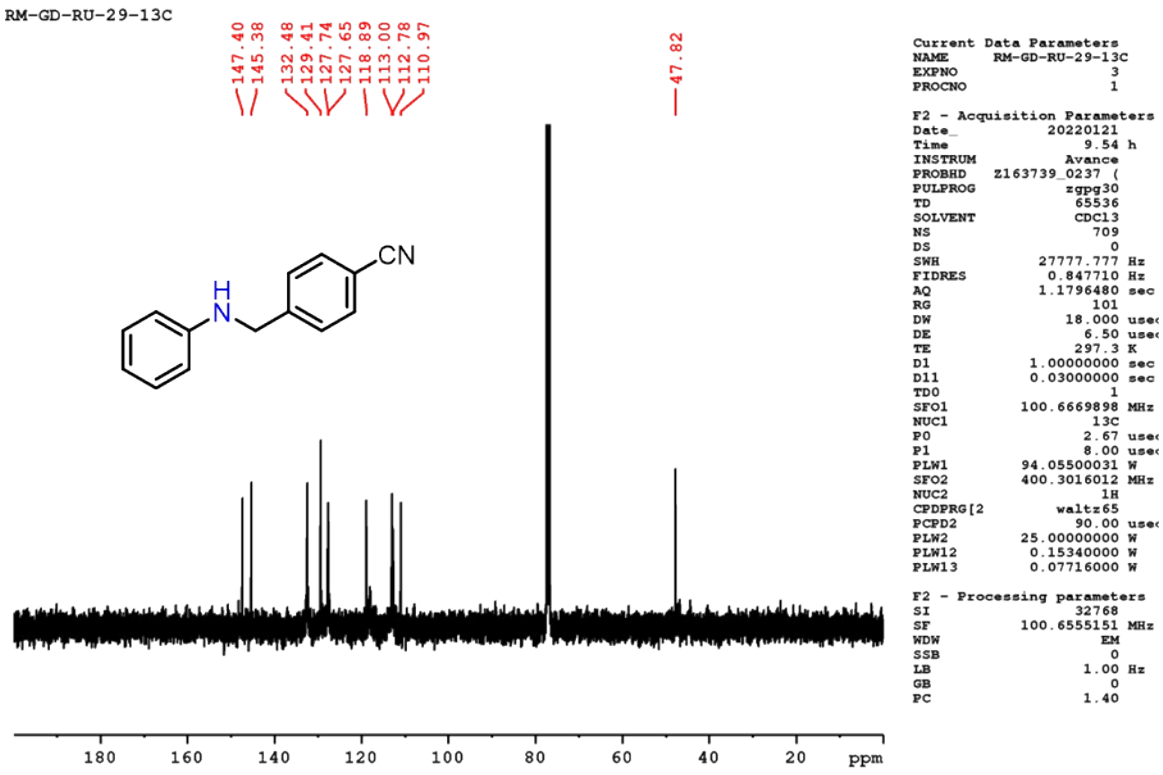

Figure S54. ^{13}C NMR spectrum of complex **2c** in $CDCl_3$ (100 MHz).

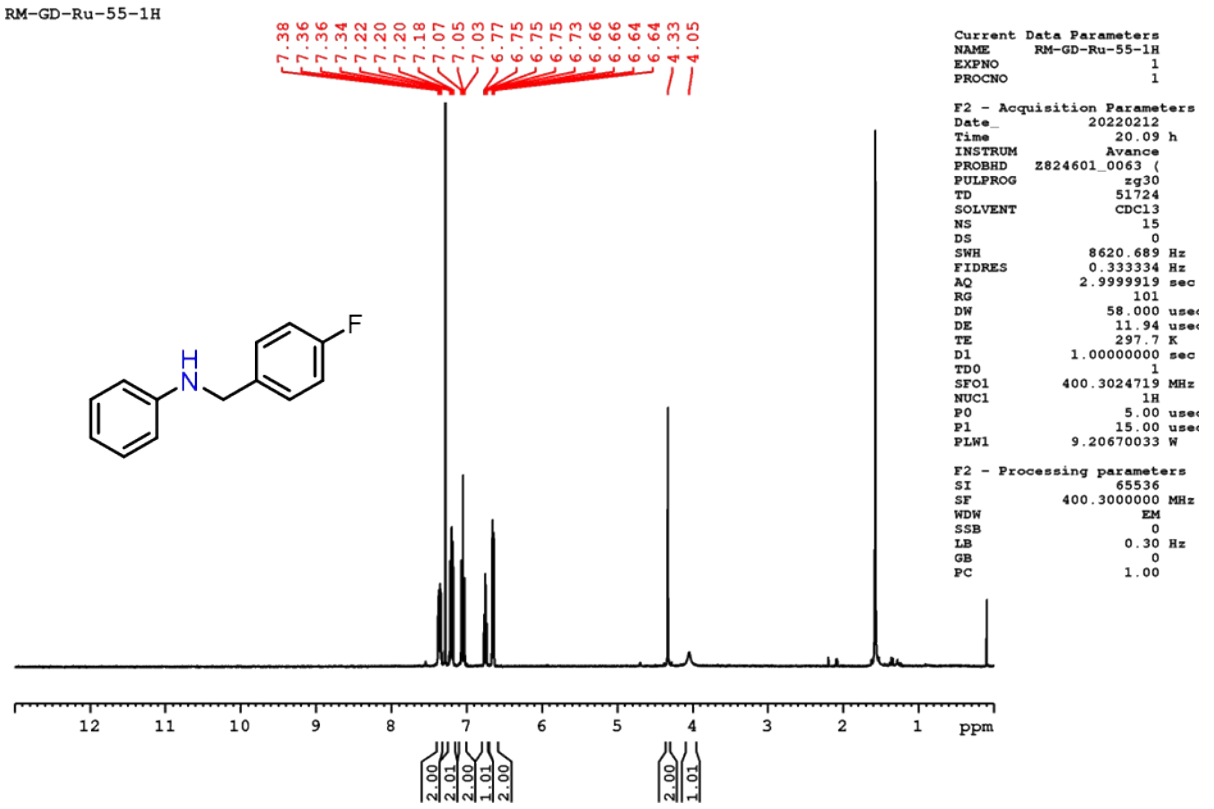

Figure S55. ^{1}H NMR spectrum of complex **2f** in $CDCl_3$ (400 MHz).

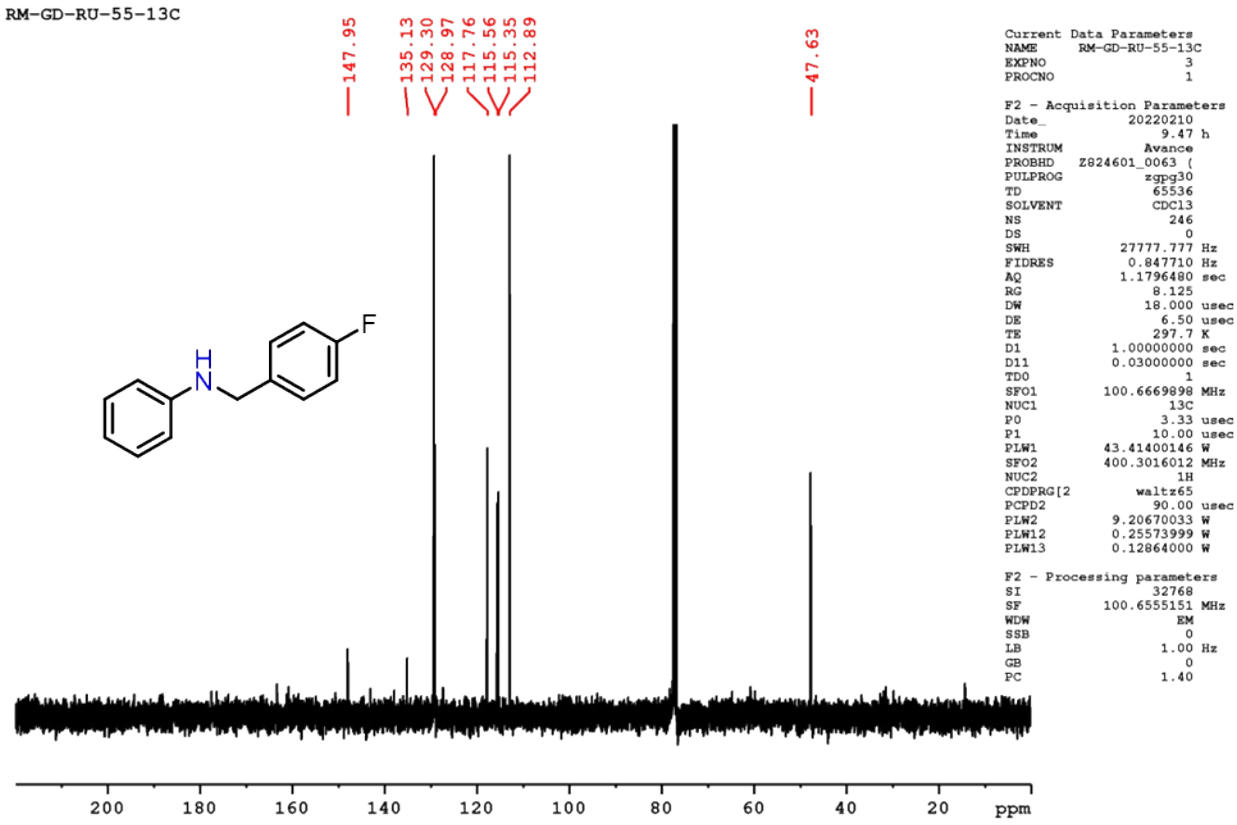

Figure S60. ^{13}C NMR spectrum of complex **2f** in $CDCl_3$ (100 MHz).

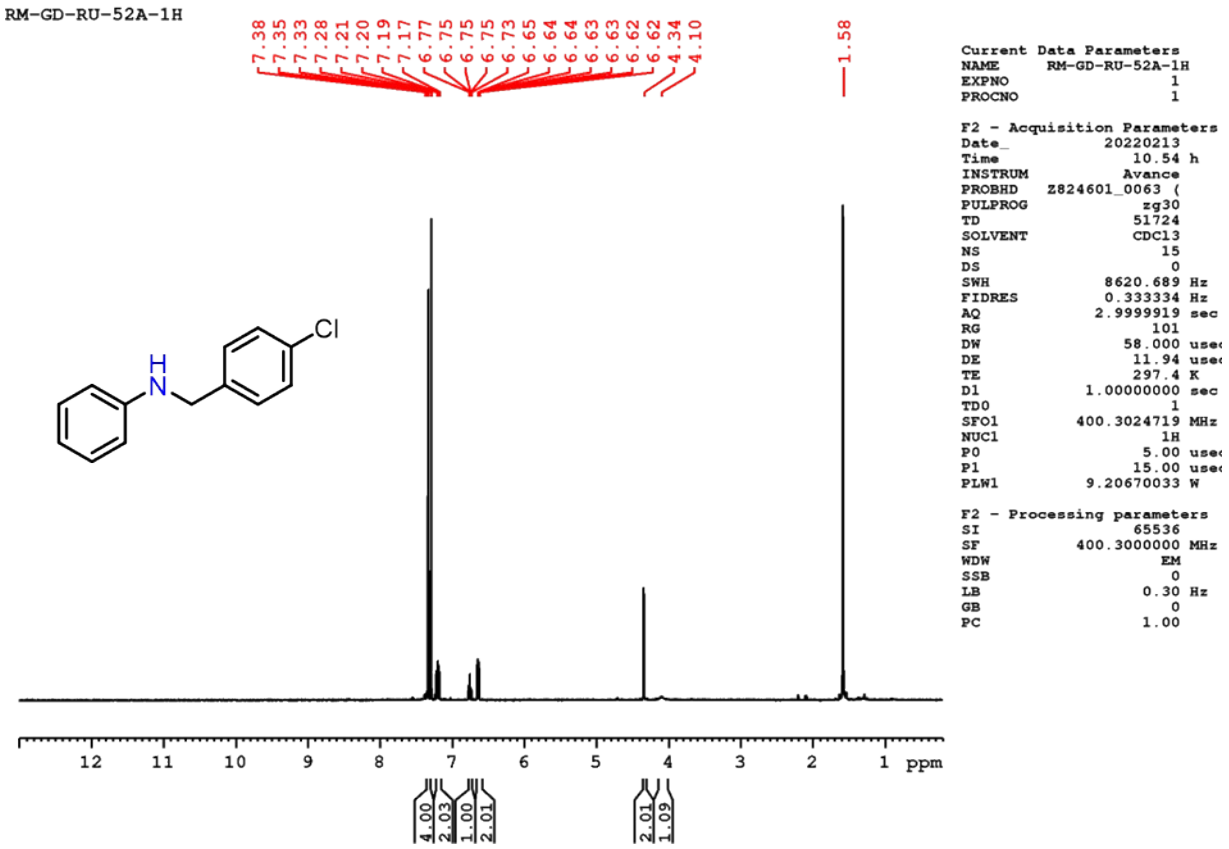

Figure S61. ^{1}H NMR spectrum of complex **2g** in $CDCl_3$ (400 MHz).

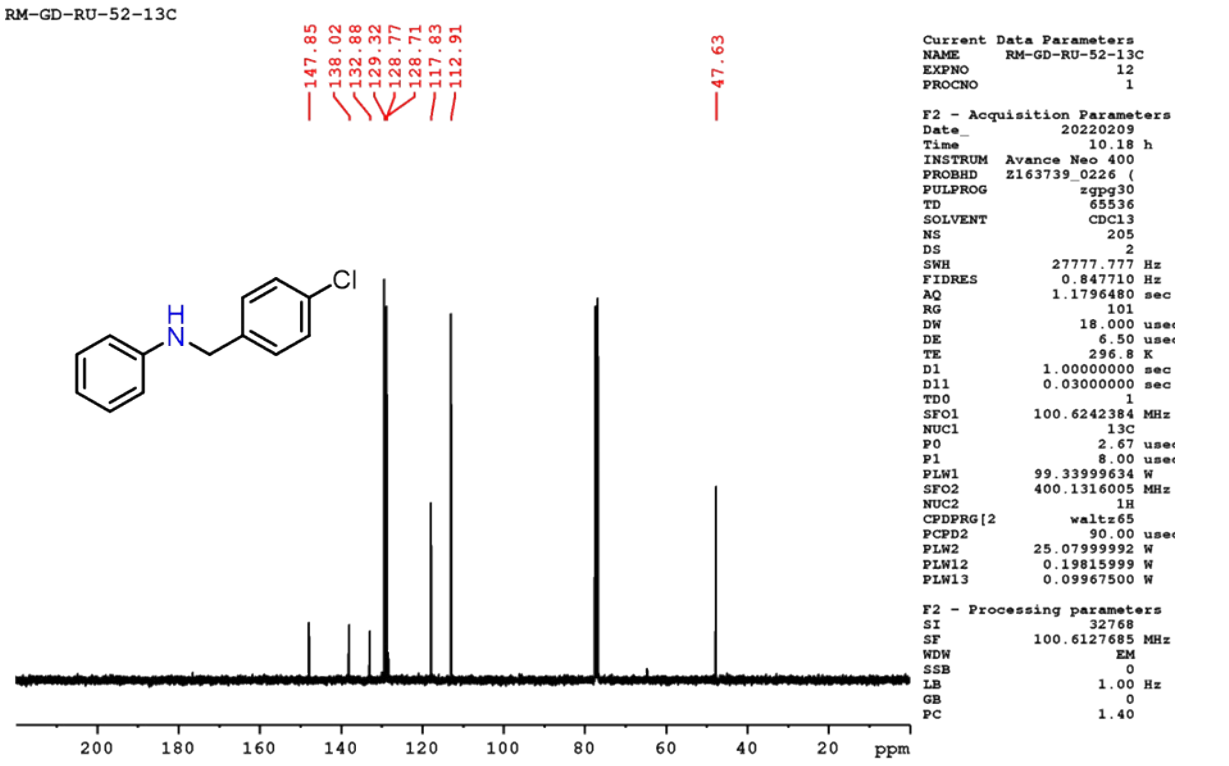

Figure S62. ^{13}C NMR spectrum of complex **2g** in $CDCl_3$ (100 MHz).

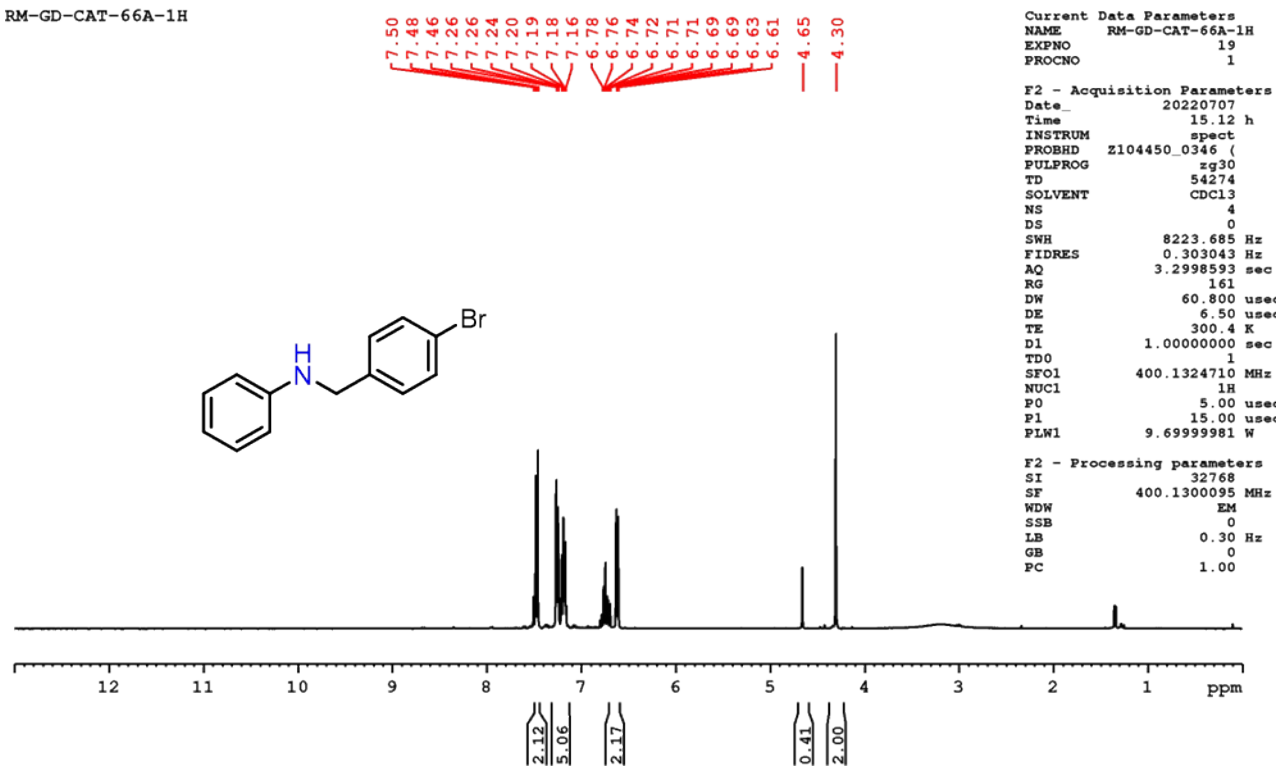

Figure S63. ^{1}H NMR spectrum of complex **2h** in $CDCl_3$ (400 MHz).

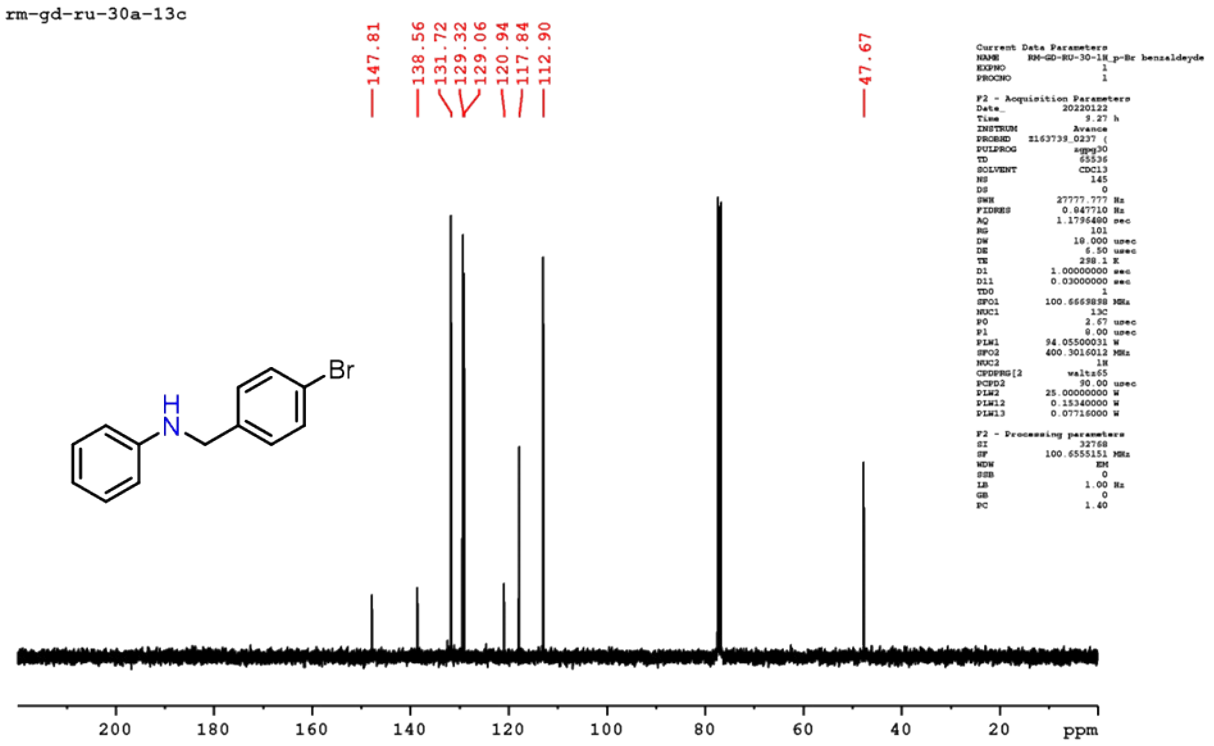

Figure S64. ^{13}C NMR spectrum of complex **2h** in $CDCl_3$ (100 MHz).

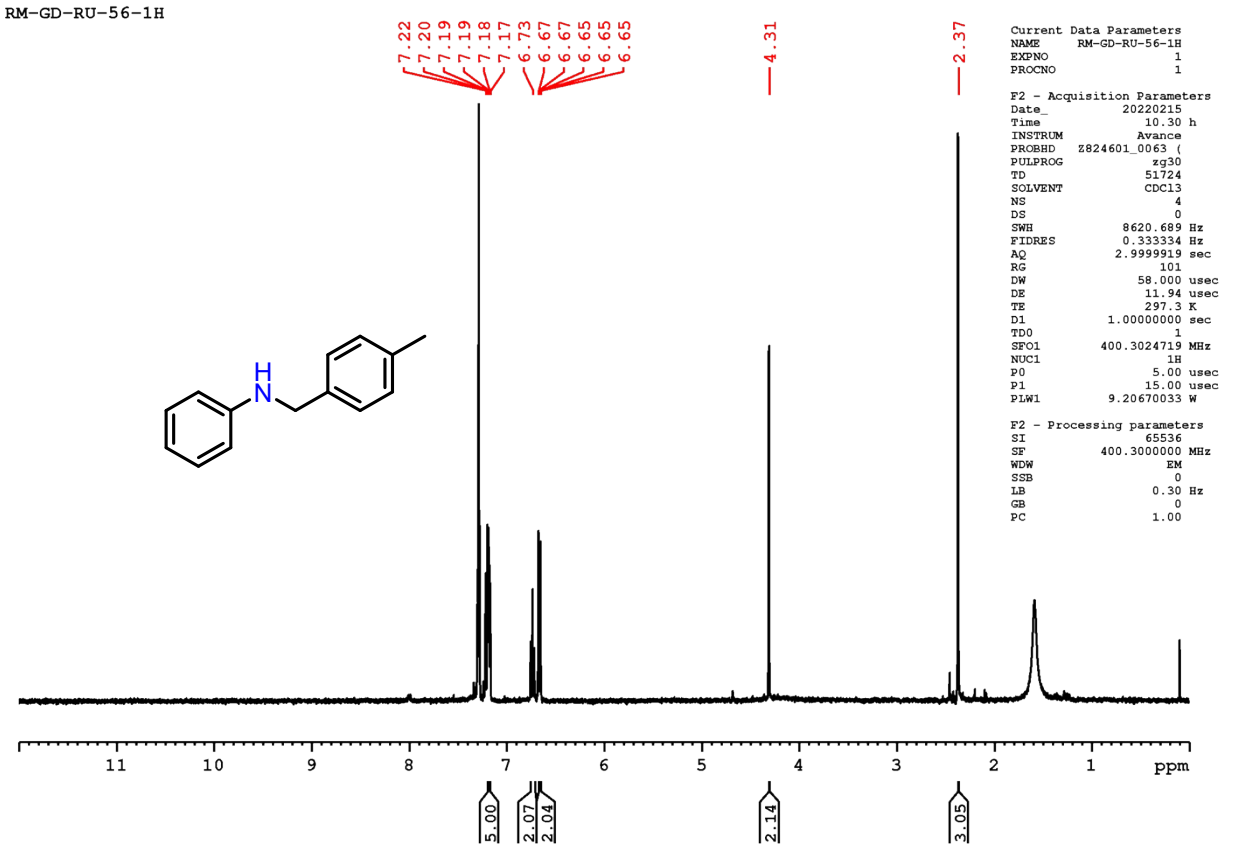

Figure S65. ^{1}H NMR spectrum of complex **2d** in $CDCl_3$ (400 MHz).

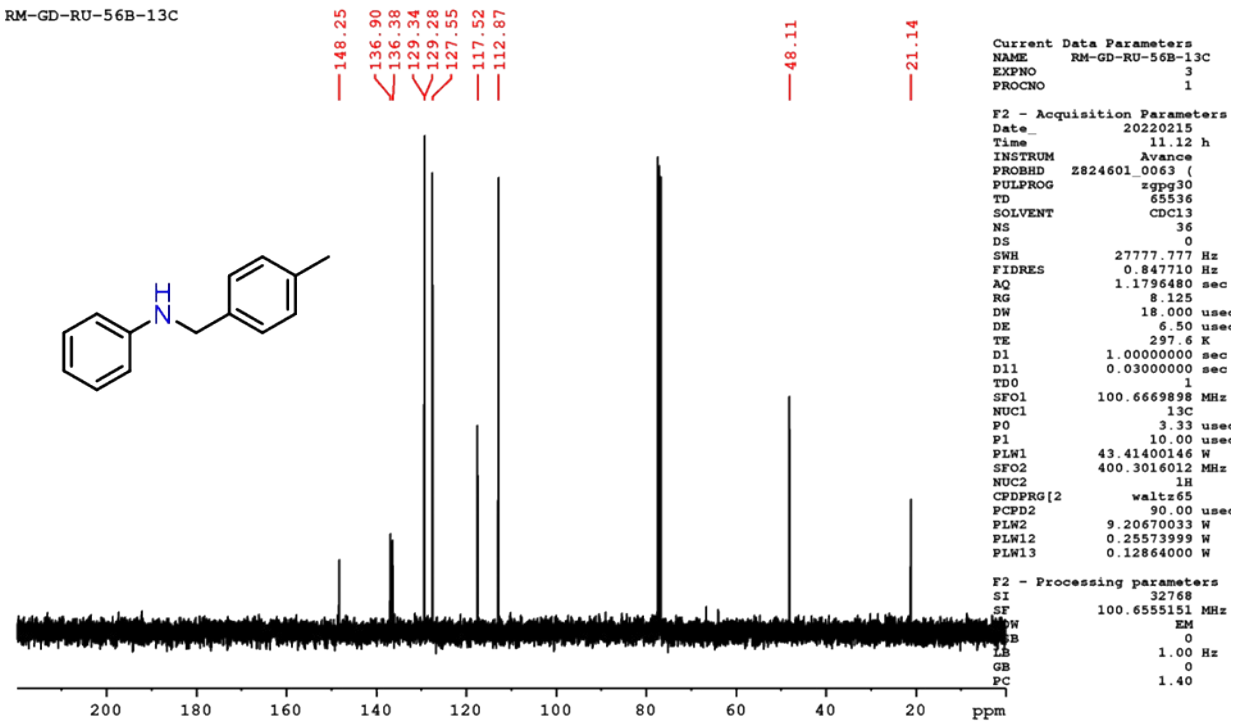

Figure S66. ^{13}C NMR spectrum of complex **2d** in $CDCl_3$ (100 MHz).

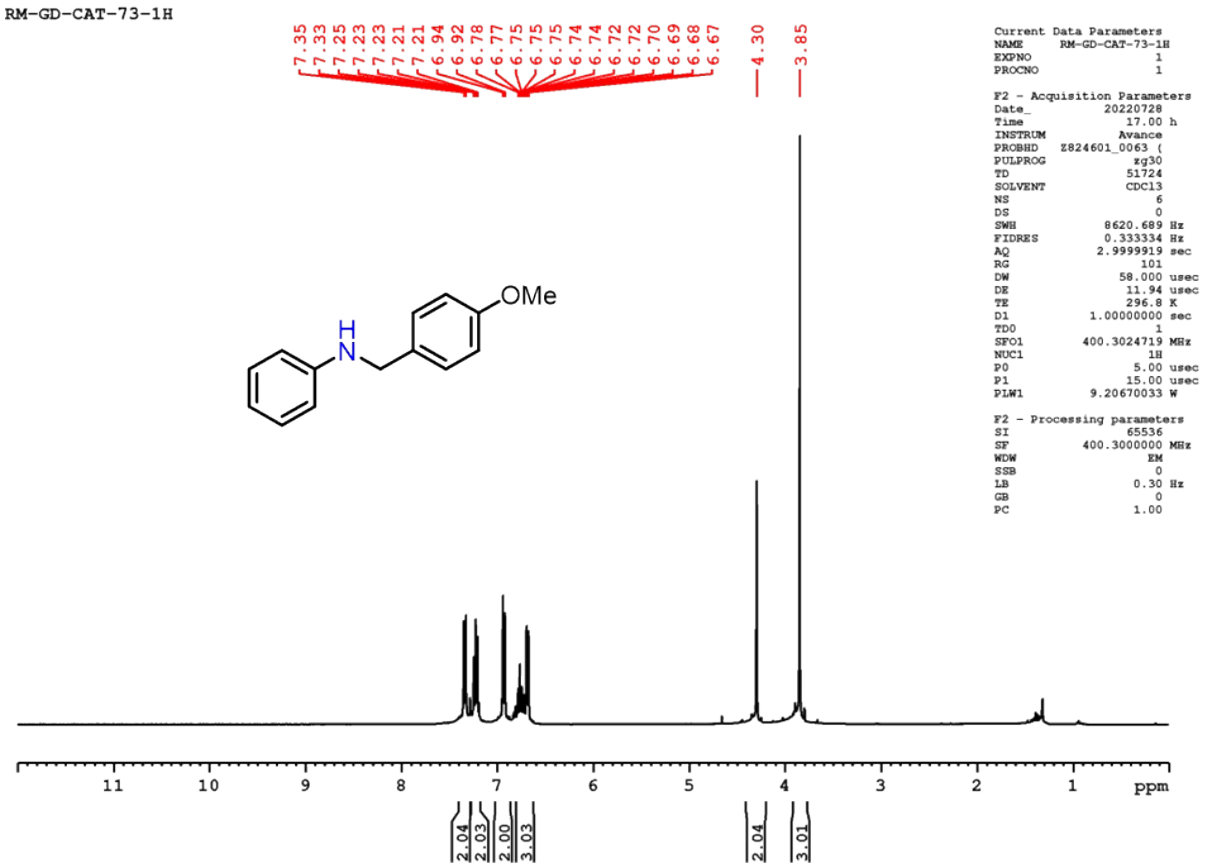

Figure S67. ^{1}H NMR spectrum of complex **2e** in $CDCl_3$ (400 MHz).

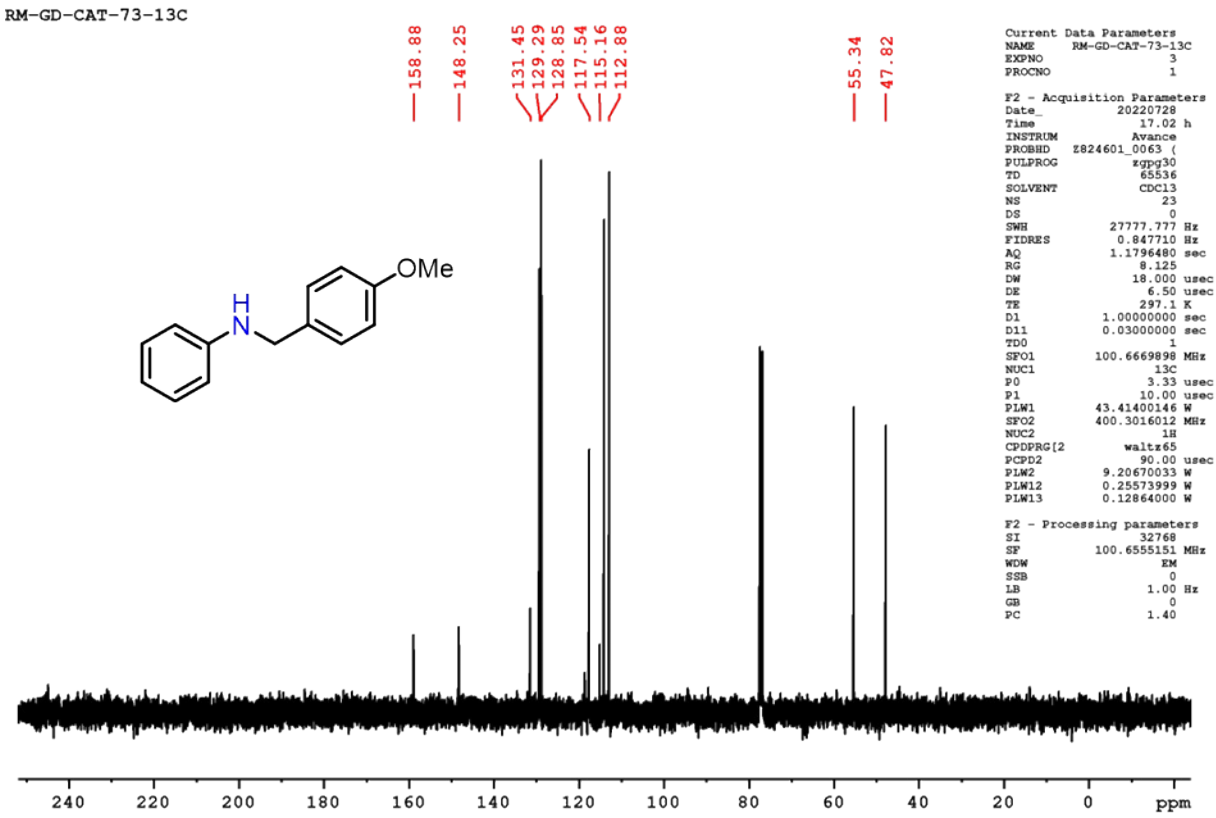

Figure S68. ^{13}C NMR spectrum of complex **2e** in $CDCl_3$ (100 MHz).

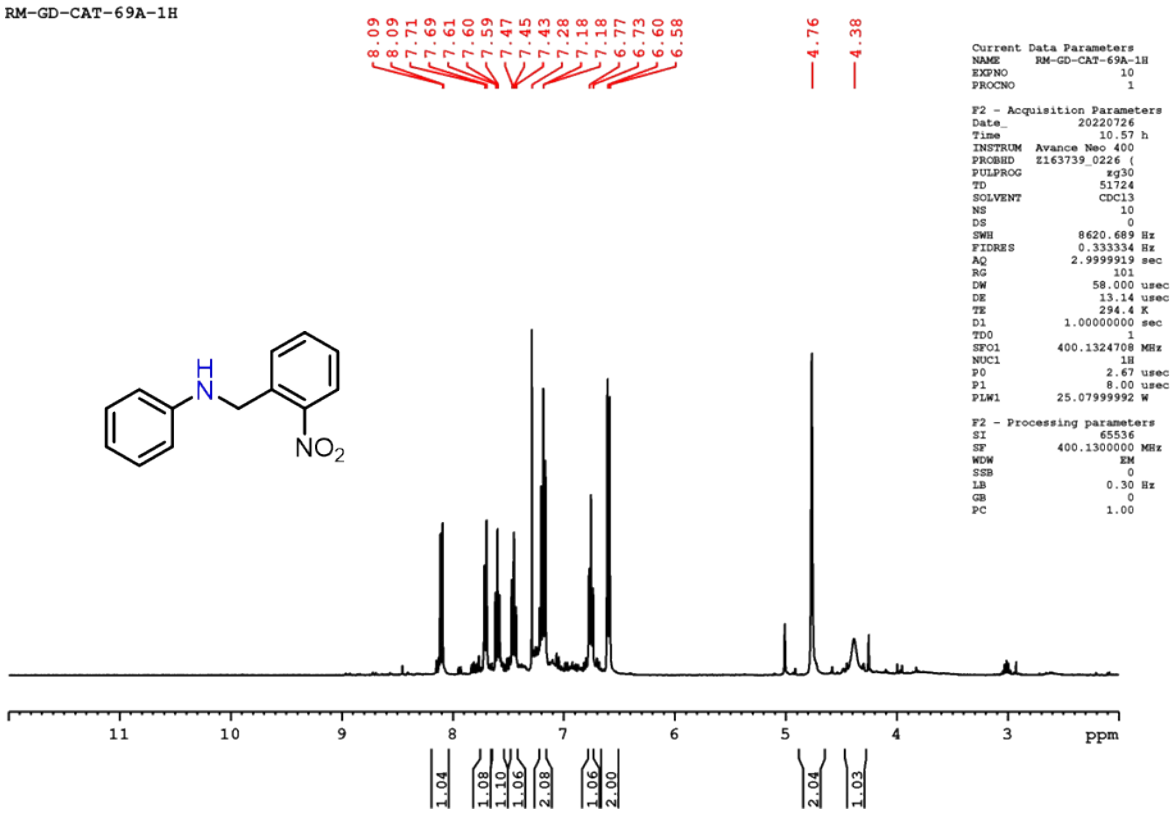

Figure S69. ^{1}H NMR spectrum of complex **2i** in $CDCl_3$ (400 MHz).

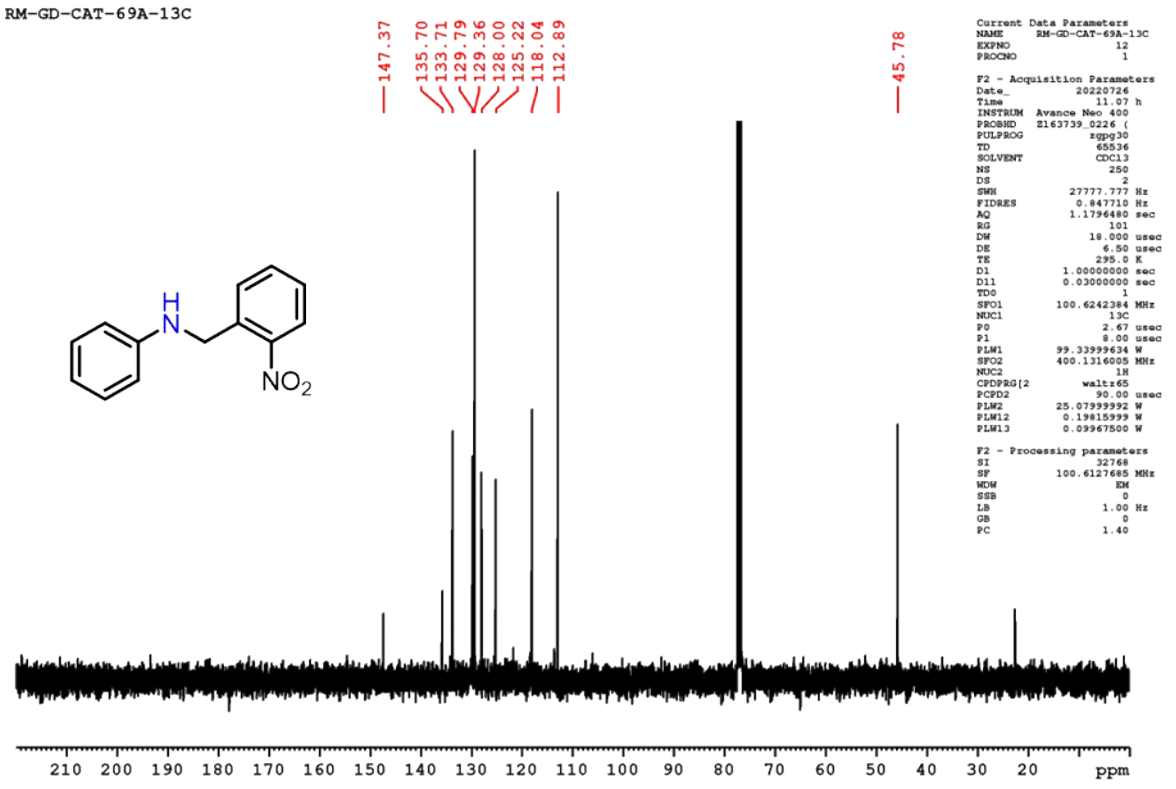

Figure S70. ^{13}C NMR spectrum of complex **2i** in $CDCl_3$ (100 MHz).

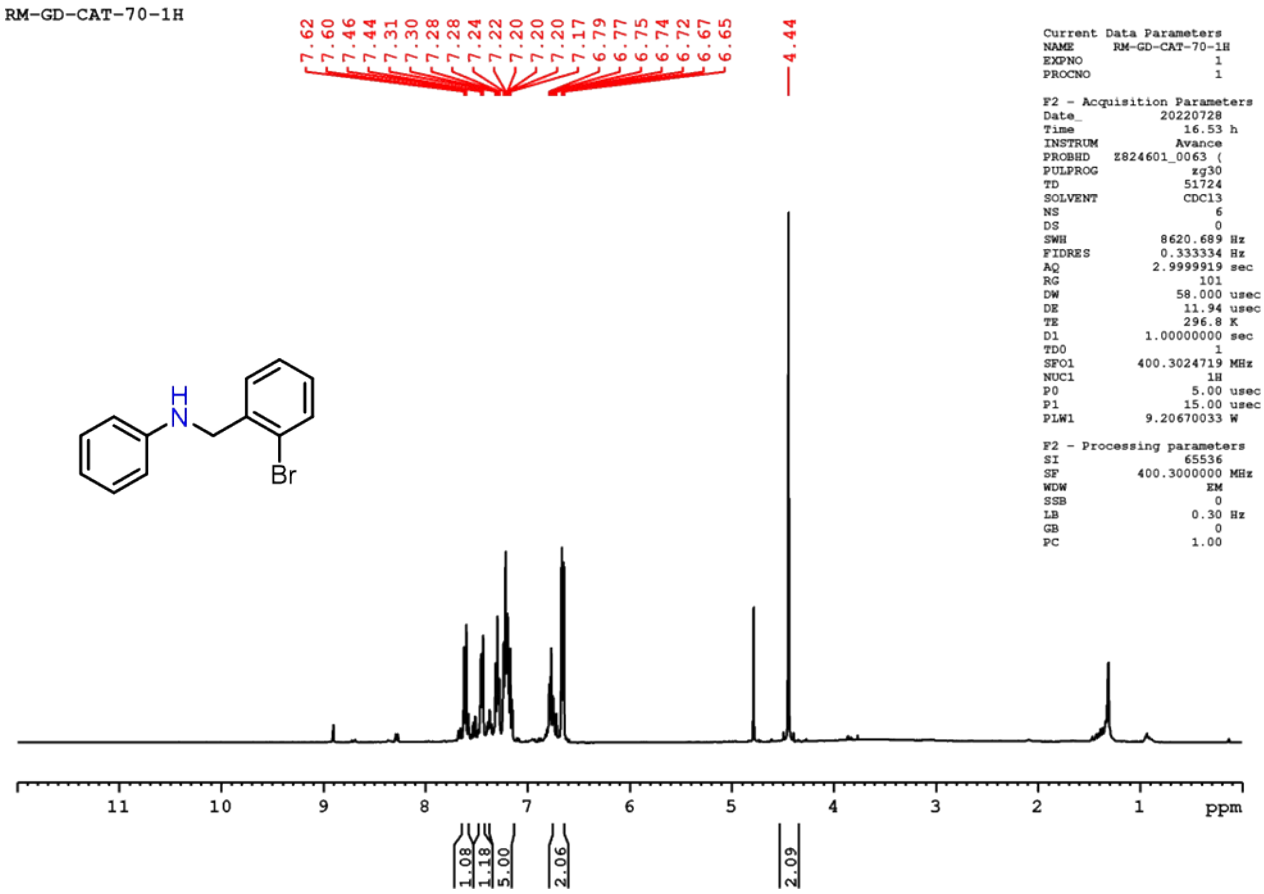

Figure S71. ^{1}H NMR spectrum of complex **2j** in $CDCl_3$ (400 MHz).

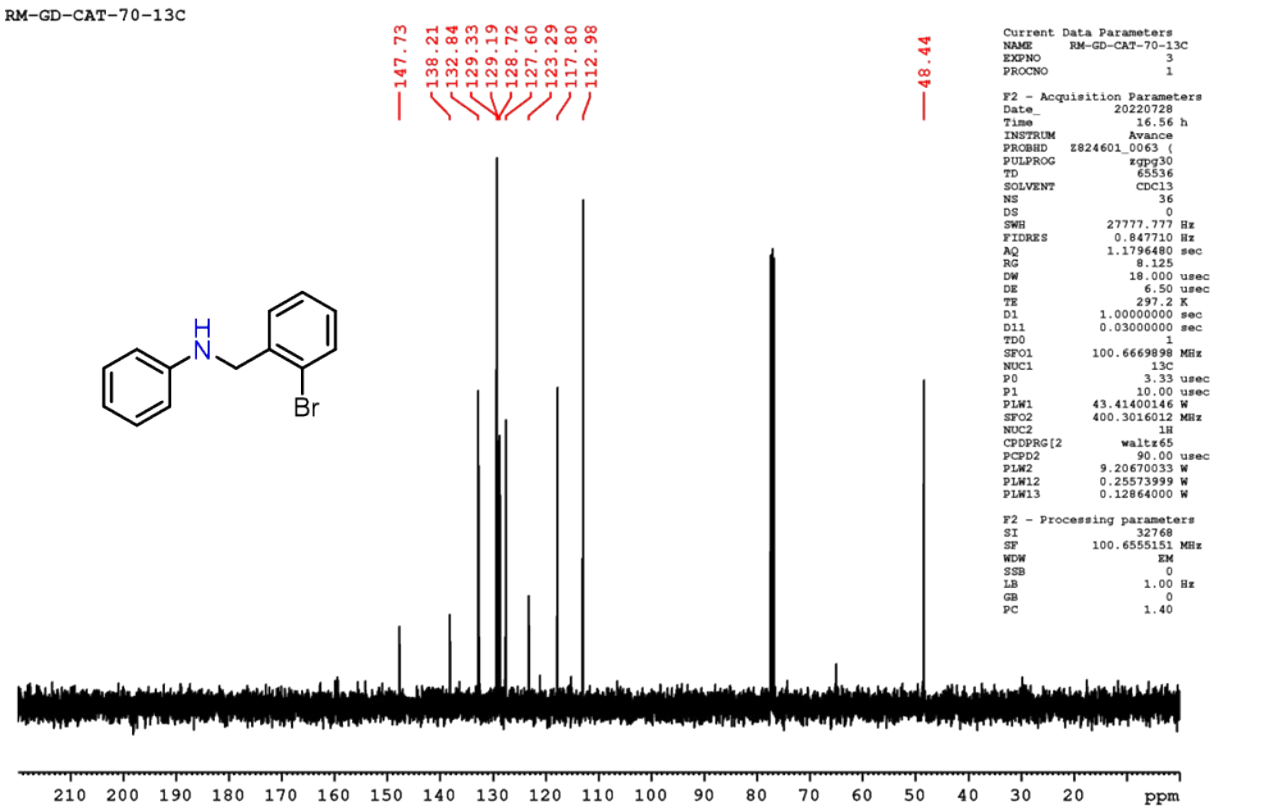

Figure S72. ^{13}C NMR spectrum of complex **2j** in $CDCl_3$ (100 MHz).

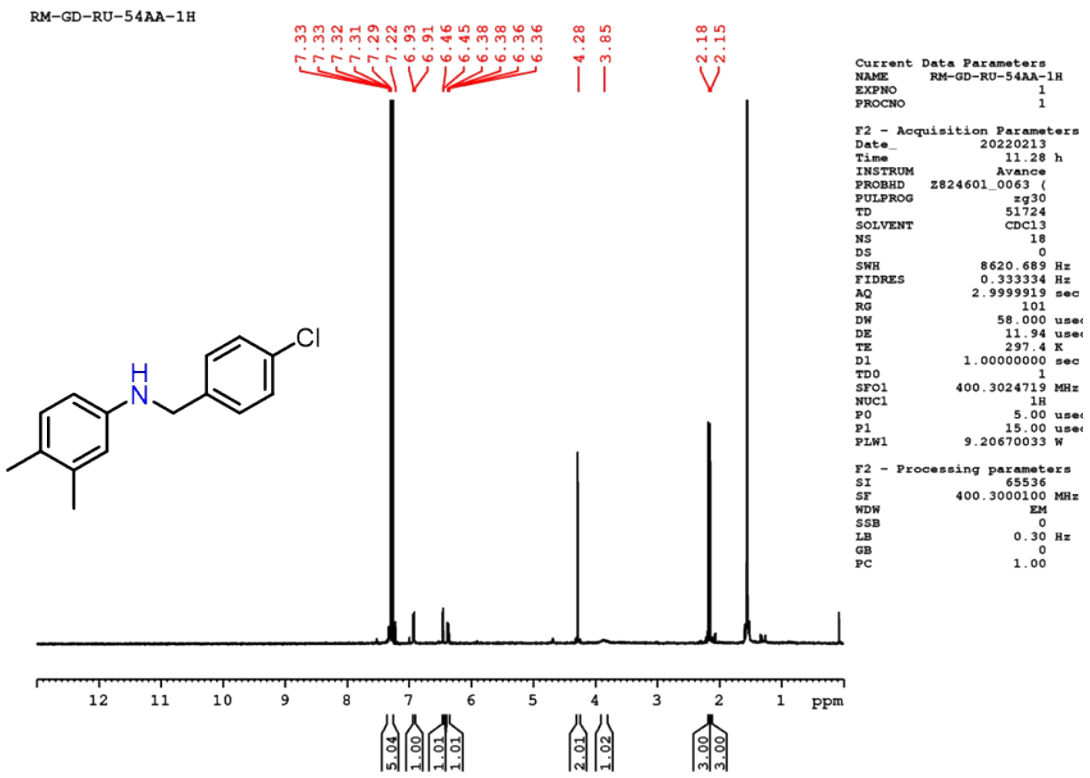

Figure S73. ^{1}H NMR spectrum of complex **2p** in $CDCl_3$ (400 MHz).

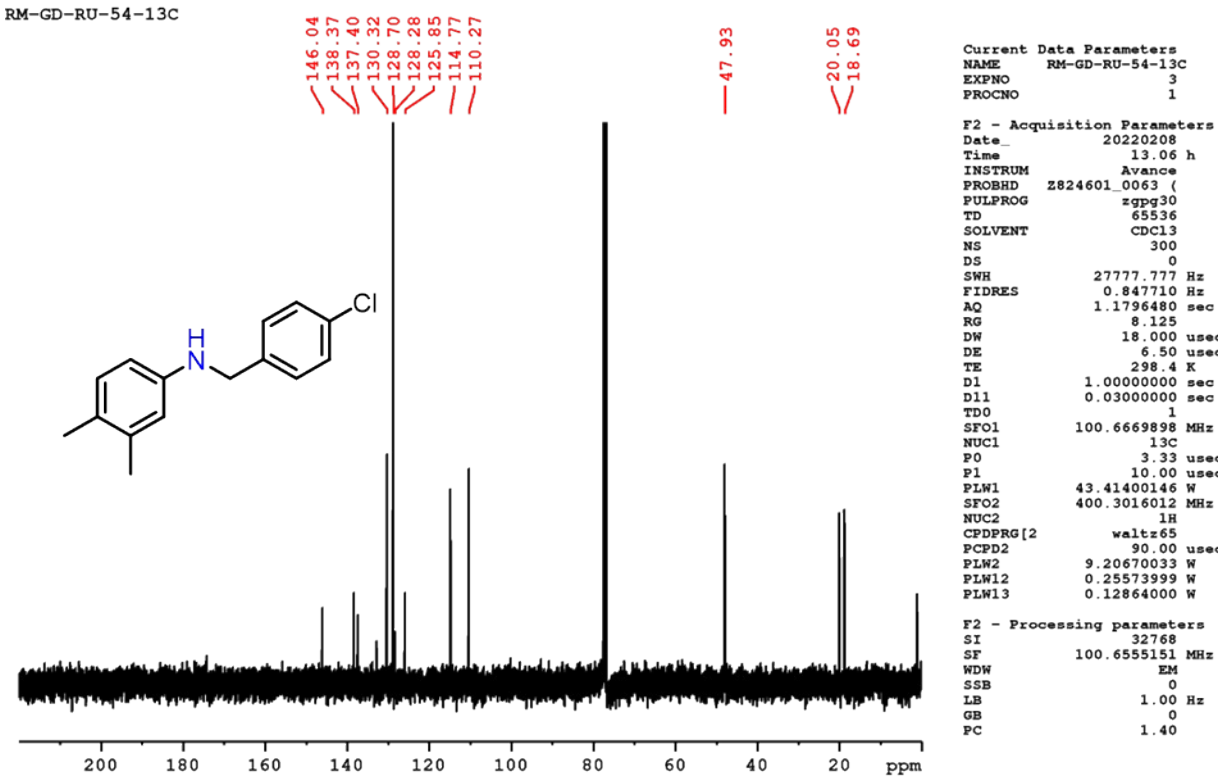

Figure S74. ^{13}C NMR spectrum of complex **2p** in $CDCl_3$ (100 MHz).

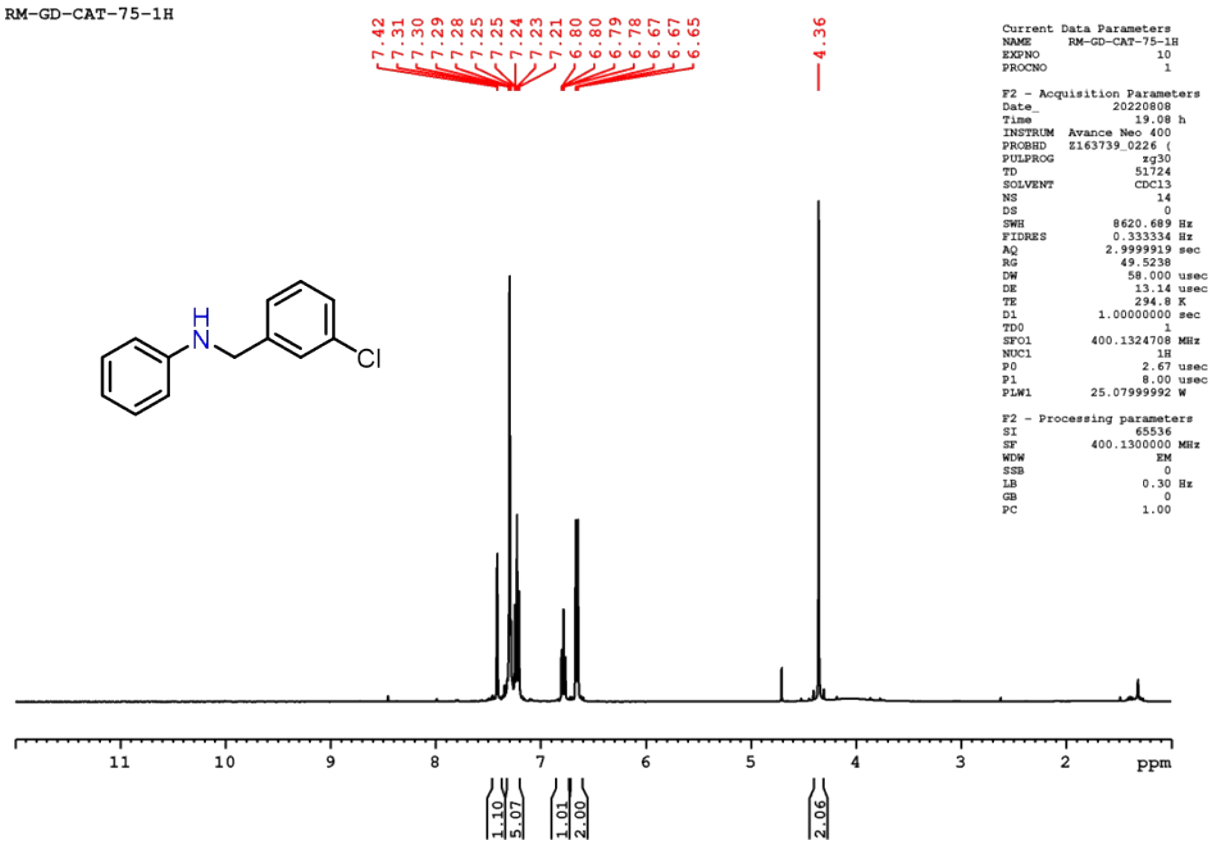

Figure S75. ^{1}H NMR spectrum of complex **2k** in $CDCl_3$ (400 MHz).

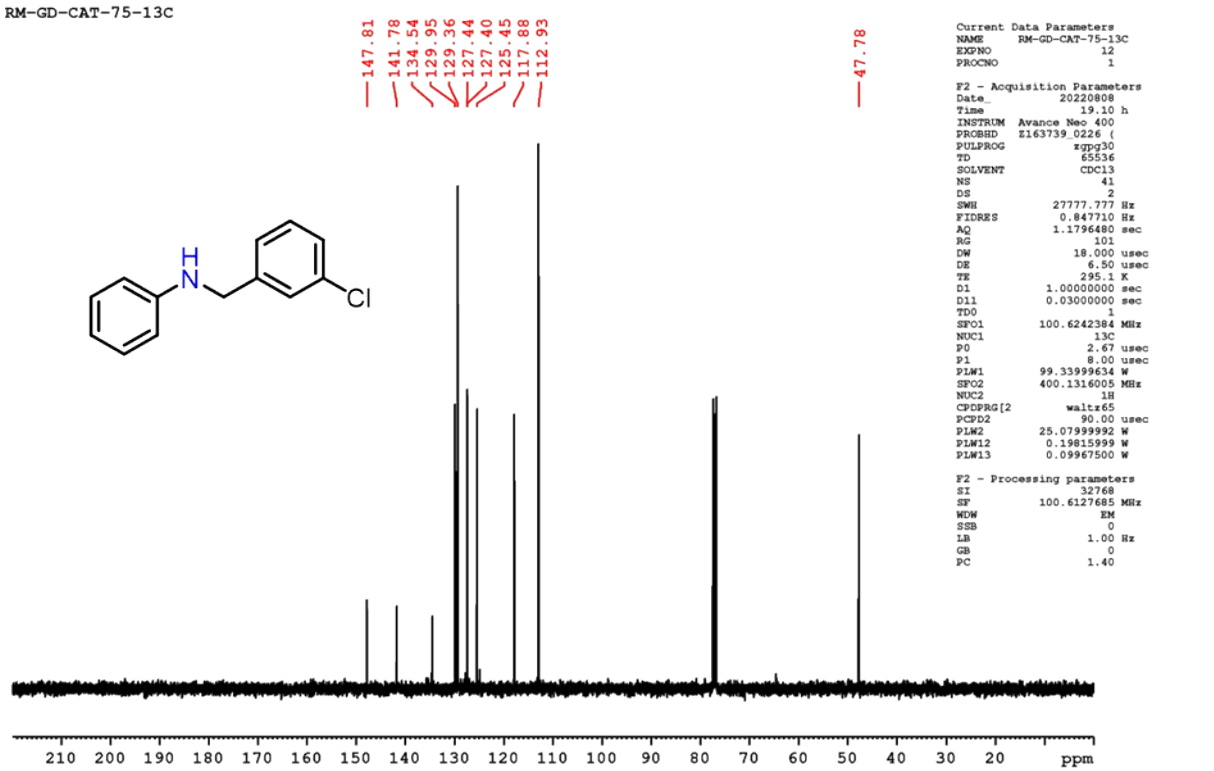

Figure S76. ^{13}C NMR spectrum of complex **2k** in $CDCl_3$ (100 MHz).

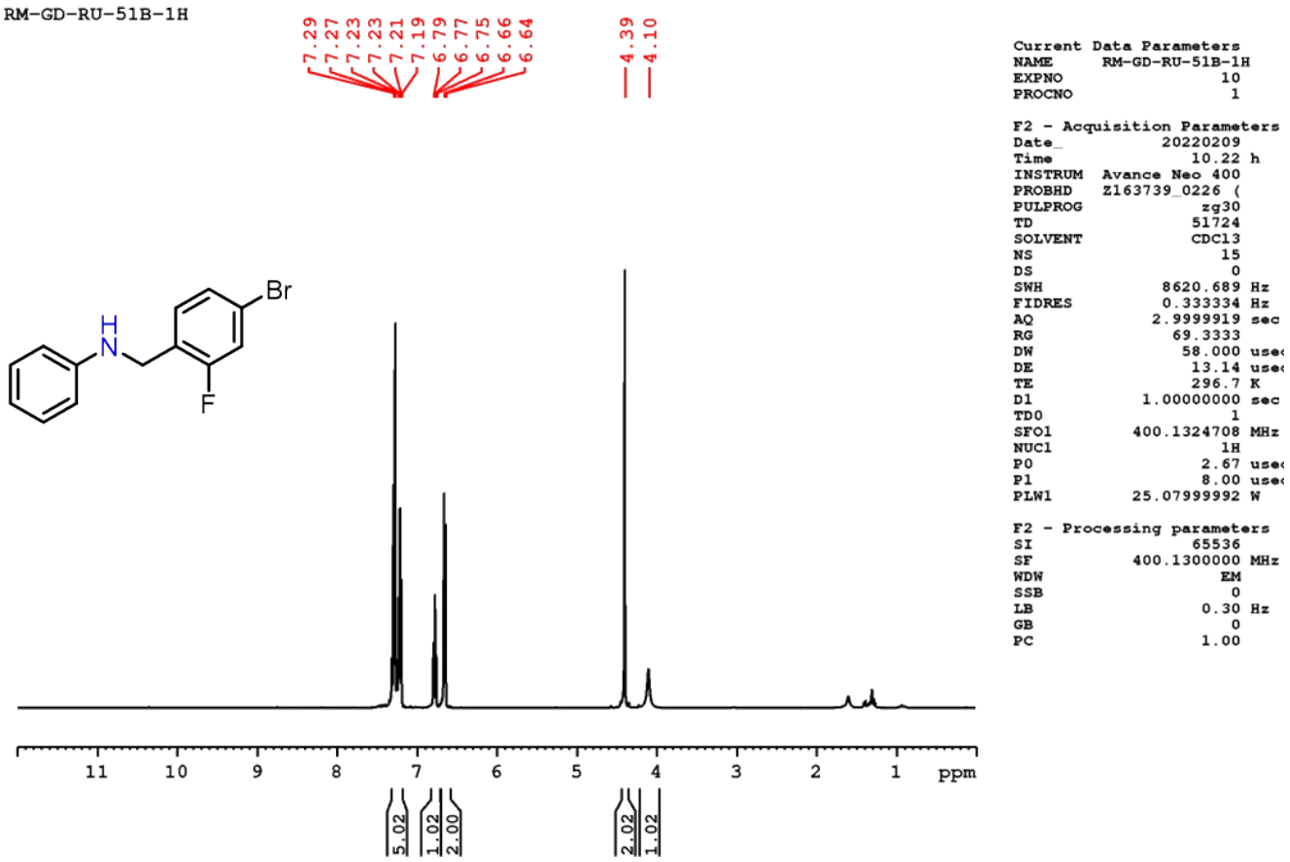

Figure S77. ^{1}H NMR spectrum of complex **2l** in $CDCl_3$ (400 MHz).

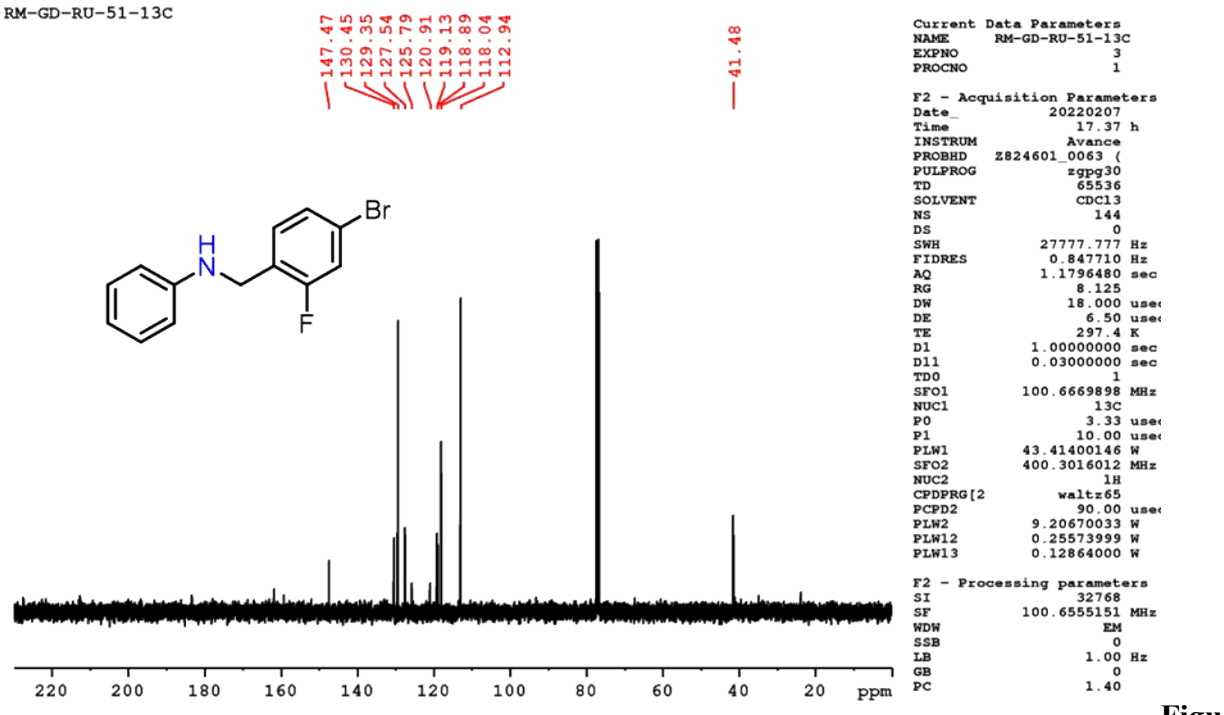

Figure S78. ^{13}C NMR spectrum of complex **2l** in $CDCl_3$ (100 MHz).

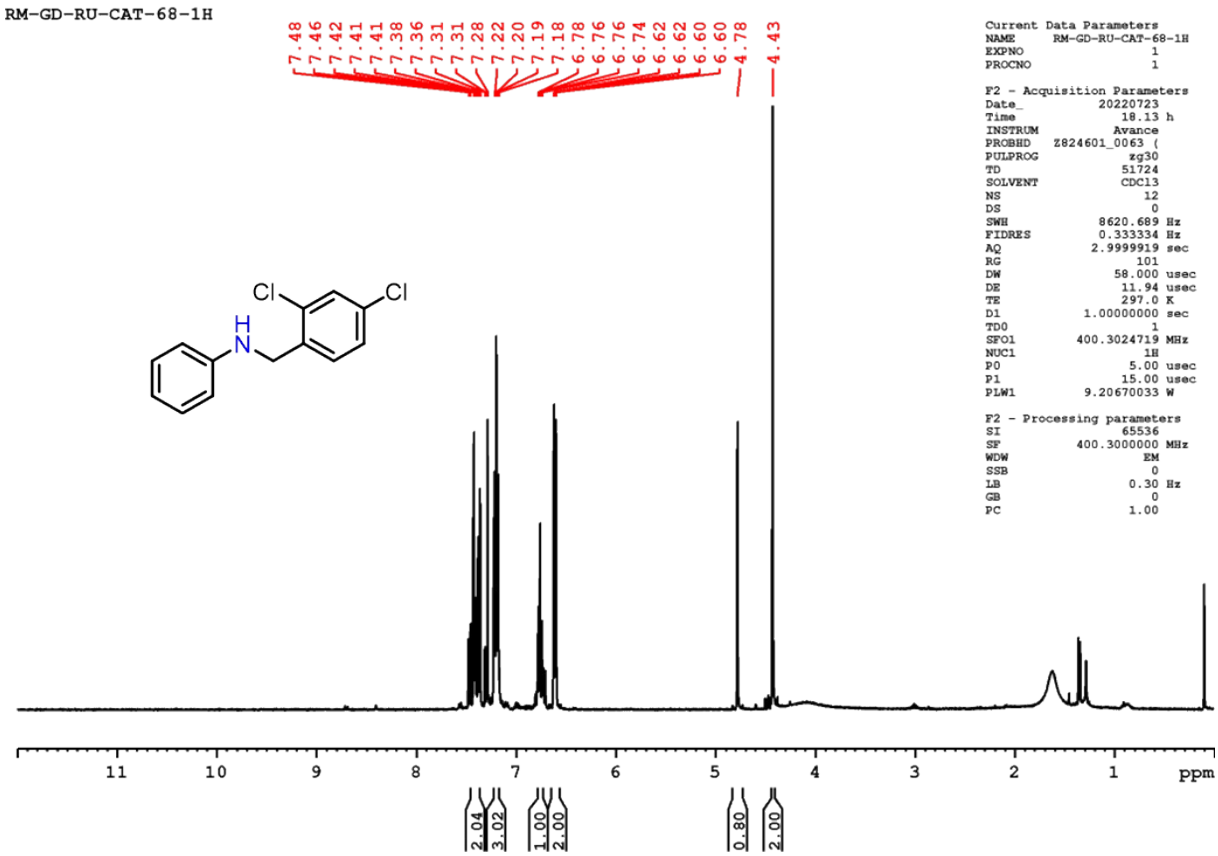

Figure S79. ^{1}H NMR spectrum of complex **2m** in $CDCl_3$ (400 MHz).

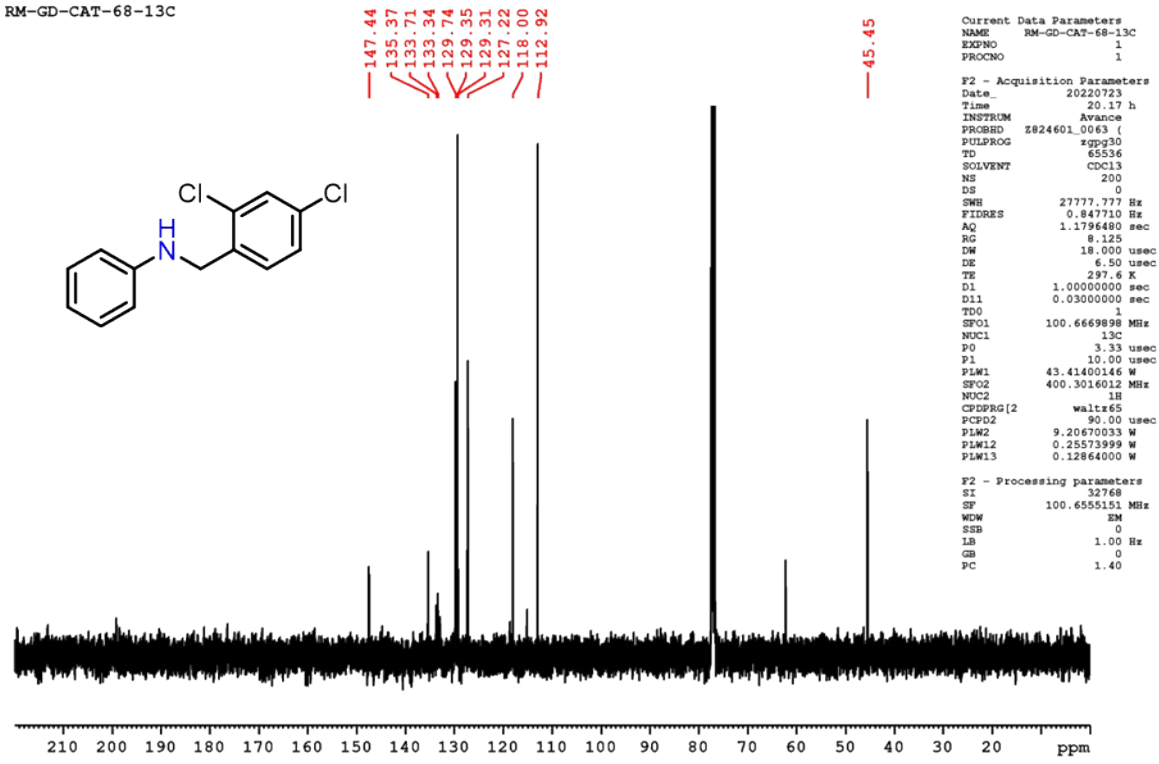

Figure S80. ^{13}C NMR spectrum of complex **2m** in $CDCl_3$ (100 MHz).

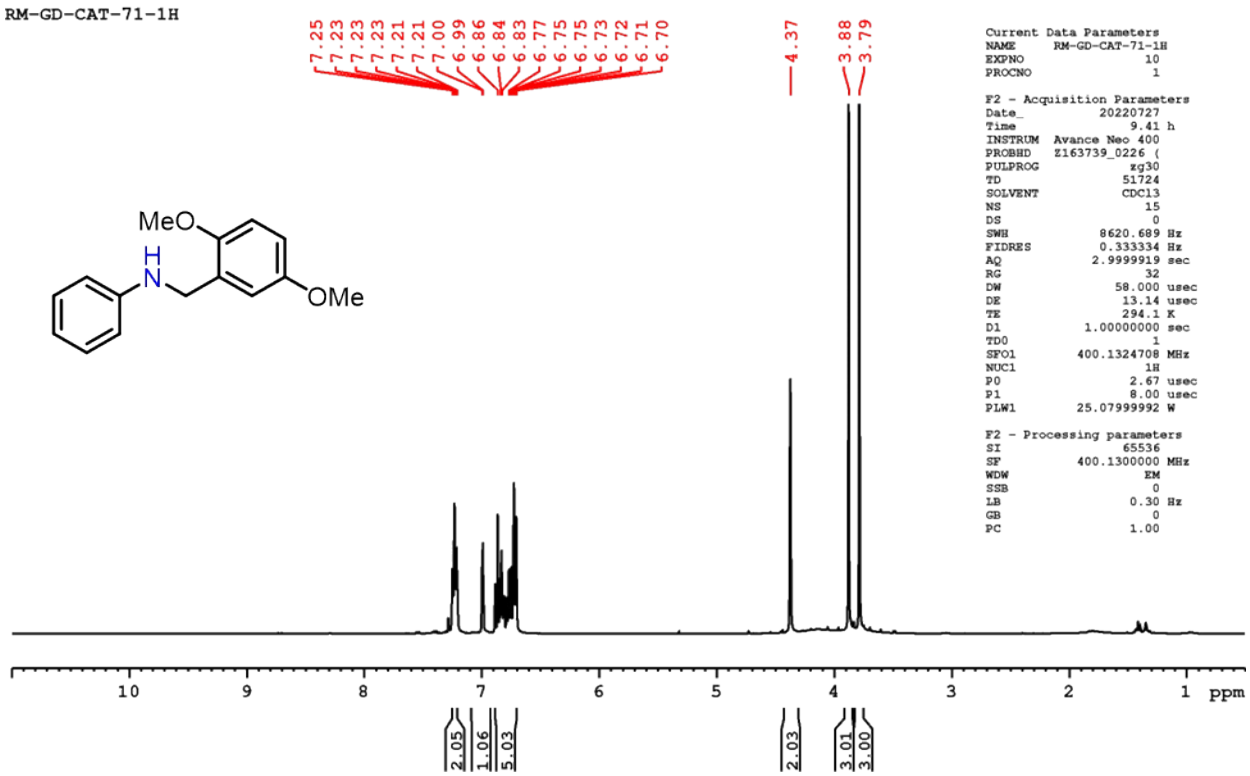

Figure S81. ^{1}H NMR spectrum of complex **2n** in $CDCl_3$ (400 MHz).

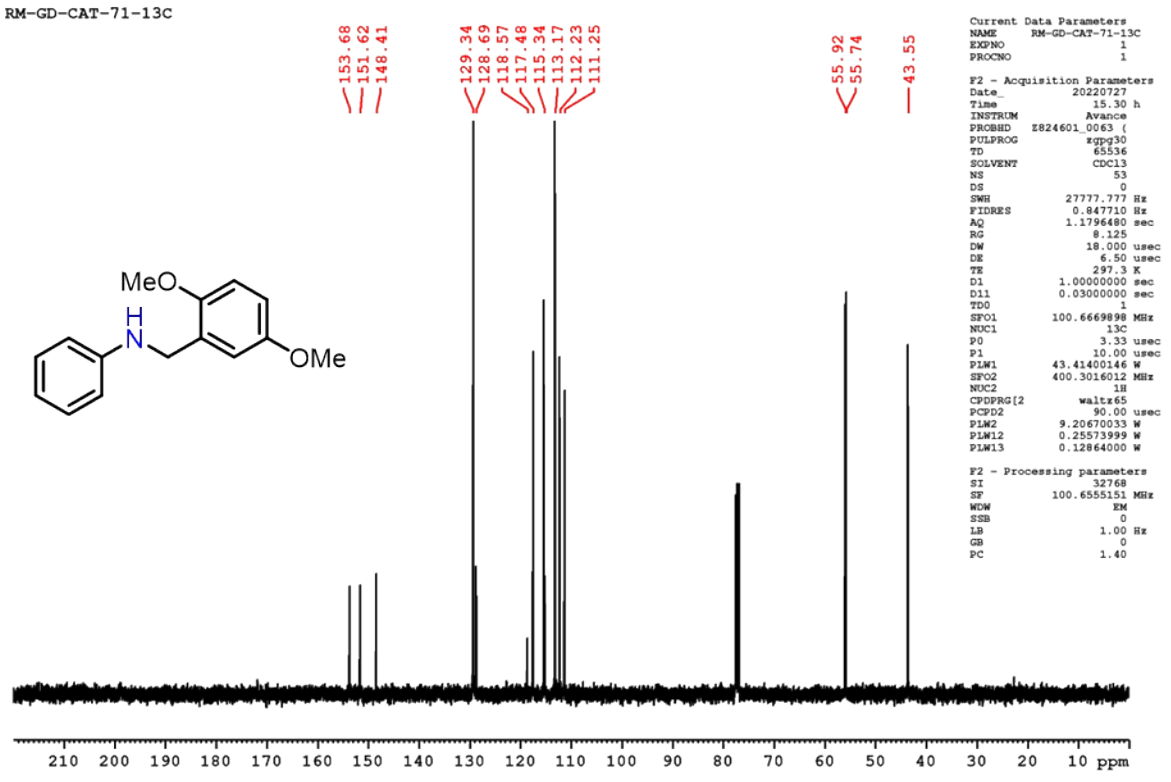

Figure S82. ^{13}C NMR spectrum of complex **2n** in $CDCl_3$ (100 MHz).

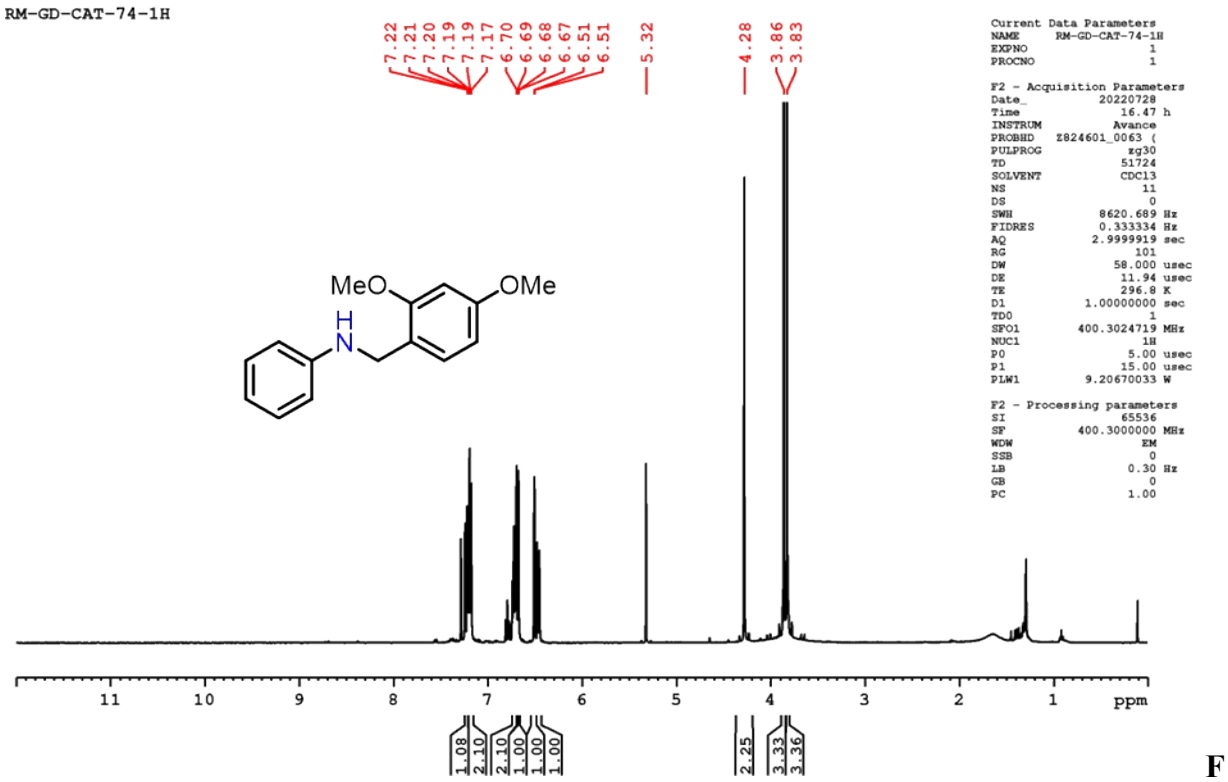

F

igure S83. ^{1}H NMR spectrum of complex **2o** in $CDCl_3$ (400 MHz).

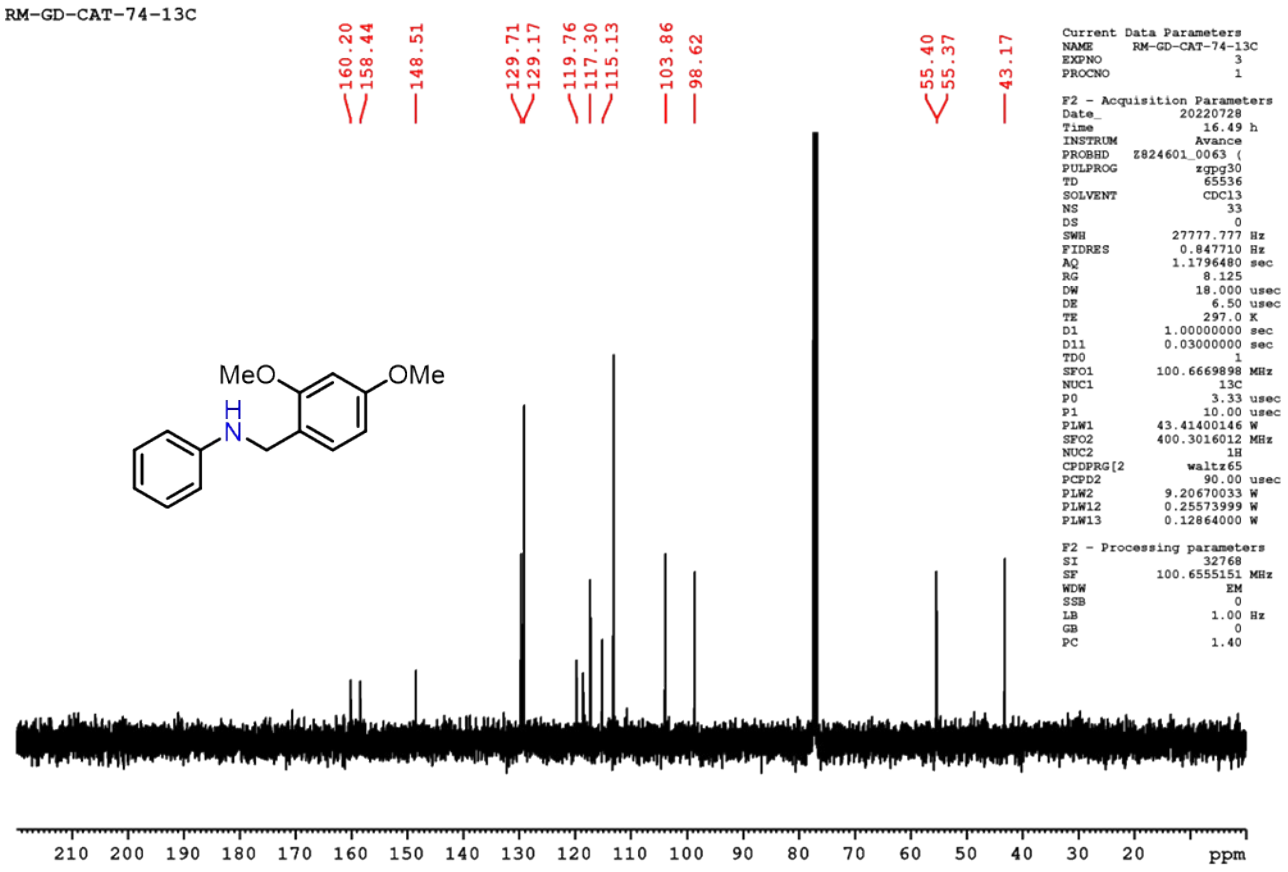

Figure S84. ^{13}C NMR spectrum of complex **2o** in $CDCl_3$ (100 MHz).

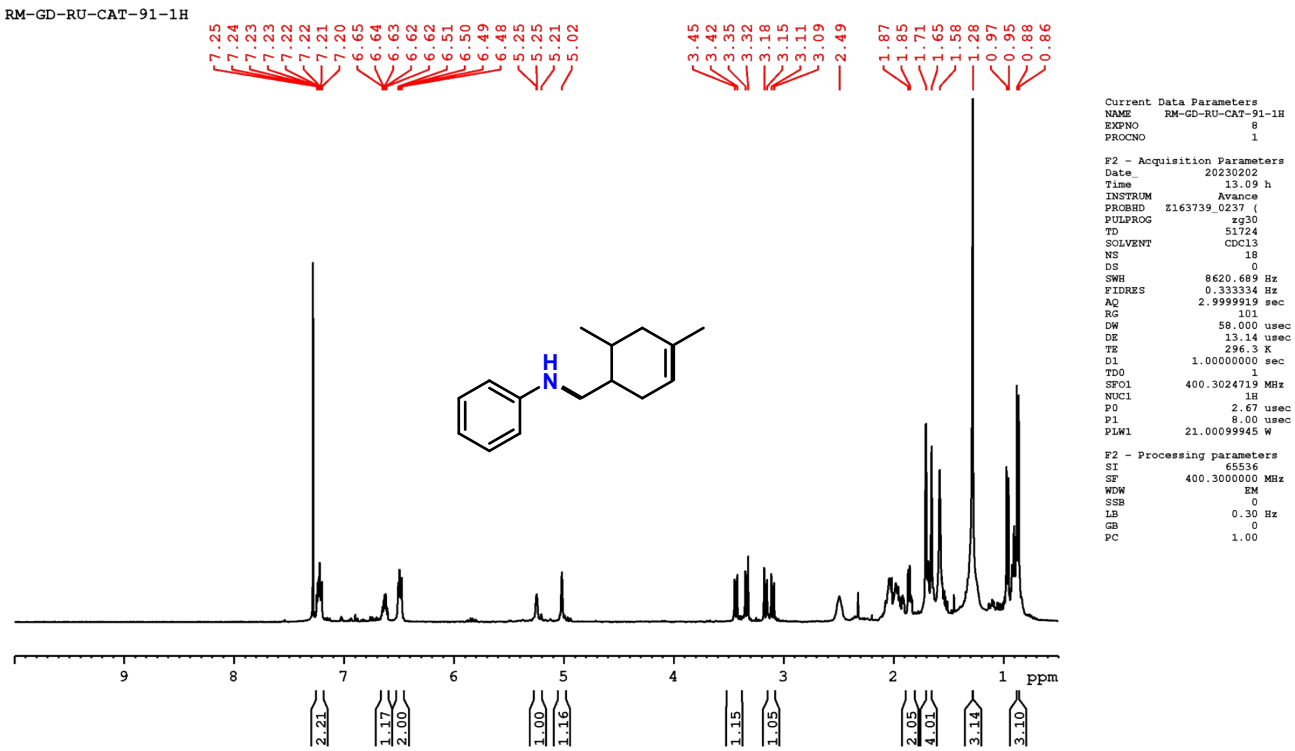

Figure S85. ^{1}H NMR spectrum of complex **2r** in $CDCl_3$ (400 MHz).

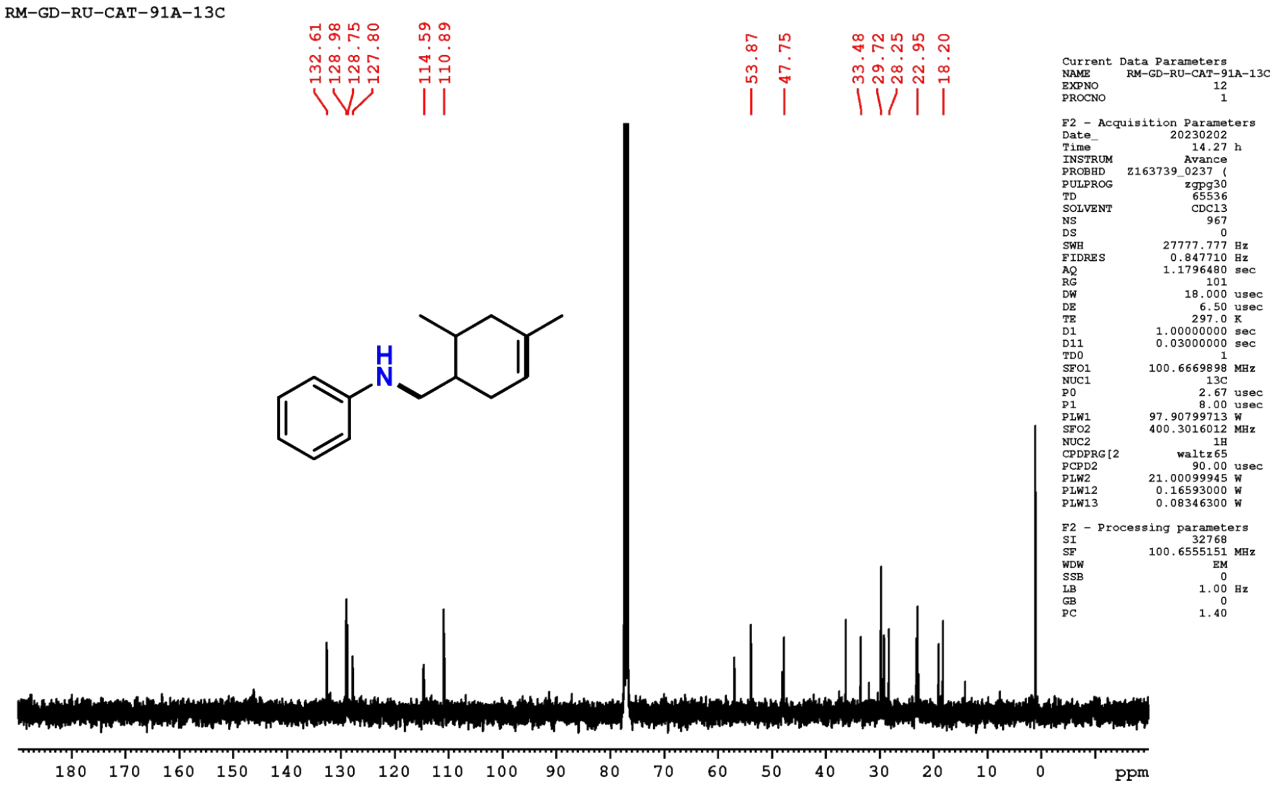

Figure S46. ^{13}C NMR spectrum of complex **2r** in $CDCl_3$ (100 MHz).

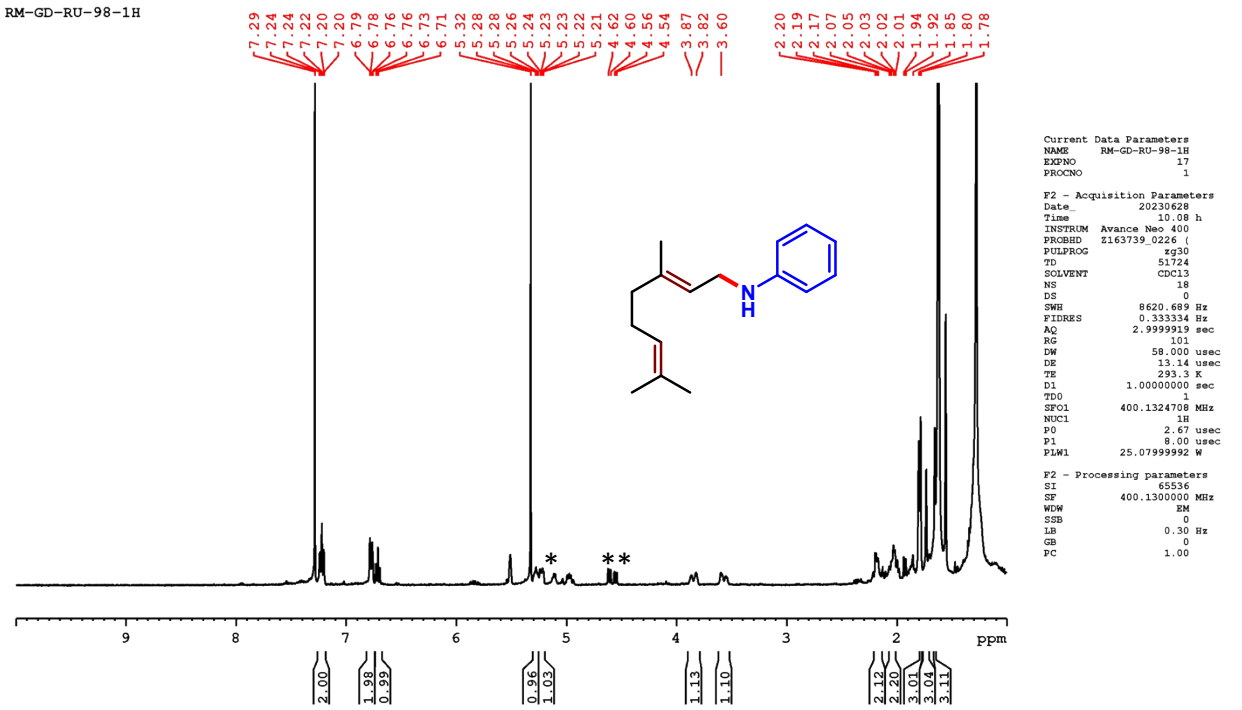

Figure S87. ^{1}H NMR spectrum of complex **2q** in $CDCl_3$ (400 MHz).

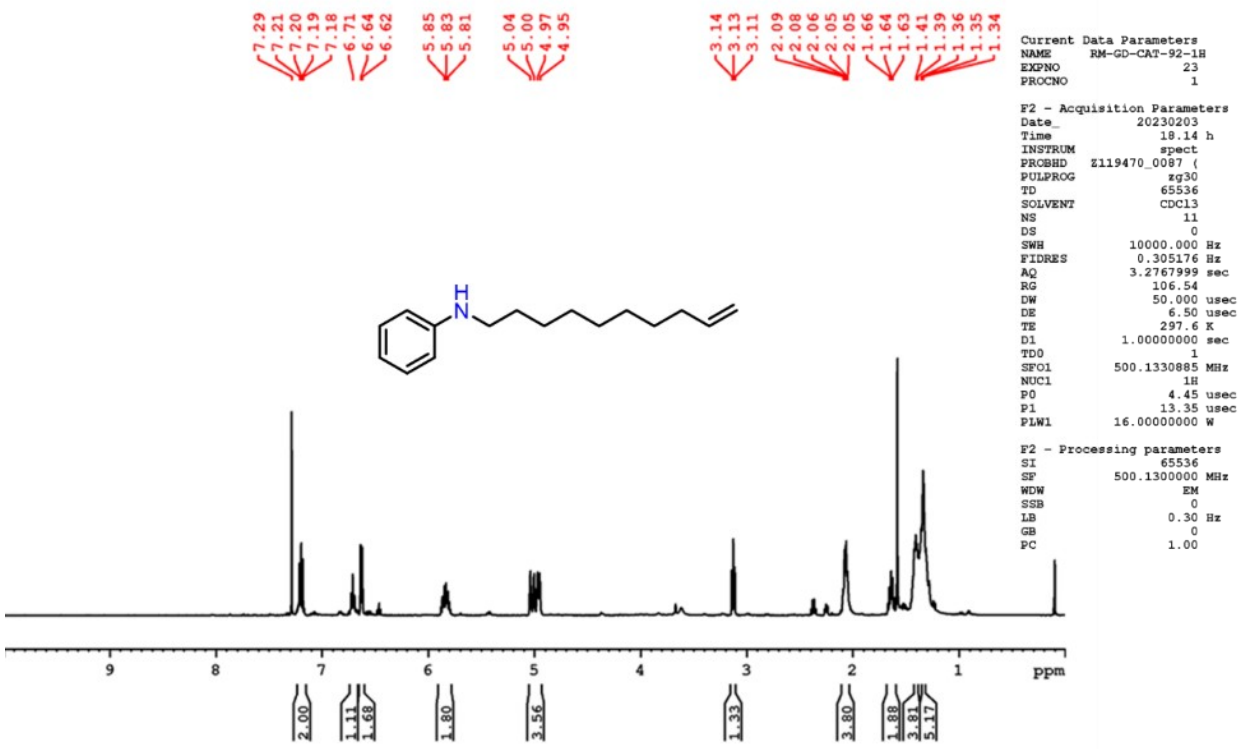

Figure S89. ^{1}H NMR spectrum of complex **2s** in $CDCl_3$ (400 MHz).

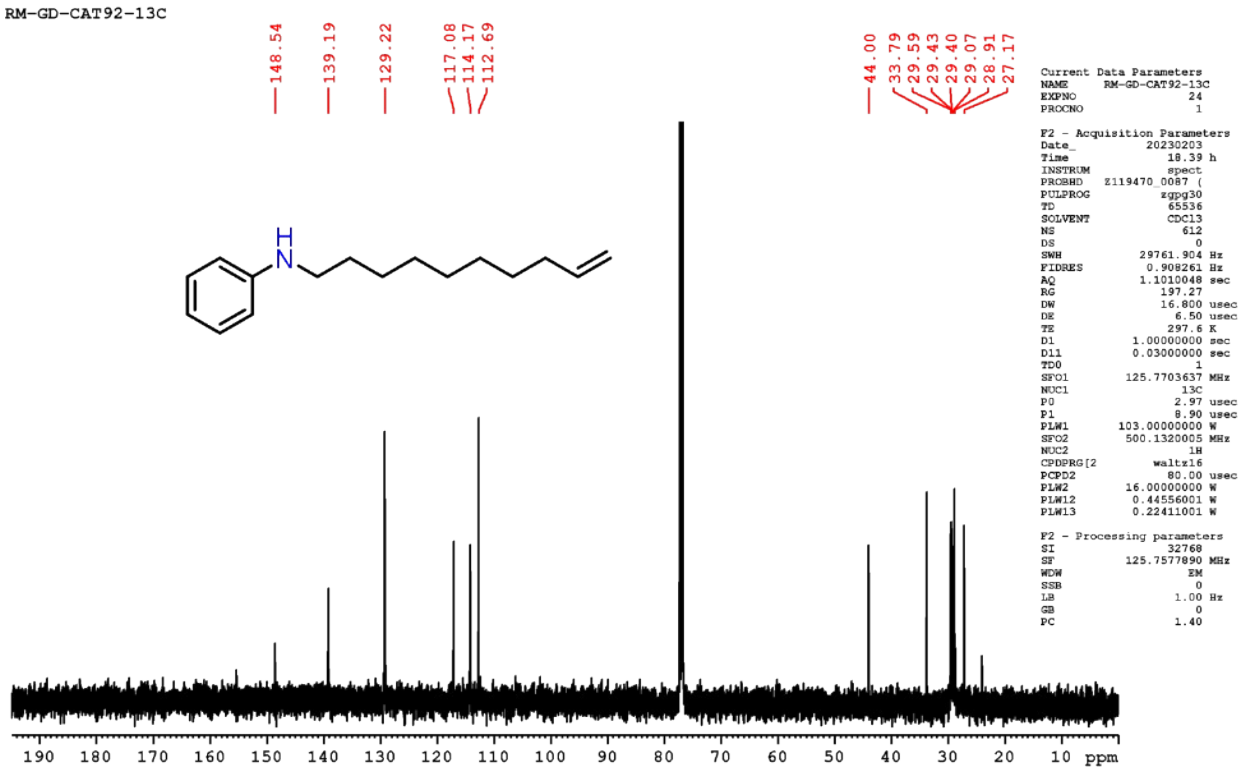

Figure S90. ^{13}C NMR spectrum of complex **2s** in $CDCl_3$ (100 MHz).

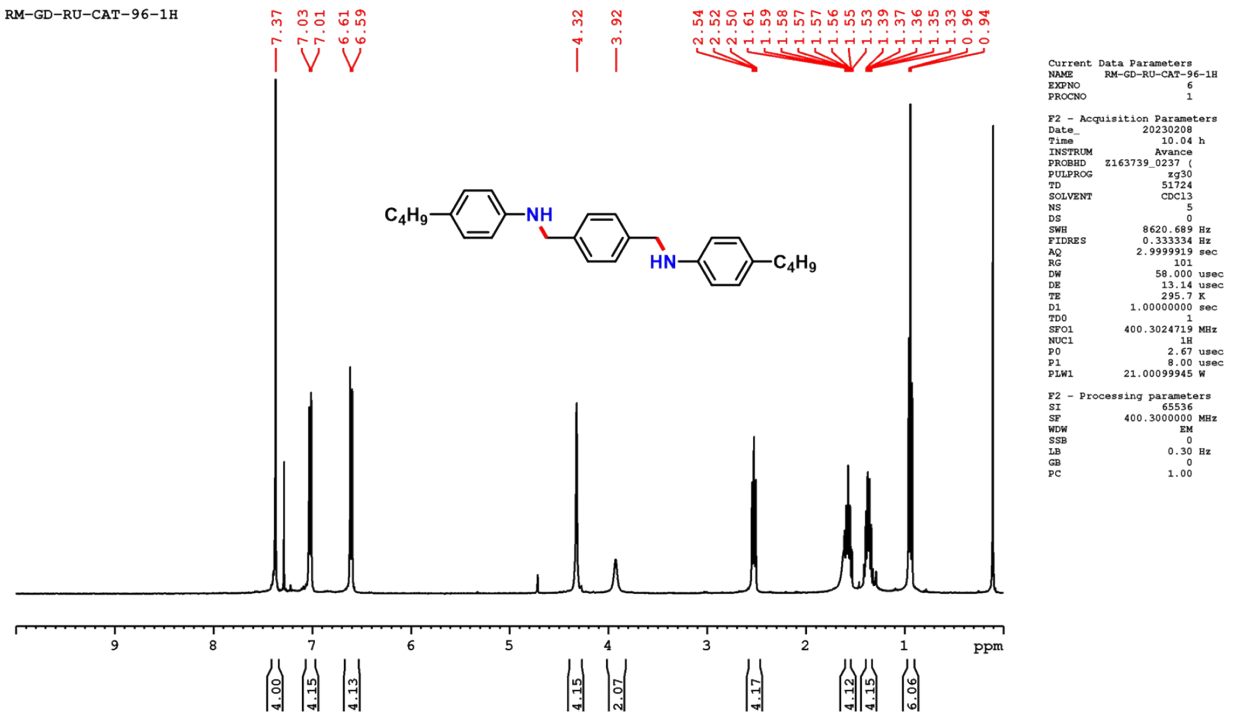

Figure S91. ^{1}H NMR spectrum of complex **3j** in $CDCl_3$ (400 MHz).

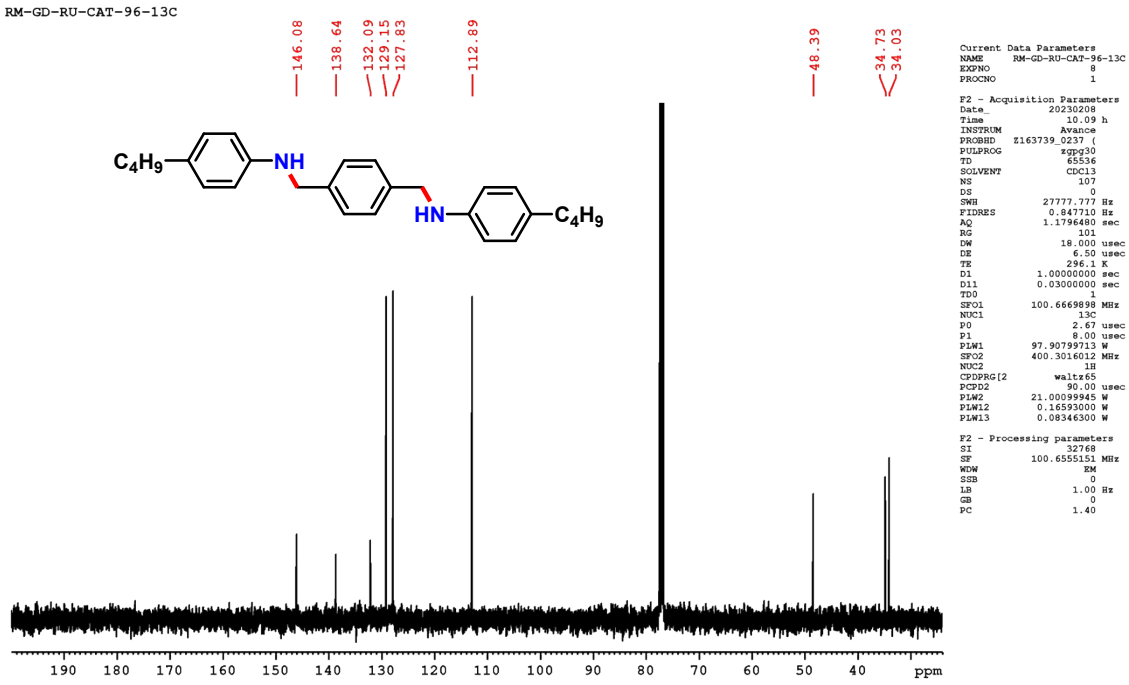

Figure S92. ^{13}C NMR spectrum of complex **3j** in $CDCl_3$ (100 MHz).

Selected GC-MS plots for reaction conducted to determine TON and TOF .

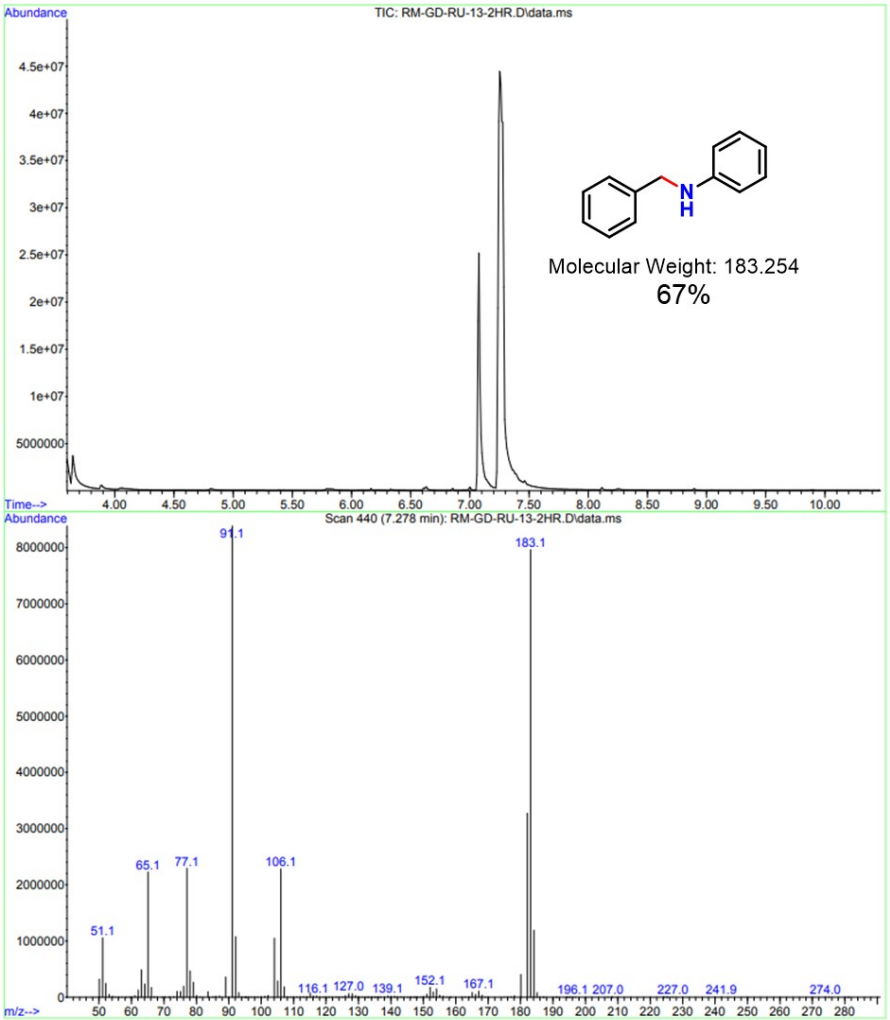

Figure S93. GC-MS plot for Table S1, entry 2.

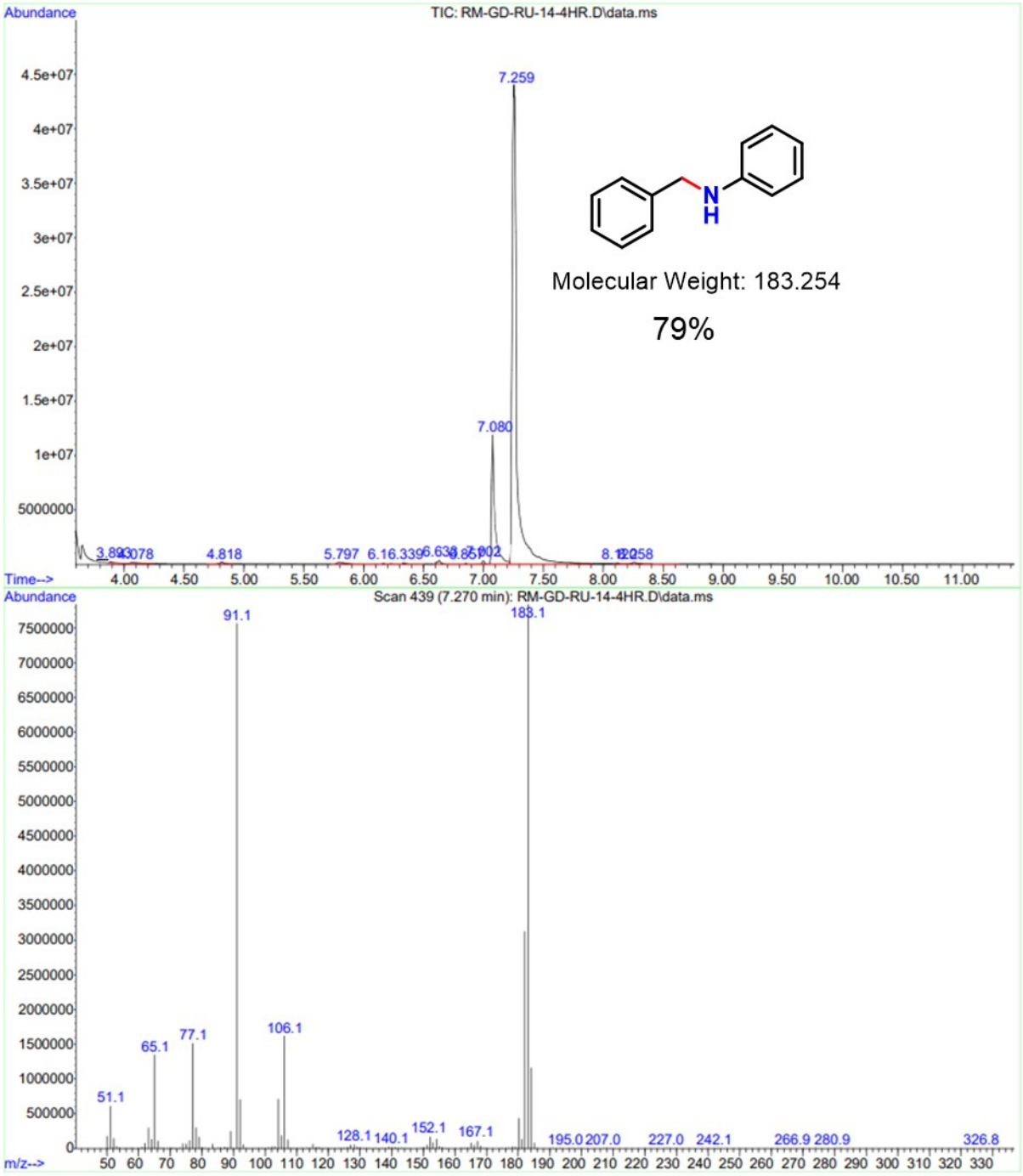

Figure S94. GC-MS plot for Table S1, entry 3.

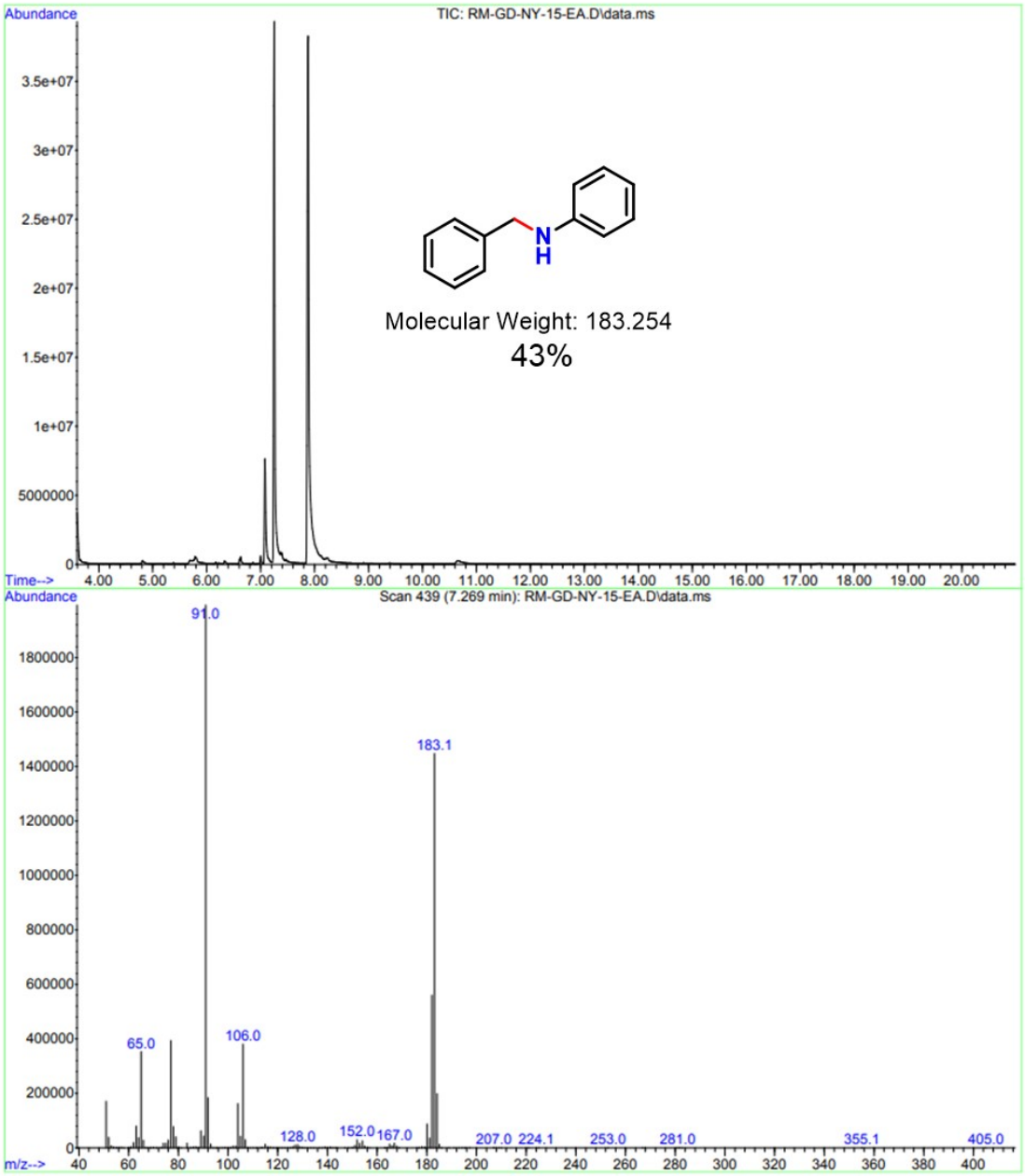

Figure S95. GC-MS plot for Table S1, entry 4.